



Available online at [www.sciencedirect.com](http://www.sciencedirect.com)

ScienceDirect

European Journal of Protistology 61 (2017) 194–232

European Journal of  
PROTISTOLOGY

[www.elsevier.com/locate/ejop](http://www.elsevier.com/locate/ejop)

# Morphologic and molecular characterization of seven species of the remarkably diverse and widely distributed metopid genus *Urostomides* Jankowski, 1964 (Armophorea, Ciliophora)

William Bourland<sup>a,\*</sup>, Johana Rotterová<sup>b</sup>, Ivan Čepička<sup>b</sup>

<sup>a</sup>Boise State University, Department of Biological Sciences, Boise, ID 83725-1515, USA

<sup>b</sup>Department of Zoology, Faculty of Science, Charles University, Prague, Czech Republic

Received 28 February 2017; received in revised form 6 July 2017; accepted 13 July 2017

Available online 20 July 2017

## Abstract

The free-living ciliates of the order Metopida Jankowski, 1980 are pivotal players in the microbial food web of the sulfuretum, acting as hosts to prokaryotic endo- and ectosymbionts. They are also of interest in the study of the function and evolution of their mitochondrion-related organelle, the hydrogenosome. The taxonomy and phylogeny of this group remains confused, due, in large part, to the fact that most of its taxa have not been characterized by modern methods including molecular sequencing. In this report we provide morphologic and molecular characterization of seven taxa from the poorly-known resurrected genus *Urostomides* obtained in the course of broad geographic sampling. Foissner (2016) established the family Apometopidae to include *Apometopus* (a junior synonym of *Urostomides*) and *Cirranter* Jankowski, 1964. These two genera differ from all other metopid genera in having a four-rowed perizonal ciliary stripe, the only currently recognizable morphologic synapomorphy for the family. The members of *Urostomides* show remarkable morphologic diversity. The genus has a broad geographic distribution, occurring on six continents. *Urostomides* species form a strongly supported clade in phylogenetic analyses. Relationships within the genus itself are less clearly resolved. The diagnoses of Apometopidae and *Urostomides* are emended.

© 2017 Elsevier GmbH. All rights reserved.

**Keywords:** Anaerobic ciliates; *Cirranter*; Metopida; Phylogeny; Protargol impregnation; 18S rRNA gene

## Introduction

The free-living anaerobic ciliates of the order Metopida Jankowski, 1980 have recently garnered increased attention from protistologists for a variety of reasons: (1) they are pivotal players in the microbial food web of the sulfuretum, (2) as hosts to a wide variety of prokaryotic ecto- and endosymbionts, they can provide models for the study

of eukaryote–prokaryote symbioses and their evolution, (3) their hydrogenosomes are of interest to those studying the biochemistry, genetics, and evolution of mitochondrion-related organelles and adaptation of eukaryotes to extreme environments, (4) the taxonomy and phylogeny of this group and its relationships with the other Armophorea is far from settled since the majority of taxa have been described without benefit of modern methods (Biagini et al. 1997; Bourland and Wendell 2014; Bourland et al. 2017; Esteban et al. 1995; Foissner and Agatha 1999; Hu 2014; Saccà 2012).

\*Corresponding author. Fax: +1 815 301 89858.

E-mail address: [willbour@me.com](mailto:willbour@me.com) (W. Bourland).

Genus *Metopus* Claparède and Lachmann, 1858 is the largest of the type family, Metopidae Kahl, 1927, and efforts to redescribe the known species by modern methods and to resolve their phylogeny are only just beginning (Bourland et al. 2014, 2017; Bourland and Wendell 2014; Foissner 2016a,b; Foissner et al. 2002; Foissner and Agatha 1999; Paiva et al. 2013; Silva-Neto et al. 2016). With the growing interest in this group and the recent findings that the type species of the two most species-rich genera *Metopus* and *Brachonella* Jankowski, 1964 appear to be very closely related (Bourland et al. 2017), the need to reclassify a number of species originally assigned to these genera is becoming critical (Omar et al. 2017). Only family Apometopidae Foissner, 2016b and six new genera, *Atopospira* Jankowski, 1964, *Brachonella* Jankowski, 1964, *Cirranter* Jankowski, 1964, *Parametopidium* Aesch, 2001, and *Heterometopus* Foissner, 2015, have been added to Metopidae in the last 52 years (Jankowski 1964a,b; Aesch 2001; Foissner 2016a). The current study redescribes seven metopid species having four-rowed perizonal ciliary stripes and examines their phylogeny based on 18S rRNA gene sequences. Six of these species, previously classified within *Metopus* and *Brachonella*, are herein transferred to *Urostomides* Jankowski, 1964, a poorly characterized genus until now.

## Material and Methods

### Organisms (Table 1)

Freshwater sediment samples from around the world were collected and most cultured as described by Bourland et al. (2017). Briefly, non-clonal cultures including undetermined bacteria and, sometimes, various flagellates and amoebae, were established by inoculating fresh samples into 15 ml Falcon tubes containing 9 ml of Sonneborn's *Paramecium* medium (Sonneborn 1970) and subcultures were made at approximately two-week intervals and maintained at room temperature. The seven USA populations were not cultured but, rather, maintained in raw samples (Table 1).

### Light microscopy

The morphology of living, methyl green-rhodamine B-stained (Waldeck, Münster, DE), silver carbonate-impregnated, and protargol-impregnated (Polysciences Inc., Warrington, PA) cells was examined with a compound microscope. Differential interference contrast was used to observe living cells. Protargol impregnation was done as previously described (Bourland and Wendell 2014). Protargol-impregnated specimens were measured with an ocular micrometer at 1000 $\times$  magnification. In vivo measurements were made from microphotographs with calibrated Spot imaging software (Diagnostic Instruments, Inc., Sterling Heights, MI, USA) and calibrated Quickphoto imaging

software (Promicra, CZ). Drawings of live specimens were done free hand and those of silver-impregnated specimens with the aid of a microscope drawing attachment. Fluorescence microscopy was done with a Zeiss CFL-40 microscope and Zeiss filter set No. 38.

### Scanning electron microscopy

For scanning electron microscopy, ciliates were selected from raw samples or cultures under the dissecting microscope, washed in filtered (0.22  $\mu$ m, Millipore, Billerica, MA, USA) Eau de Volvic (French table water), fixed in a solution of glutaraldehyde and osmium tetroxide (2.5% and 1% final concentration respectively), and processed as previously described (Bourland and Wendell 2014). Gold-sputtered specimens were examined in a Hitachi SU3500 scanning electron microscope (Hitachi High Technologies America, Inc., Schaumburg, IL, USA), and JEOL JSM-6380 (JEOL Ltd., Tokyo, Japan). Where indicated, image stacking was done with Helicon Focus (Helicon Soft Ltd., Kharkiv, UA). Images were adjusted for brightness, contrast and background removal with Photoshop CS6 (Adobe Systems Inc., San Jose, CA, USA).

### DNA extraction, amplification, cloning, and sequencing

For the North American populations (Table 1), total DNA was extracted from washed single cells with 5% Chelex, the 18S rRNA gene was amplified by PCR using Medlin et al. (1988) primers EukA (5'-AACCTGGTTGATC-CTGCCAGT-3') and EukB (5'-TGATCCTGCAGGTTCACCTAC-3') with an annealing temperature of 60 °C. Sequencing was done by GeneWiz (South Plainfield, NJ, USA) as previously described (Bourland et al. 2012).

For the remaining isolates (Table 1), 1.5 ml of thriving cultures were centrifuged for 8 min at 500  $\times$  g, 1400  $\mu$ l of the supernatant was removed, and the remaining 100  $\mu$ l was resuspended and used for DNA isolation. Genomic DNA was isolated from the cultures using the DNA isolation kit (Genomic DNA Minikit, Geneaid, New Taipei City, Taiwan; DNeasy Blood & Tissue Kit, Qiagen, Hilden, Germany; or ZR Genomic DNA Kit II TM, Zymo Research, Irvine, CA, USA) according to the manufacturer's instructions. The DNA was stored at -20 °C. The 18S rRNA gene was amplified with degenerate primers designed for Armophorida, ArmF1 (5'-GCGAYATRTCATTCAAGT-3') and ArmR4 (5'-GWGGTTWTCCACACAGTC-3') (Bourland et al. 2017) and an annealing temperature of 60 °C. In most cases, direct sequencing of PCR products was possible. In cases where there were several related ciliate species present in the culture, it was necessary to clone selected amplicons to obtain the sequence of interest. Cloning was done using cloning kit (pGEM-T Easy Vector System, Promega, Madison, WI,

**Table 1.** *Urostomides* strains included in this study.

Strain <sup>a</sup>	Species	Locality	Coordinates <sup>b</sup>	Sample type <sup>c</sup>
<b>1.ABACBLUFF</b>	<i>Urostomides bacillatus</i>	8th Street Bluff pond, Idaho, USA	43°38'31.37"N 116°11'12.01"W	Sediment, pond
<b>2.STAN5</b>	<i>Urostomides bacillatus</i>	Beaver Lake, Stanley, Canada	49°18'06.14"N 123°08'30.12"W	Sediment
<b>3.ACADBLUFF</b>	<i>Urostomides caducus</i>	8th street Bluff pond, Idaho, USA	43°38'31.37"N 116°11'12.01"W	Sediment, pond
4. ACADGLEN	<i>Urostomides caducus</i>	Riverside Park, Idaho USA	43°39'43.42"N 116°16'22.21"W	Sediment, stream
<b>5.ACAMTR</b>	<i>Urostomides campanula</i>	Aquaculture trough, Idaho, USA	43°33'04.57"N 116°17'07.95"W	Sediment
<b>6.ADARBOT</b>	<i>Urostomides darwini</i>	Idaho Botanical Gardens, Idaho, USA	43°36'05.73"N 116°09'37.34"W	Sediment, stream
<b>7.KLAN2BC</b>	<i>Urostomides pullus</i>	Prague, CZ	50°05'42.48"N 14°40'09.68"E	Sediment, stream
8. APOG1	<i>Urostomides denarius</i>	Guam, USA	13°25'23"N, 144°46'51"E	Sediment
9. BORNEOLB	<i>Urostomides denarius</i>	Borneo, Indonesia	1°43'07.2"N 110°26'47.3"E	Sediment
10. EBOGO	<i>Urostomides denarius</i>	Nyong-et-So, Cameroon	3°22'47.2"N 11°27'51.2"E	Sediment
11. LOIRABC	<i>Urostomides denarius</i>	Loire River, near Le Puygrenet, France	46°19'57.35"N 1°02'40.30"E	Sediment, river
<b>12.MOLUKY4</b>	<i>Urostomides denarius</i>	Moluku, Indonesia	3°31'22.33"S 130°25'37.84"E	Sediment
13. PIET4B	<i>Urostomides denarius</i>	Pietermaritzburg, JAR	29°36'16.70"S 30°20'48.60"E	Sediment
14. REU1	<i>Urostomides denarius</i>	Reunion Island, France	21°12'35.50"S 55°20'12.50"E	Sediment
<b>15.SUSBARB</b>	<i>Urostomides denarius</i>	Bako NP, Malaysia	1°43'00.00"N 110°28'00.00"E	Sediment
16. 1VLADECH	<i>Urostomides striatus</i>	Prague, CZ	50°00'48.25"N 14°30'30.24"E	Sediment
17. 3ELI	<i>Urostomides striatus</i>	n.a.	n.a.	Sediment
18. CASTILLO	<i>Urostomides striatus</i>	Cerro Castillo, Andes, Chile	45° 59.648'N 72°4.359'E	Sediment
19. RADUŇ	<i>Urostomides striatus</i>	Raduň, CZ	49°53'34.33"N 17°56'35.70"E	Sediment
<b>20.RAJ2AN</b>	<i>Urostomides striatus</i>	Bohemian Paradise PA, CZ	50°30'57.80"N 15°03'48.15"E	Sediment
21. SCHOOONERS	<i>Urostomides striatus</i>	Vancouver Island, Canada	49°04'N 125°46'W	Sediment
22. STOVIK	<i>Urostomides striatus</i>	Botanical Garden CU, Prague, CZ	50°04'20.00"N 14°24'24.00"E	Sediment, pond
23. V5MS	<i>Urostomides striatus</i>	Botanical Garden CU, Prague, CZ	50°04'20.00"N 14°24'24.00"E	Sediment, pond
24. <b>ASTRTUB<sup>d</sup></b>	<i>Urostomides striatus</i>	Garden tub mesocosm, Idaho, USA	43°37'40.82"N 116°11'17.59"W	Sediment, mesocosm

<sup>a</sup> All cultured except for those from USA which were maintained in original raw samples. Strains with detailed morphometrics and 18S rDNA sequences in bold, those with only 18S rDNA sequences in regular font.

<sup>b</sup> Approximate coordinates, obtained from Google Earth (accessed 11/4/2017).

<sup>c</sup> All freshwater.

<sup>d</sup> Listed as *Metopus striatus*, accession number KF607085 in GenBank.

USA) and JM109 competent cells of *Escherichia coli* (High Efficiency Competent Cells, Promega, Madison, WI, USA). Sanger DNA sequencing was done in the Laboratory of DNA Sequencing at Charles University, which is equipped with an ABI PRISM 3100 sequencer (Applied Biosystems, Foster City, CA, USA).

## Phylogenetic analyses

We created a data set of 18S rRNA gene sequences consisting of 22 newly determined sequences of *Urostomides*, 33 sequences of other Metopida and environmental sequences affiliated with Metopida by BLAST, 12 sequences of Cleavelandellida, and 15 sequences of Armophorida, Litostomatea, Spirotrichaea, and Cariacotrichaea. The sequences were aligned using MAFFT (Katoh et al. 2002) on the MAFFT 7 server <http://mafft.cbrc.jp/alignment/server/> with G-INS-i algorithm at default settings. The alignment was manually edited using BioEdit 7.0.9.0 (Hall 1999). The final data set of unambiguously aligned characters consisted of 1639 positions and is available upon request. Phylogenetic trees were constructed by maximum likelihood (ML) and Bayesian methods. ML analysis was performed in RAxML 8.0.0 (Stamatakis 2014) under the GTRGAMMAI model. Node support was assessed by ML analysis of 1000 bootstrap data sets. Bayesian analysis was performed using MrBayes 3.2.2. (Ronquist et al. 2012) using the GTR + I + Γ + covarion model with four discrete categories. Four MCMCs were run for 2,000,000 generations, with a sampling frequency of 500 generations, until the mean standard deviation of split frequencies based on last 75% was lower than 0.01. First 25% of trees were removed as burn-in.

## Terminology

Terminology used in this study is mainly according to Foissner and Agatha (1999), Bourland et al. (2014), and Lynn (2008) except as noted. We define the “preoral dome” as that portion of the cell anterior to the level of the cytostome. The use of the term “somatic kineties” excludes perizonal stripe kineties. We define the term “dome kineties” as kineties the anterior ends of which lie at or above the level of the anterior end of the perizonal stripe and those confined completely to the preoral dome. Classification follows Jankowski (2007) and Foissner (2016b) except as noted.

## Results and Discussion

### Morphologic characterization of species

*Urostomides caducus* (Kahl, 1927) comb. nov. (original combination *Metopus caducus* Kahl, 1927) (Figs. 1A–G, 2A–L, Tables 1 and 2)

**Improved diagnosis based on Idaho strains ACAD-BLUFF and ACADGLEN, original description (Kahl 1927), and redescription (Kahl 1932).** Body size about 70–110 × 50–70 μm in vivo. Body shape obpyriform, not twisted, dorsoventrally flattened. Preoral dome massive. Posterior body obconical, posterior end truncate. Macronucleus globular, in preoral dome. Extrusomes, inconspicuous oblong to ellipsoidal. Cortical granules in about 20 interkinetal rows. Cortex conspicuously furrowed by kineties. Preoral dome granule aggregate absent. Total of about 35 ciliary rows, invariably seven extending as widely spaced rows onto preoral dome, posterior body rows closely spaced. Eccentric tuft of long, nonmotile caudal cilia on right margin of posterior end. Perizonal ciliary stripe never arranged in false kineties. Adoral zone spirals ≥ one full turn around long axis.

**Remarks.** Terms of anatomic orientation in metopids were particularly confusing in the older literature. Kahl (1927) described the eccentric tuft of long caudal cilia as being on the left margin of the posterior end. This reflects his unusual designation of ventral and dorsal sides in this and other metopids. We consider the view presented in Kahl (1927, his Fig. 20c) as the ventral surface, thus the caudal ciliary tuft is located on the right margin of the posterior end according to our definition (Bourland et al. 2014).

**Description of Idaho strain ACADBLUFF.** Size in vivo 71–97 × 47–67 μm and in protargol-impregnated specimens 59–77 × 36–62 μm. Shape broadly obpyriform in ventral view, strongly flattened dorsoventrally (Fig. 2L), about 1:3.5. Length:width ratio including preoral dome 1.4:1 on average. Preoral dome massive, asymmetric, left margin convex, bluntly rounded right anterior end usually overhangs right posterior body margin; dome brim broad, flat, not overhanging adoral zone (Fig. 1A–C); preoral dome occupies about 70% of body length when viewed ventrally (Figs. 1A–C, 2A, G, J). Body part posterior to preoral dome truncate inverted cone. Macronucleus globular, in preoral dome, occupies about 30% of body length in protargol preparations, scattered 3 μm-sized nucleoli. Micronucleus globular, about 6 μm in diameter, adjacent to macronucleus (Figs. 1A–C, G, 2F). Extrusomes about 2.5 μm long (range 1.5–3 μm), oblong to ellipsoidal, inconspicuous in vivo (Fig. 1E), stain pink with methyl green-rhodamine B, explode to form mucus coat around distressed cells (Fig. 2D, E). Contractile vacuole terminal, excretory pore not observed. Cytopygae not visible (Figs. 1A, 2A). Cortex flexible, prominent kinetal furrows at 2.5 μm intervals in posterior part of cell, 10 μm apart in preoral dome. Tiny cortical granules in about twenty interkinetal rows, impregnate strongly with silver carbonate but not with protargol (Fig. 2C, K). Cytoplasm colorless to faint golden-brown in vivo, apical granule aggregate absent. Many food vacuoles up to 13 μm in diameter. (Figs. 1A, 2A). Swims slowly, rotating on long axis.

Ordinary somatic cilia about 10 μm long in vivo, perizonal stripe cilia about 25 μm in vivo, cilia of preoral dome kineties about 12–15 μm long, beat in metachronal waves;

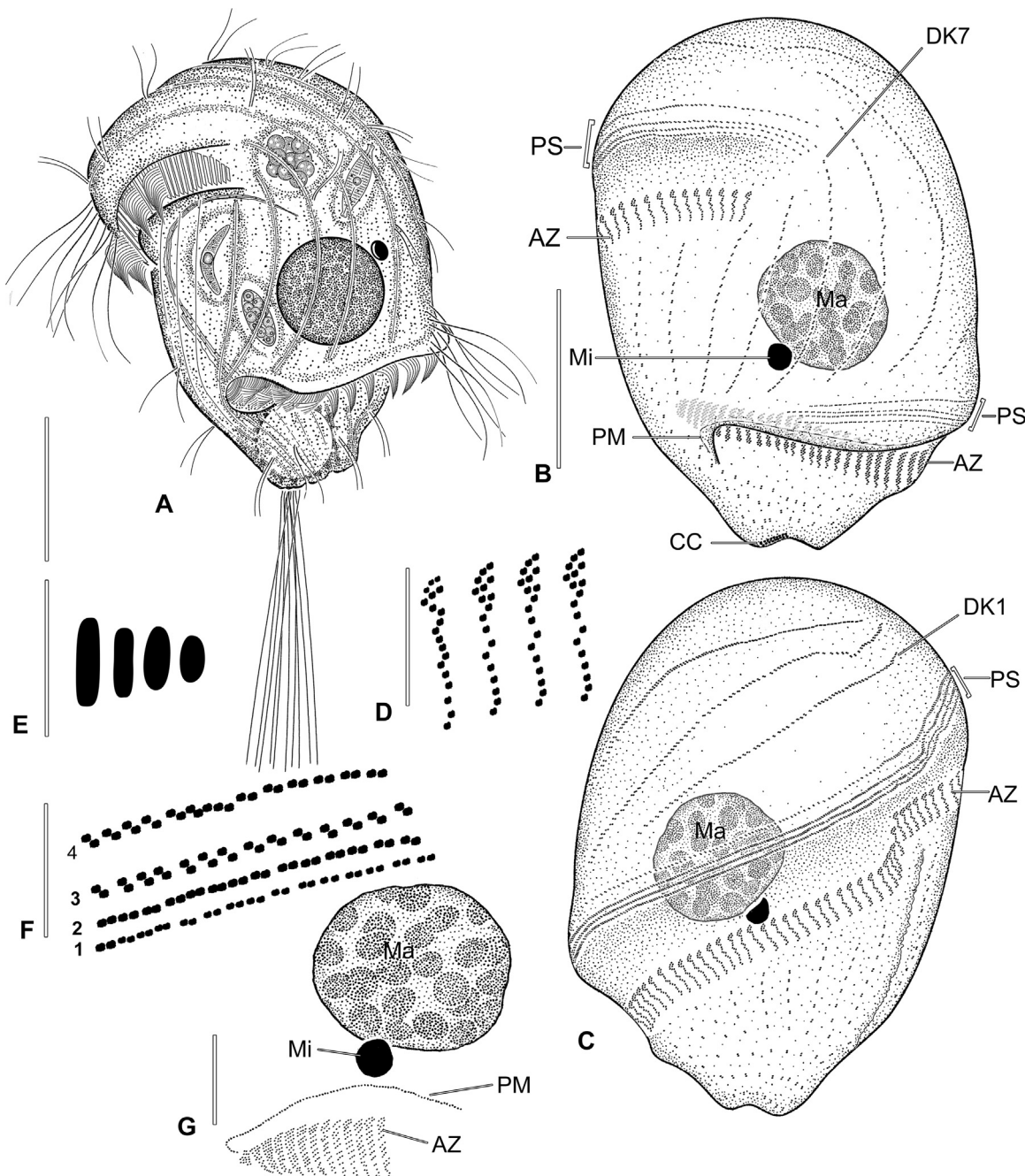


**Fig. 1.** (A–G) *Urostomides caducus* comb. nov., Idaho population (ACADBLUFF) from life (A) and after protargol impregnation (B–G). (A) Ventral view of a representative specimen. (B, C) Ventral (B) and dorsal (C) view of same specimen. (D) Structure of membranelles from mid-portion of the adoral zone. (E) Extrusomes. (F) Structure of the four-rowed perizonal ciliary stripe. Row 1 lies along the margin of the preoral dome, row 4 lies between row 3 and preoral dome kinety 1. (G) Detail of posterior part of buccal region. AZ, adoral zone; CC, basal bodies of caudal ciliary tuft; DK1, 7, preoral dome kineties 1 and 7; Ma macronucleus, Mi, micronucleus; PM, paroral membrane; PS, perizonal ciliary stripe. Scale bars: 25 µm (A–C), 10 µm (G), 5 µm (D–F).

nonmotile caudal cilia, about 50 µm long, grouped in eccentric tuft at right margin of posterior end (Figs. 1A, B, 2A, F, I, J, L). On average 35 (range 27–38) somatic kineties about 2.5 µm apart in the posterior body portion, invariably seven widely-spaced dome kineties (about 10 µm apart), widest gap between dome kinety 1 and perizonal ciliary stripe row 4 (Figs. 1B, C, 2B, H, J). Somatic kineties in posterior

body portion comprised of ordinarily spaced dikinetids usually with only posterior basal body ciliated. Perizonal stripe four-rowed, composed of densely spaced dikinetids, shorter than adoral zone proximally, extends further than adoral zone distally, rows 1–3 closely-spaced, separated from row 4 by distinct gap, dikinetids of rows 1 and 2 parallel to kinety axis, those of rows 3 and 4 obliquely inclined, never form

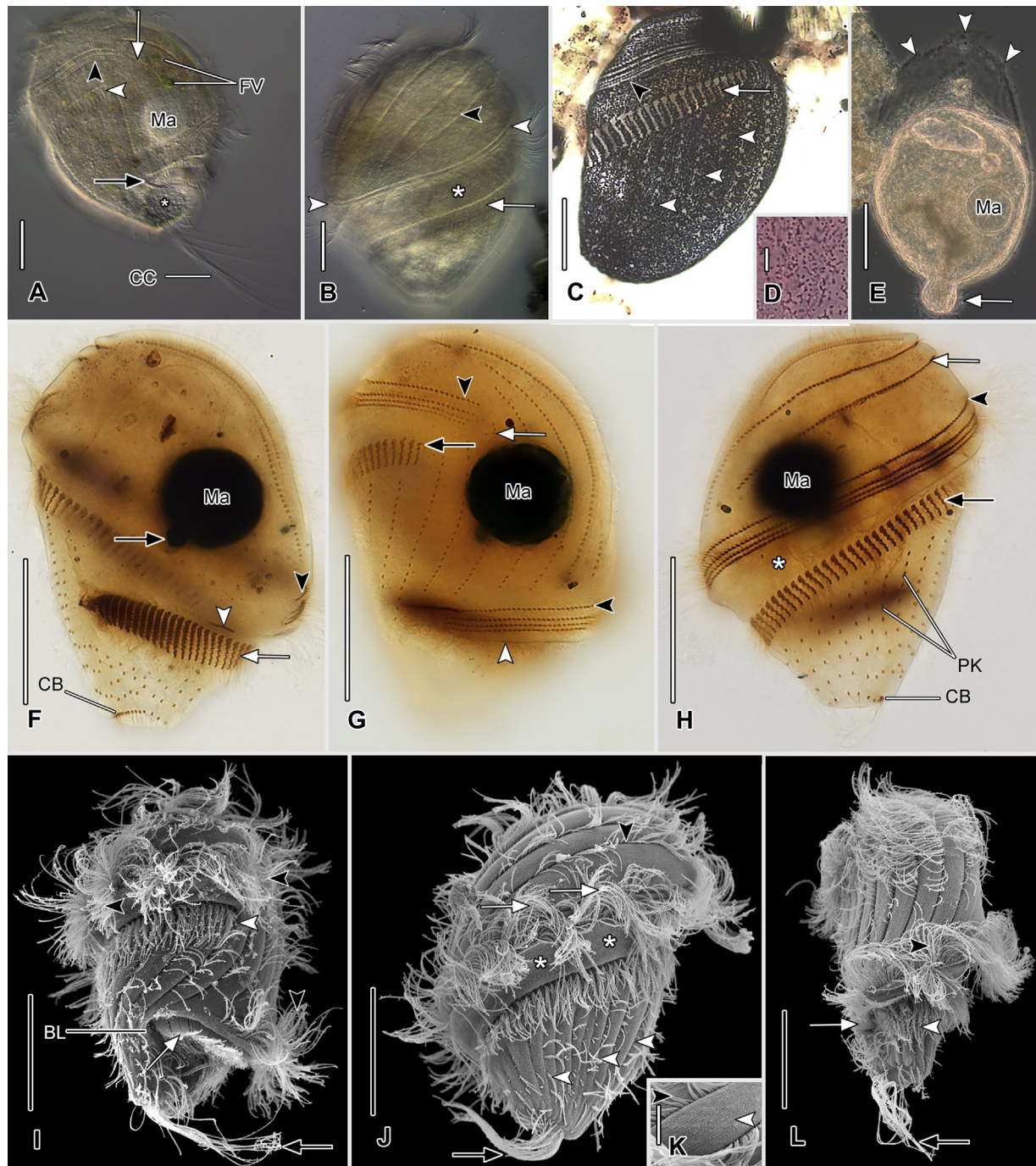


**Fig. 2. (A–L)** *Urostomides caducus* comb. nov., Idaho population (ACADBLUFF) from life (A, B, differential interference contrast; E, phase contrast), after silver carbonate impregnation (C, brightfield), after methyl green-rhodamine B (D, brightfield), after protargol impregnation (F–H, brightfield), and in scanning electron microscope (I–L). (A) Ventral view showing anterior part of perizonal ciliary stripe (black arrowhead), anterior part of adoral zone (white arrowhead), preoral dome kinety 1 (white arrow), proximal margin of buccal cavity (black arrow), and contractile vacuole (asterisk). (B) Dorsal view of perizonal ciliary stripe (white arrowheads), adoral zone (white arrow), preoral dome kinety 1 (black arrowhead), and expanded glabrous margin of preoral dome (asterisk). (C) Argyrophilic cortical granules of the perizonal stripe (black arrowhead), the adoral zone (arrow), and the interkinetal cortex (white arrowheads). (D) Cortical granules (extrusomes). (E) Distressed individual partially extruding (white arrow) from mucous sheath (white arrowheads). (F) Optical section, ventral aspect showing perizonal stripe (black arrowhead), distal part of paroral membrane (white arrowhead), adoral membranelles (white arrow), and micronucleus (black arrow). (G) Ventral view at a more superficial focal plane showing margin of the preoral dome (white arrowhead), perizonal ciliary stripe row 4 (black arrowheads), distal end of adoral zone (black arrow), and distal end of preoral dome kinety 7 (white arrow). (H) Dorsal view of same specimen as (F, G) showing perizonal ciliary stripe row 4 (black arrowhead), preoral dome kinety 1, adoral membranelles (white arrow), and distal part of paroral membrane (white arrowhead).

false kinetics (Figs. 1B, C, F, 2G, H). Dikinetids of perizonal stripe and somatic kinetics completely ciliated. Dikinetids of dome kinetics progressively more densely spaced from right to left (Figs. 1B, C, 2G, H). Dome kinetics often bear syncilia (Fig. 2I, J, L).

Adoral zone comprises about 77 membranelles on average, begins and ends on ventral surface (i.e. makes  $\geq 360^\circ$  spiral around long axis), level of anterior end of adoral zone about 30  $\mu\text{m}$  anterior to level of posterior end, posterior end partly enclosed in buccal cavity (Figs. 1A–C, 2A–C, F–J, L). Posterior-most 13 membranelles rectangular to triangular (Figs. 1G, 2F), composed of three to four long rows; membranelles of ventral part of adoral zone longest (about 7  $\mu\text{m}$ ), composed of three long rows of basal bodies with three basal bodies in triangular array to the left of the anterior end of membranelle (Figs. 1D, 2H). Paroral membrane originates in, and protrudes from, buccal cavity at posterior end of adoral zone, extends to undersurface of preoral dome, comprised of single row of ciliated basal bodies (Figs. 1G, 2F, G, I, L). Cytopharyngeal fibers curve anteriorly from cytostome, extend to level of distal adoral zone (Fig. 1A). Resting cysts, conjugants, and dividers not observed. Attempts to induce encystment by starvation resulted in cell death within hours.

**Strain ACADGLEN.** Morphometric data were available only for protargol-impregnated specimens of this strain (Table 2). The *U. caducus* strain ACADGLEN shows minor morphometric differences from ACADBLUFF in: size, number of adoral membranelles, and number of somatic kinetics although values for both strains overlap broadly. Otherwise, the ACADGLEN matches the ACADBLUFF strain very closely.

**Occurrence and ecology (Table 1).** Two populations of *U. caducus* were collected in Boise, Idaho, U.S.A, one (ACADGLEN) from sulfidic sediments of a lentic outflow creek during April, 2015, and the other (ACADBLUFF) from a eutrophic permanent pond bordered by *Typha latifolia* during June 2016. Sample site characteristics for ACADBLUFF included: pH 7.59, temperature 19.8 °C, salinity 332  $\mu\text{S}/\text{cm}$  (234 mg/L). Food organisms include purple sulfur bacteria, green algae, fungal spores, and pennate diatoms.

**Voucher material.** One slide with protargol-impregnated specimens from the ACADBLUFF population is deposited in the Biology Centre of the Upper Austrian Museum in Linz, Austria (accession no. 2017264). Relevant specimens are marked on the slide with black ink circles.

***Urostomides campanula* (Kahl, 1932) comb. nov.** (original combination *Metopus campanula* Kahl, 1932) (Figs. 3A–G, 4A–J, Tables 1 and 3)

(black arrow) and expanded glabrous margin of preoral dome (asterisk). (I) Ventral view showing the distal end of the adoral zone (white arrowhead), the paroral membrane (white arrow), and caudal ciliary tuft (black arrow). (J) Dorsal view showing preoral dome kinety 1 (black arrowhead), metachronal waves of perizonal stripe cilia (white arrows), postoral kinetics (white arrowheads), caudal ciliary tuft (black arrow), and the expanded glabrous margin of the preoral dome (asterisks). (K) Cortical granules (white arrowhead) and syncilium (black arrowhead). (L) Slightly left ventrolateral view showing flattening of body and paroral membrane (white arrow) perizonal stripe cilia (black arrowhead), adoral membranelles (white arrowhead), and caudal cilia (black arrow). BL, buccal lip, CB, basal bodies of caudal ciliary tuft; CC, caudal cilia; FV, food vacuoles with green algae; Ma, macronucleus; PK, postoral kinetics. Scale bars: 25  $\mu\text{m}$  (A–C, E–J, L), 5  $\mu\text{m}$  (D), 2.5  $\mu\text{m}$  (K).

**Remarks.** The species name, L. f. noun “campanula” = “small bell”, is used in apposition.

**Improved diagnosis based on Idaho strain ACAMTR, original description (Kahl 1927), and redescription by Kahl (1932).** Body size about 35–90  $\times$  30–40  $\mu\text{m}$  in vivo. Body shape broadly obpyriform to campanulate. Preoral dome wider than posterior body. Posterior body obconical, posterior end truncate. Macronucleus globular, in preoral dome. Extrosomes oblong, conspicuous. Total of about 13 ciliary rows, invariably five widely spaced rows in deep cortical furrows on preoral dome; crown kinety (dome kinety 3) thigmotactically specialized. Eccentric tuft of elongated caudal cilia on right margin of posterior end. Perizonal ciliary stripe four-rowed, never arranged in false kinetics, longer than adoral zone distally. Adoral zone horizontal composed of 33 membranelles on average, makes about 270° turn around long axis. Paroral stichomonad. Swimming pattern distinctive, twitching from side to side.

**Description of Idaho strain ACAMTR.** Size in vivo 33–46  $\times$  29–40  $\mu\text{m}$  in vivo and in protargol-impregnated specimens 30–51  $\times$  27–44  $\mu\text{m}$ . Shape broadly obpyriform to campanulate. Length:width ratio including preoral dome 1.1:1 on average. Preoral dome more or less symmetric, hemispherical to broadly conical, occupies about 70% of body length. Body posterior to preoral dome broad, truncate inverted cone (Figs. 3A–C, 4A, B, D–J). Macronucleus globular, in preoral dome, occupies about 30% of body length in protargol preparations; chromatin finely granular, sparse scattered 1  $\mu\text{m}$ -sized nucleoli in protargol preparations. Micronucleus about 3  $\mu\text{m}$  in length, ellipsoidal, usually adjacent to macronucleus but in separate envelope (Figs. 3A, F, 4A, D, E). Extrosomes prominent, ellipsoidal to short blunt rods, about 2–3  $\mu\text{m}$  long, seen as refractive peripheral fringe in vivo, form scattered cortical bumps in scanning electron microscope preparations, impregnate with silver carbonate but not protargol, do not stain with methyl green-rhodamine B, explode to form mucus coat around distressed cells (Figs. 3A, 4A, C, D, H–J). Contractile vacuole terminal, excretory pore and cytopype not observed (Figs. 3A, 4A, B). Cortex flexible, prominent kinetal furrows in preoral dome, cortical granules absent. Cytoplasm colorless to faintly brownish in vivo, many food vacuoles (Figs. 3A, 4E, F). Swims at moderate pace with distinctive side-to-side twitching movement while rotating on long axis (Fig. 3G).

On average 13 (range 11–15) somatic kinetics about 6  $\mu\text{m}$  apart in the posterior body portion; invariably five more widely spaced dome kinetics (Figs. 3B, C, 4E–J). Kinetics of posterior body part composed of dikinetids, longest of these

kineties just to right of proximal buccal margin composed of about nine dikinetids, most postoral kineties reduced, sometimes to only one dikinetid, often with only anterior basal body ciliated (Figs. 3A, 4A, H–J). Perizonal stripe composed of closely spaced dikinetids arranged in four rows, longer than

adoral zone anteriorly, rows 1–3 closely-spaced, separated from row 4 by gap, dikinetids of rows 1 and 2 parallel to kinety axis, those of rows 3 and 4 obliquely inclined, never form false kineties (Figs. 3B–D, 4E–H). Dikinetids of perizonal stripe and most dome kineties have both basal bodies cili-

**Table 2.** Morphometric data for *Urostomides caducus*, Idaho strains ACADBLUFF and ACADGLEN.

Characteristic <sup>a</sup>	Strain	Method <sup>b</sup>	Mean	M	SD	CV	Min	Max	n
Body, length	ACADBLUFF	in vivo	84.0	83.0	8.44	10.0	71.0	97.0	20
		P	69.0	70.0	3.95	5.7	59.0	77.0	25
	ACADGLEN	P	77.0	76.5	13.21	17.2	58.0	100.0	12
Body, width <sup>c</sup>	ACADBLUFF	in vivo	58.1	59.0	5.66	9.7	47.0	67.0	20
		P	49.1	49.0	5.68	11.6	36.0	62.0	25
	ACADGLEN	P	59.2	60.0	7.67	13.0	45.0	74.0	12
Body, length-width, ratio	ACADBLUFF	in vivo	1.4	1.5	0.07	4.7	1.3	1.5	20
		P	1.4	1.4	0.13	9.4	1.1	1.6	25
	ACADGLEN	P	1.3	1.3	0.13	9.8	1.1	1.5	12
Anterior pole to posterior end of adoral zone, distance	ACADBLUFF	in vivo	63.4	63.0	7.48	11.8	53.0	77.0	20
		P	48.6	49.0	3.55	7.3	41.0	55.0	25
	ACADGLEN	P	55.6	53.5	12.2	21.9	35.0	76.0	12
Distance anterior pole to posterior end of adoral zone:body length, %	ACADBLUFF	in vivo	75.6	75.0	4.85	6.4	67.0	83.0	20
		P	70.4	70.0	3.26	4.6	63.0	78.0	25
	ACADGLEN	P	71.8	73.5	5.70	7.9	57.0	78.0	12
Anterior pole to posterior end of macronucleus, distance	ACADBLUFF	in vivo	56.5	57.0	7.09	12.6	46.0	69.0	20
		P	43.8	45.0	6.18	14.1	31.0	53.0	25
	ACADGLEN	P	55.7	51.5	11.66	21.0	41.0	80.0	12
Distance anterior pole to posterior end of macronucleus:body length, %	ACADBLUFF	in vivo	67.3	67.5	5.50	8.2	57.0	78.0	20
		P	63.7	65.0	8.32	13.1	45.0	76.0	25
	ACADGLEN	P	72.1	72.5	6.61	9.2	60.0	81.0	12
Anterior pole to anterior end of adoral zone, distance	ACADBLUFF	P	21.3	22.0	2.08	9.7	16.0	24.0	25
		ACADGLEN	P	26.3	26.0	4.22	16.1	22.0	36.0
	ACADGLEN	P	34.5	34.5	4.08	11.8	30.0	40.0	12
Macronucleus, length	ACADBLUFF	in vivo	21.3	21.0	1.87	8.8	18.0	26.0	20
		P	18.0	18.0	1.53	8.5	15.0	21.0	25
	ACADGLEN	P	22.6	23.5	3.20	14.2	19.0	29.0	12
Macronucleus, width	ACADBLUFF	in vivo	19.2	19.5	1.99	10.4	15.0	22.0	20
		P	16.4	16.0	1.86	11.3	13.5	21.0	25
	ACADGLEN	P	19.9	19.5	3.85	19.3	14.0	29.0	12
Micronucleus, length	ACADBLUFF	P	4.1	4.0	0.47	11.3	3.5	5.0	19
	ACADGLEN	P	4.6	4.0	0.86	19.0	4.0	6.5	10
Adoral membranelles, number	ACADBLUFF	P	77.0	78.0	4.01	5.2	67.0	83.0	25
	ACADGLEN	P	84.4	85.0	4.13	4.9	76.0	90.0	9
Somatic kineties, number <sup>d</sup>	ACADBLUFF	P	33.4	35.0	3.51	10.5	27.0	38.0	23
	ACADGLEN	P	37.2	37.0	1.71	4.6	34.0	40.0	12
Preoral dome kineties, number	ACADBLUFF	P	7.0	7.0	0.00	0.0	7.0	7.0	25
	ACADGLEN	P	7.0	7.0	0.00	0.0	7.0	7.0	12
Paroral membrane, length <sup>e</sup>	ACADBLUFF	P	25.7	25.5	2.26	8.8	22.0	30.0	22
	ACADGLEN	P	27.5	27.5	2.07	7.5	25.0	30.0	8
Perizonal ciliary stripe rows, number	ACADBLUFF	P	4.0	4.0	0.00	0.0	4.0	4.0	25
	ACADGLEN	P	4.0	4.0	0.00	0.0	4.0	4.0	12

Table 2 (Continued)

Characteristic <sup>a</sup>	Strain	Method <sup>b</sup>	Mean	M	SD	CV	Min	Max	n
Caudal cilia dikinetids, number	ACADBLUFFACADGLEN	P	12.0	12.0	1.26	10.5	10.0	15.0	20
	ACADGLEN	P	13.2	14.0	2.22	16.8	9.0	16.0	9
Caudal cilia, length	ACADBLUFF	in vivo	49.4	51.0	5.09	10.2	34.0	57.0	19

<sup>a</sup>All distances in μm.<sup>b</sup>Measurements and counts (in vivo) made from digital images using calibrated software, (P) made from formalin-fixed protargol-impregnated permanent preparations using ocular micrometer.<sup>c</sup>Measured from right cell margin to left edge of preoral dome.<sup>d</sup>Posterior body kinetics plus dome kineties, excluding perizonal stripe rows.<sup>e</sup>Measured as the chord. CV, coefficient of variation (%); M, median; Max, maximum value; Min, minimum value; n, number of cells studied; P, protargol; SD, standard deviation of the mean.Table 3. Morphometric data for *Urostomides campanula*, Idaho strain ACAMTR.

Characteristic <sup>a</sup>	Method <sup>b</sup>	Mean	M	SD	CV	Min	Max	n
Body, length	in vivo	38.6	39.0	3.45	8.9	33.0	46.0	24
	P	40.1	40.5	5.31	13.2	30.0	51.0	40
Body, width <sup>c</sup>	in vivo	33.2	33.0	2.74	8.2	29.0	40.0	24
	P	35.4	35.0	4.49	12.7	27.0	44.0	40
Body, length-width, ratio	in vivo	1.2	1.2	0.06	5.3	1.0	1.3	24
	P	1.1	1.1	0.08	7.1	1.0	1.4	40
Anterior pole to posterior end of adoral zone, distance	in vivo	25.0	24.0	3.19	12.8	20.0	31.0	24
	P	28.4	27.5	4.26	15.0	21.0	40.0	40
Distance anterior pole to posterior end of adoral zone:body length, %	in vivo	64.8	63.5	5.31	8.2	56.0	64.8	24
	P	70.8	70.0	5.22	7.4	61.0	82.0	40
Anterior pole to posterior end of macronucleus, distance	in vivo	23.2	22.0	2.95	12.7	19.0	31.0	22
	P	25.0	25.0	4.35	17.4	18.0	38.0	40
Distance anterior pole to posterior end of macronucleus:body length, %	in vivo	60.0	59.0	7.16	11.9	46.0	76.0	22
	P	62.3	62.0	6.56	10.5	48.0	75.0	40
Anterior pole to anterior end of adoral zone, distance	P	25.7	24.0	5.77	22.5	18.0	38.0	38
Distance anterior pole to anterior end of adoral zone:body length, %	P	64.1	61.5	10.06	15.7	46.0	90.0	38
Macronucleus, length	in vivo	13.7	13.0	2.43	17.7	12.0	23.0	22
	P	11.1	11.0	1.01	9.1	9.0	13.0	40
Macronucleus, width	in vivo	12.1	12.0	2.65	21.9	9.0	22.0	22
	P	10.3	10.0	0.94	9.2	9.0	12.0	40
Micronucleus, length	P	2.9	3.0	0.35	11.9	2.0	4.0	38
Adoral membranelles, number	P	32.6	33.0	2.19	6.7	26.0	36.0	35
Somatic kineties, number <sup>d</sup>	P	12.8	13.0	1.24	9.8	11.0	15.0	32
Preoral dome kineties, number	P	5.0	5.0	0.00	0.0	5.0	5.0	40
Paroral membrane, length <sup>e</sup>	P	12.1	12.0	2.79	23.0	8.0	18.0	30
Perizonal ciliary stripe rows, number	P	4.0	4.0	0.00	0.0	4.0	4.0	40
Length of midventral adoral membranelle base	P	6.2	6.0	0.96	15.6	4.0	8.0	38

<sup>a</sup>All distances in μm.<sup>b</sup>Measurements and counts (in vivo) made from digital images using calibrated software, (P) made from formalin-fixed protargol-impregnated permanent preparations using ocular micrometer.<sup>c</sup>Measured from right cell margin to left edge of preoral dome.<sup>d</sup>Posterior body kineties plus dome kineties, excluding perizonal stripe rows.<sup>e</sup>Measured as the chord. CV, coefficient of variation (%); M, median; Max, maximum value; Min, minimum value; n, number of cells studied; P, protargol; SD, standard deviation of the mean.

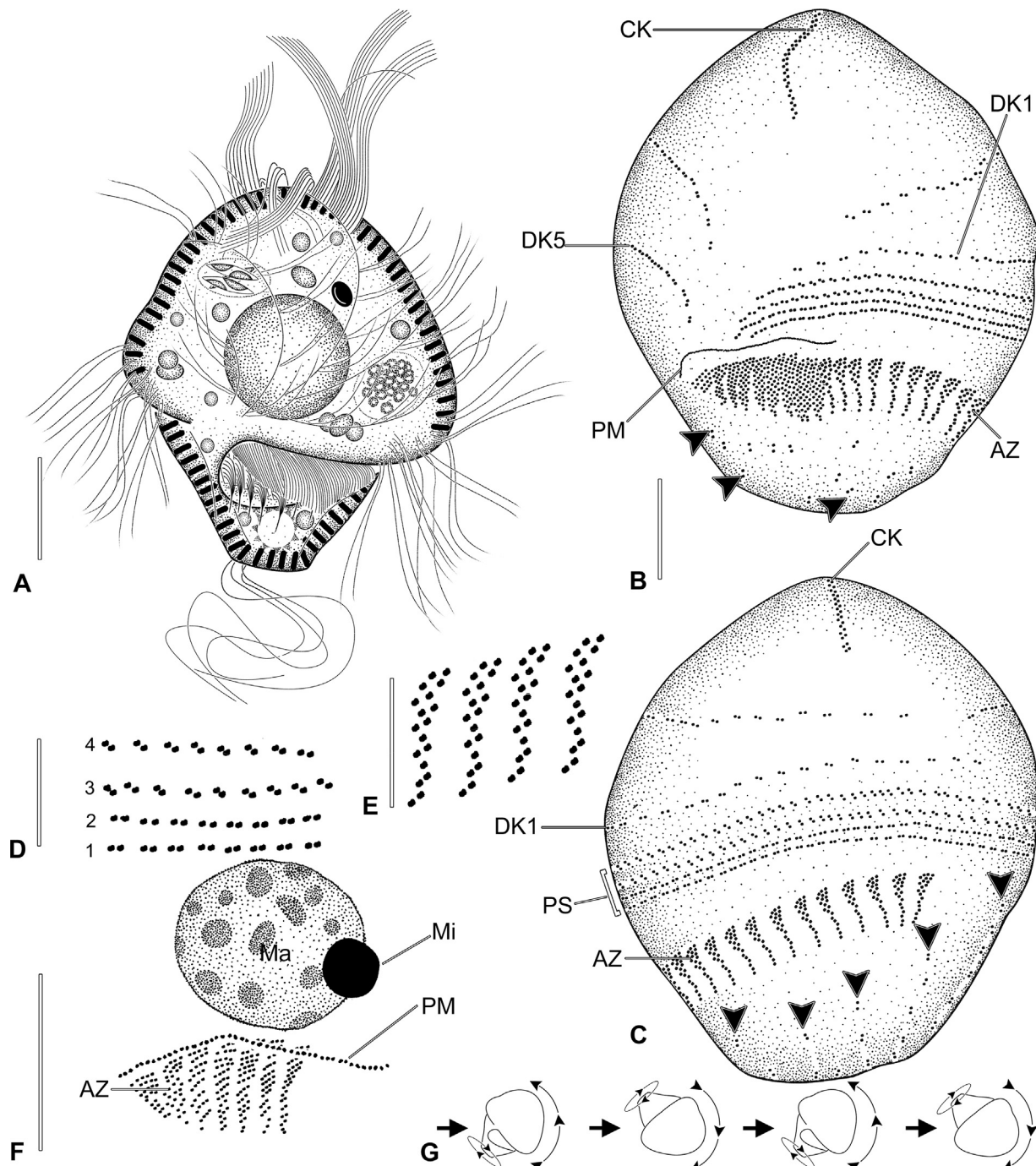


**Fig. 3. (A–G)** *Urostomides campanula* comb. nov., Idaho population (ACAMTR) from life (A, G) and after protargol impregnation (B–F). (A) Ventral view of a representative specimen. (B, C) Ventral (B) and dorsal (C) view of same specimen showing reduced postoral kinetics (arrowheads). Preoral dome kinety 3, the “crown” kinety (CK) is comprised of closely spaced inclined dikinetids that give rise to membranelle-like adherent syncilia. (D) Structure of the four-rowed perizonal ciliary stripe. Row 1 lies along the margin of the preoral dome, row 4 lies between row 3 and dorsal kinety 5. (E) Structure of membranelles from mid-portion of the adoral zone. (F) Detail of proximal part of buccal area. (G) Schematic of characteristic swimming motion (see description). AZ, adoral zone; CK, “crown” preoral dome kinety; DK1 and 5, preoral dome kineties 1 and 5; Ma, macronucleus; Mi, micronucleus; PM, paroral membrane; PS, perizonal ciliary stripe; 1–5, perizonal ciliary stripe rows 1–5. Scale bars: 10 µm (A–C, F), 5 µm (D, E).

ated. Dikinetids of dome normally spaced except specialized row 3 where dikinetids are densely spaced in zigzag arrangement (Figs. 3B, C, 4E–J). Cilia of preoral dome kineties often

form syncilia, dome kinety 3 thigmotactically specialized, cilia about 20 µm long, adhere to form sagittal pseudomembrane (Figs. 3A, 4H–J). Nonmotile caudal cilia grouped in

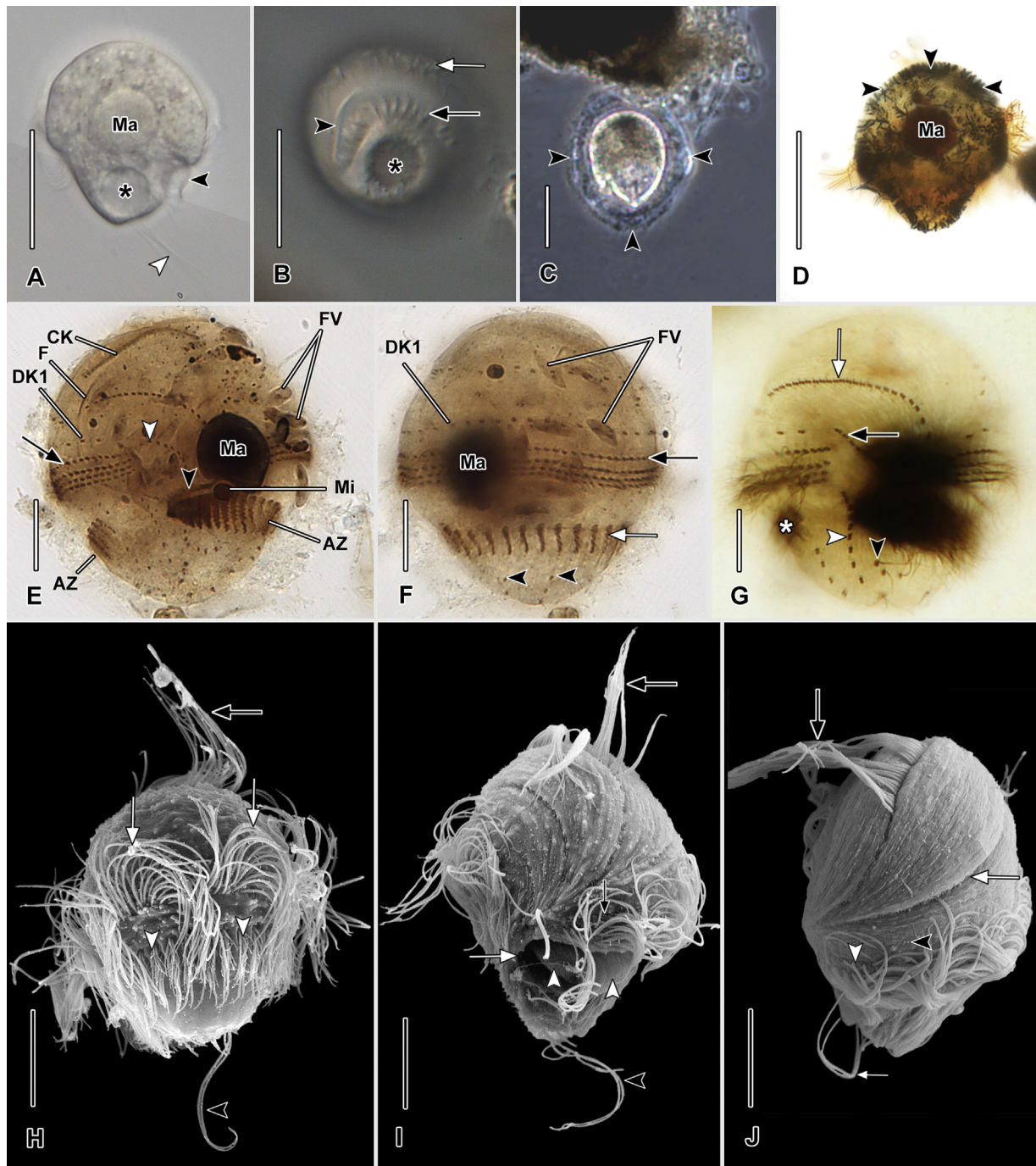


**Fig. 4.** (A–J) *Urostomides campanula*, comb nov., Idaho population (ACAMTR) from life (A, B, differential interference contrast; C, phase contrast), after silver carbonate impregnation (D, brightfield), protargol impregnation (E–G, brightfield), and in scanning electron microscope (H–J). (A) Optical section showing paroral membrane (black arrowhead), caudal cilia (white arrowhead), and contractile vacuole (asterisk). (B) Posterior view showing perizonal stripe cilia (white arrow), adoral membranelles (black arrow), paroral membrane (black arrowhead), and contractile vacuole (asterisk). (C) Distressed individual forming mucous sheath (black arrowheads). (D) Rounded rod-shaped extrusomes (black arrowheads) impregnate with silver carbonate but not protargol (cf. E–G). (E) Ventral aspect (stacked image) showing perizonal stripe row 4 (black arrow), distal end of preoral dome kinety 1 (white arrowhead), and the paroral membrane (black arrowhead). (F) Dorsal view of same specimen as (E) showing perizonal stripe row 4 (black arrowhead), adoral membranelles (white arrowhead), and shortened postoral kinetics (black arrowheads). (G) Posterior view showing perizonal stripe row 1 (white arrow) and adoral zone (black arrow). (H) Dorsal view showing metachronal waves of perizonal stripe cilia (white arrows), adoral membranelles (white arrowheads), syncilia of preoral dome kinety 3, the membrane-like “crown” kinety (black arrow), and the elongated caudal cilia (black arrowhead). The caudal cilia are quite fragile and are often lost during processing. (I) Ventral view showing the paroral membrane (white arrowheads), the proximal margin of the buccal cavity

eccentric tuft at right margin of posterior end, about 30  $\mu\text{m}$  long (Figs. 3A, 4A, H–J).

Adoral zone comprises 33 membranelles on average (range 26–36), begins on ventral surface and ends at same level on right margin (i.e. horizontally oriented, makes about 270° turn around long axis), proximal end not enclosed in buccal cavity (Figs. 3A, B, F, 4B, E–J). Proximal-most membranelle rhomboidal, next seven or eight membranelles longest, composed of four long rows of basal bodies (Figs. 3B, F, 4B, E, I); mid adoral zone membranelles about 6  $\mu\text{m}$  long, composed of three rows of steeply inclined basal bodies with three basal bodies in triangular array to the left of anterior end of membranelle (Fig. 3B, C, E). Paroral membrane stichomonad, originates in, but protrudes only slightly from, buccal cavity at posterior end of adoral zone (Figs. 3A, B, E, 4I). Cytopharyngeal fibers inconspicuous, curve anteriorly from cytostome into preoral dome (Fig. 4E).

**Occurrence and ecology** (Table 1). A single population was collected from bottom sediments of a commercial freshwater plant aquaculture tub with a dense growth of *Typha angustifolia*, *Oenanthe* sp., *Lemna* sp. and abundant water snails in Boise, Idaho, during July 2015. Sample site characteristics included: pH 6.50 and salinity 407  $\mu\text{S}/\text{cm}$  (260 mg/L). Food includes purple sulfur bacteria (*Lamprocystis* sp.) and green algae.

**Voucher material.** One slide with protargol-impregnated specimens is deposited in the Biology Centre of the Upper Austrian Museum in Linz, Austria. Relevant specimens are marked on the slide with black ink circles.

***Urostomides darwini* (Kahl, 1927) comb. nov.** (original combination *Metopus darwini* Kahl, 1927) (Figs. 5A–H, 6A–M, Tables 1 and 4)

**Improved diagnosis based on the Idaho strain ADARBOT, the original and subsequent descriptions** (Kahl 1927, 1932): Body size about 80–130 × 35–50  $\mu\text{m}$  in vivo. Body outline clavate, laterally compressed. Preoral dome massive, wider than posterior body. Body immediately posterior to preoral dome obconical, right surface with bulbous protuberance, ends in ciliated, narrowly tapered tail. Usually 25 ciliary rows, ten of which are widely spaced in deep cortical furrows on preoral dome. Preoral dome granule aggregate absent. Inconspicuous elongated cilia on tail. Perizonal ciliary stripe same length as adoral zone, never arranged in false kineties. Adoral zone steeply oblique, composed of about 54 adoral membranelles, makes ≥ 360° turn around long axis, begins at posterior margin of preoral dome, ends subapically.

#### Description of Idaho population ADARBOT.

**Remarks.** The lateral compression of this species presents some problems in precisely determining anatomic directions (i.e. ventral, dorsal, lateral) since the posterior end of the

adoral zone is usually displaced onto the narrowest aspect of the cell and thus defines this as the ventral surface (Bourland and Wendell 2014). However, since there is variability in the lateral compression there can be some minor ambiguity in defining this morphologic aspect (Figs. 1H, 2K–M).

Size in vivo 81–132 × 35–50  $\mu\text{m}$  and in protargol-impregnated specimens 71–116 × 20–53  $\mu\text{m}$ . Body outline clavate with slightly curved, acutely tapered tail, preoral dome laterally compressed about 1.5:1. Length:width ratio including preoral dome about 2.5:1 in lateral view. Preoral dome massive, asymmetric, dorsal margin convex, left margin more or less straight, anterior end bluntly rounded, dome occupies about 50% of body length, originates and ends on ventral surface; dome brim forms thickened, glabrous lip proximally, overhangs adoral zone, (Fig. 6A–D, K–M). Body posterior to preoral dome attenuate, right surface bears short protuberant keel with posteriorly convergent cortical furrows (Figs. 5A–C, H, 6A–D, G, H, K–M). Macronucleus globular, in preoral dome, chromatin finely granular, scattered 2–3  $\mu\text{m}$  diameter nucleoli. Micronucleus planoconvex, flat side adjacent to macronucleus, about 5  $\mu\text{m}$  in length (Figs. 5A–C, E, 6A, B, G, H). Contractile vacuole in mid posterior body portion at base of tail, excretory pore not observed (Figs. 5A, 6A–D). Cytopype not observed. Extrosomes inconspicuous, fine rods 1.5–2.0  $\mu\text{m}$  long, colorless in vivo but form thin, refractive peripheral fringe, do not stain with methyl green-rhodamine B or protargol, explode to form mucus coat around distressed cells (Figs. 5F, 6B, F). Cortex slightly flexible, kinetal furrows prominent, more widely spaced in preoral dome. Cortical granules about 1  $\mu\text{m}$  diameter, in about eight loosely arranged interkinetal rows, stain pink with methyl green-rhodamine B (Fig. 6E). Cytoplasm colorless, numerous approximately 3.5  $\mu\text{m}$  refractive globules, anterior granule aggregate absent. Food vacuoles sparse (Fig. 5A). Swims at moderate pace; rotates on long axis.

On average, 25 (range 22–27) somatic kineties, posterior body kineties spiral slightly to end of tail except for shortened kineties of keel region on right surface (Fig. 6K–M), 10 or 11 more widely-spaced dome kineties, none obviously specialized (Figs. 5A–C, 6G, H, K–M). Ordinary somatic cilia and preoral dome cilia about 10  $\mu\text{m}$  long in vivo, perizonal stripe cilia about 15  $\mu\text{m}$  long in vivo, about six 30  $\mu\text{m}$  long posterior cilia, easily overlooked (Fig. 6A). Perizonal stripe invariably composed of dikinetids arranged in four rows, same length as adoral zone, rows almost equidistant, dikinetids only slightly inclined, never form false kineties (Figs. 5B, C, G, 6G, H). Dikinetids of perizonal stripe and most dome kineties have both basal bodies ciliated. Dikinetids of dome kineties ordinarily spaced (Figs. 5A–C, 6E, F, I–K). Dome kineties bear scattered syncilia (Figs. 5A, 6K–M).

(white arrow), the syncilia of the “crown” kinety (black arrow), and the caudal cilia (black arrowhead). (J) Anterodorsal view showing the “crown” kinety (black arrow), dikinetids of preoral dome kinety 5, the cilia of which have been lost in processing (white arrow), perizonal stripe row 4 (white arrowhead), and the caudal cilia (small white arrow). AZ, adoral zone; CK, “crown” kinety (preoral dome kinety 5); DK5, preoral dome kinety 5; F, pharyngeal fibers; FV, algae-containing food vacuoles; Ma macronucleus; Mi, micronucleus. Scale bars: 50  $\mu\text{m}$  (C), 25  $\mu\text{m}$  (A, B, D), 10  $\mu\text{m}$  (E–J).

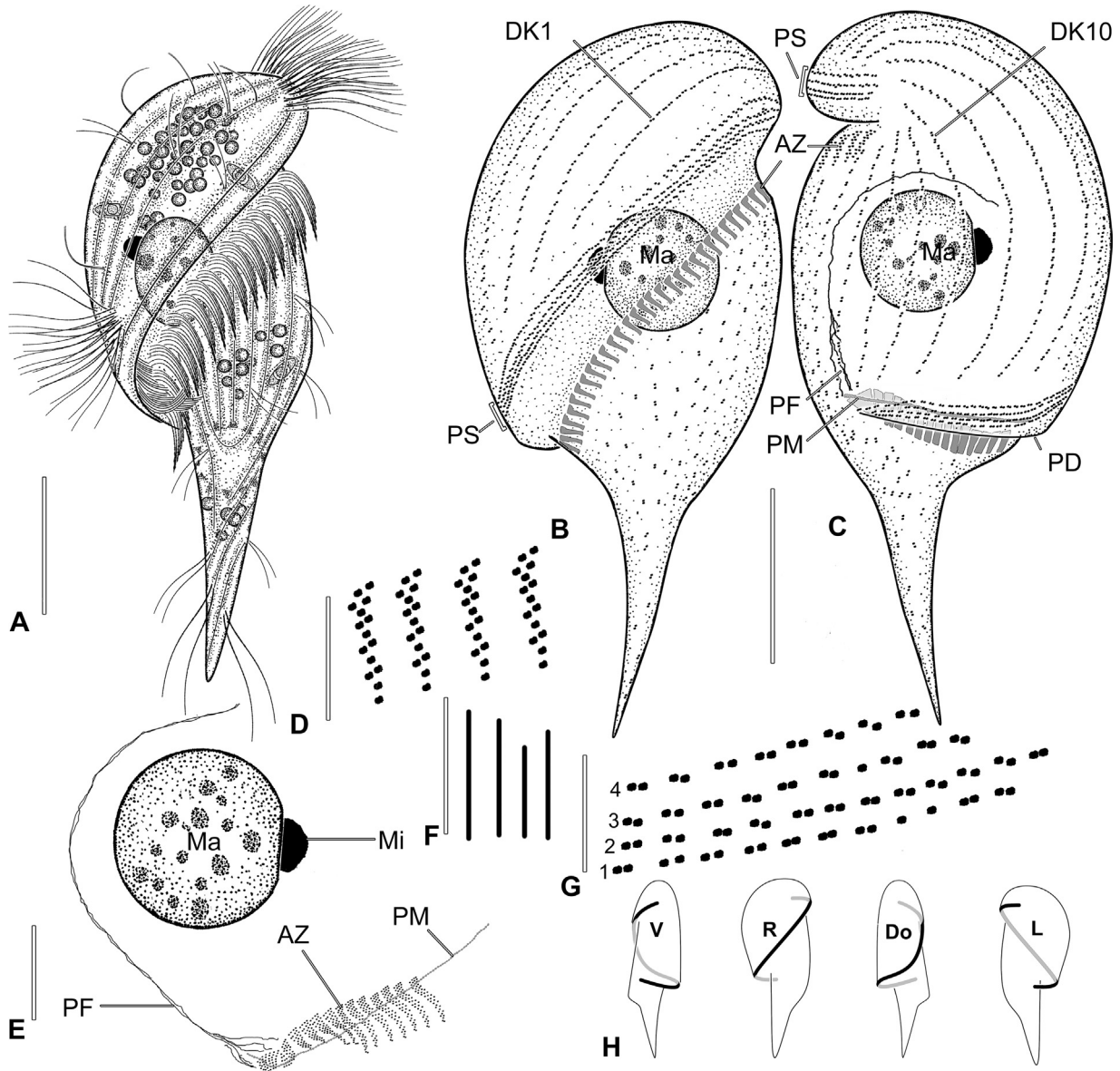


**Fig. 5.** (A–H) *Urostomides darwini* comb. nov., Idaho population (ADARBOT) from life (A, H) and after protargol impregnation (B–G). (A) Right lateral view of a representative specimen. (B, C) Right (B) and left lateral (C) views. (D) Structure of membranelles from mid-portion of the adoral zone. (E) Detail of proximal part of buccal region. (F) Extrusomes. (G) Structure of the four-rowed perizonal ciliary stripe. Row 1 lies near the margin of the preoral dome, row 4 lies between row 3 and preoral dome kinety 1. (H) Schematic showing the course of the perizonal ciliary stripe as the cell is rotated on the long axis leftward in 90° increments. AZ, adoral zone; DK1, 10, preoral dome kineties 1 and 10; Do, dorsal; L, left; Ma, macronucleus; Mi, micronucleus; PD, margin of preoral dome; PF, pharyngeal fibers; PM, paroral membrane; PS, perizonal ciliary stripe; R, right; V, ventral. Scale bars: 25 µm (A–C), 10 µm (E), 5 µm (D, G), 2.5 µm (F).

Adoral zone comprises about 54 (range 50–63) membranelles, begins and ends on left surface, makes  $\geq 360^\circ$  spiral around long axis, level of posterior and anterior ends of adoral zone about 30 µm apart, anterior end partly enclosed in buccal cavity, most of its length roofed by preoral dome (Figs. 5C, E, 6H, K, M). Proximal-most 13 membranelles rectangular to triangular, composed of three or four rows of basal bodies (Fig. 5E); membranelles longest (about 6 µm) in mid-portion of adoral zone, composed of three rows of steeply inclined basal bodies with three basal bodies in triangular

array to the left of anterior end of membranelle (Fig. 5D). Paroral membrane stichomonad, originates in, and protrudes only slightly from buccal cavity, extends onto undersurface of preoral dome (Figs. 5C, E, 6K, M). Cytopharyngeal fibers curve anteriorly from cytostome into preoral dome (Fig. 5C, E).

**Morphogenesis** (Fig. 6I, J). Only one post divider (probable proter daughter cell) was found in protargol preparations. The limited observations suggest that (1) division likely occurs in the free-swimming state. (2) Spiralization of the oral

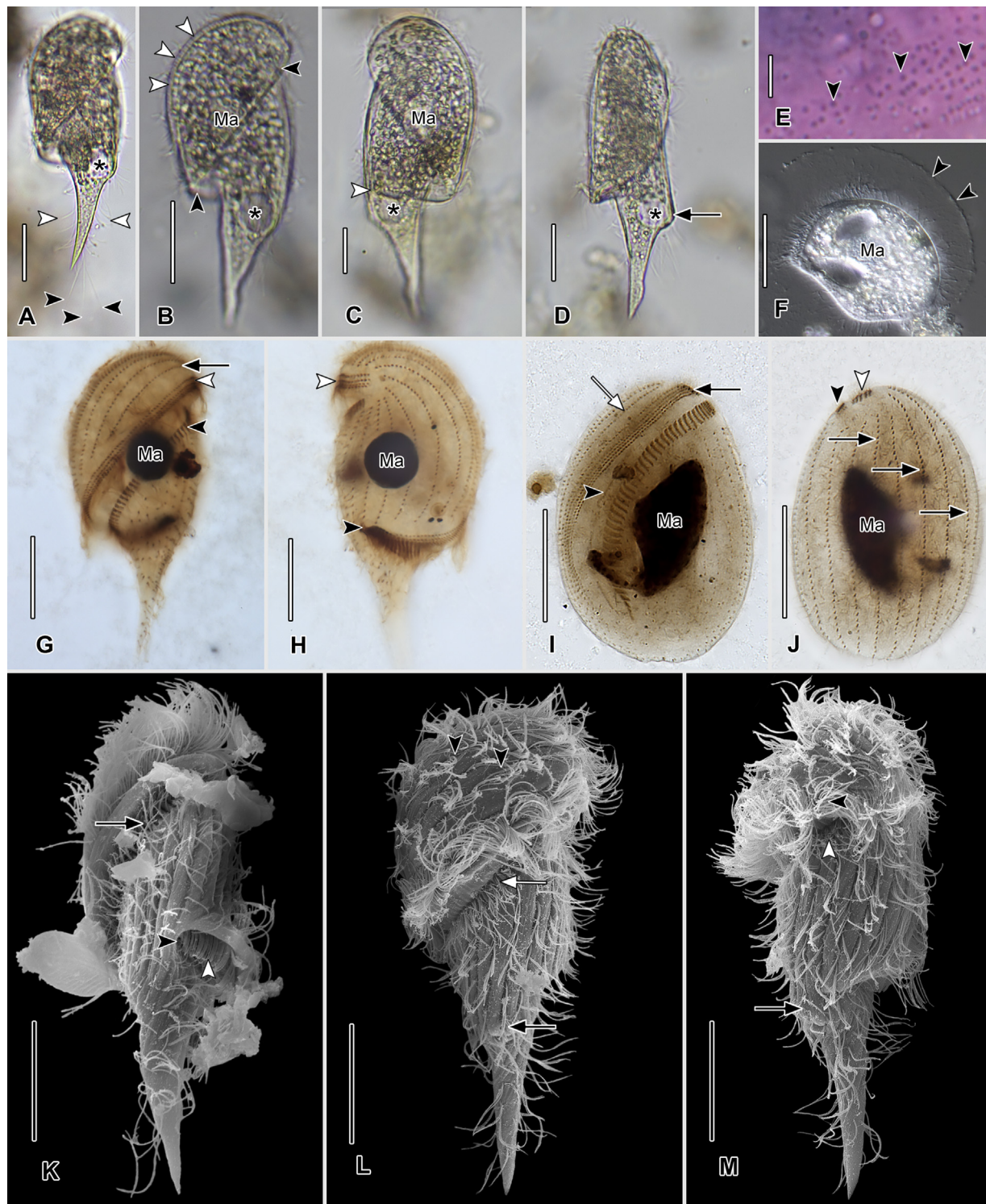


**Fig. 6.** (A–M) *Urostomides darwini* comb. nov., Idaho population (ADARBOT) from life (A–D, brightfield; F, differential interference contrast), after methyl green–rhodamine B staining (E), after protargol impregnation (G–J), and in scanning electron microscope (K–M). (A) Right dorsolateral view showing ordinary somatic cilia (white arrowheads) and elongated posterior cilia (black arrowheads). (B) Right lateral view showing margin of preoral dome (black arrowheads), extrusome layer (white arrowheads), and contractile vacuole (asterisk). (C) Left lateral view showing level of the cytostome (white arrowhead). (D) Dorsal view showing the protuberant pellicular protuberance (black arrow) and contractile vacuole (asterisk). (E) Cortical granules. (F) Distressed individual with mucous sheath (black arrowheads). (G) Right lateral view showing preoral dome kinety 1 (black arrow), perizonal ciliary stripe (white arrowhead), and adoral zone (black arrowhead). (H) Left ventrolateral view showing anterior part of perizonal ciliary stripe (white arrowhead) and the posterior end of the adoral

structures occurs rather late in morphogenesis. (3) The perizonal ciliary stripe appears five-rowed in early post-dividers, indicating that the right-most row migrates onto the dome to become the left-most dome kinety. (4) The new paroral is at least partially resorbed (i.e. shortened) in late post-division. (5) Achievement of the distinctive body shape would appear to be a late post-division event (i.e. the formation of the tail in proter cells and, probably, the preoral dome in opisthe cells, respectively).

**Occurrence and ecology.** The ADARBOT population was collected from bottom sediments of a lentic, man-made stream bordered by *Typha latifolia* at the Idaho Botanical Garden in Boise, Idaho during May 2016. The diet of *U. darwini* includes green algae and purple sulfur bacteria.

**Voucher material.** One slide with protargol-impregnated specimens is deposited in the Biology Centre of the Upper Austrian Museum in Linz, Austria (accession no. 2017265). Relevant specimens are marked on the slide with black ink circles.

***Urostomides bacillatus* (Levander, 1894) comb. nov.** (original combination *Metopus bacillatus* Levander, 1894) (Figs. 7A–F, 8I–J, Tables 1 and 5)

**Improved diagnosis based on population ABACBLUFF, original description (Levander 1894), and redescription by Kahl (1932):** Body size about  $65–100 \times 45–65 \mu\text{m}$  in vivo, obpyriform, broadly ellipsoidal in cross-section. Preoral dome broadly rounded, wider than posterior body portion, slightly overhangs left margin. Posterior body obconical, more or less triangular in cross-section, not tail-like, with elongated caudal cilia. Usually 21 ciliary rows, eight of which are widely spaced on preoral dome, none obviously specialized. Perizonal ciliary stripe not arranged in false kineties. Adoral zone steeply oblique, makes  $<180^\circ$  turn around long axis, usually about 54 adoral membranelles.

**Description of population ABACBLUFF.** Size in vivo  $84–98 \times 50–64 \mu\text{m}$ , in protargol-impregnated specimens  $65–95 \times 42–66 \mu\text{m}$ . Shape obpyriform, variable dorsoventral flattening from minimal to 1.4:1. Length:width ratio including preoral dome about 1.5:1 in protargol-impregnated specimens. Preoral dome broadly rounded, right margin convex, left anterior margin projects beyond left margin, dome occupies about two-thirds of body length, dome brim broad, glabrous, overhangs entire adoral zone. Body posterior to preoral dome obconical, more or less triangular in cross-section, posterior end rounded to obliquely truncate, not tail-like, right margin slightly concave, left margin slightly convex (Figs.

7A–C, 8A–H). Macronucleus 15–27  $\mu\text{m}$  in length, globular to reniform, located in anterior half of body, chromatin finely granular, many nucleoli of 1.5–3.0  $\mu\text{m}$  in diameter. Micronucleus ellipsoidal, relatively large, about 6  $\mu\text{m}$  long in vivo, 4.5  $\mu\text{m}$  long in protargol-impregnated specimens (Figs. 7A–C, 8A–F). Contractile vacuole subterminal, excretory pore not observed, may empty via cytopygae (Figs. 7A, 8A–C). Cytopygae subterminal, on ventral surface (Fig. 8H, I). Extrusomes narrowly ellipsoidal to oblong, 2–3  $\mu\text{m}$  long, colorless in vivo but form distinct refractive peripheral fringe in vivo, do not stain with methyl green-rhodamine B or protargol, ejection with mucus coat formation not observed (Figs. 7A, D, 8J). Cortex slightly flexible, kinetal furrows conspicuous in dome, very shallow in posterior body, cortical granules absent. Cytoplasm colorless, contains scattered refractive 2  $\mu\text{m}$  diameter globules, anterior granule aggregate absent (Fig. 8A, B). Food vacuoles up to 20  $\mu\text{m}$  diameter (Fig. 5A). Swims at moderate pace, rotates on long axis.

Twenty-three somatic kineties on average (range 21–25); about 15 kineties converge at posterior body end, posterior-most dikinetids usually bear about 12 elongated caudal cilia, invariably eight widely-spaced dome kineties, none obviously specialized (Figs. 7A–C, 8D–H). Ordinary somatic cilia and preoral dome cilia about 10  $\mu\text{m}$  long in vivo, perizonal stripe cilia about 13  $\mu\text{m}$  in vivo, elongated posterior cilia about 30  $\mu\text{m}$ . Perizonal stripe, same length as adoral zone posteriorly, slightly longer anteriorly, rows 1–3 equidistant, separated from row 4 by gap, dikinetids of rows 1–3 only slightly inclined if at all, row 4 dikinetids inclined, perizonal stripe dikinetids never form “false kineties”. Dikinetids of perizonal stripe and most dome kineties have both basal bodies ciliated. Dikinetids of dome kineties ordinarily spaced. Dome kineties often bear syncilia (Figs. 7B, C, 8D–H).

Adoral zone comprises about 42 membranelles (range 32–47), begins at right margin of ventral surface, extends obliquely about 20  $\mu\text{m}$  more anteriorly to left side of dorsal surface (i.e. makes  $<180^\circ$  turn around long axis), only a few posterior membranelles enclosed in buccal cavity. Posterior-most membranelle triangular; remaining membranelles composed of three rows of steeply inclined basal bodies with three basal bodies in triangular array to the left of anterior end of membranelle, proximal part of adoral zone makes 180° anticlockwise rotation as it descends into buccal (Figs. 7B, C, E, 8G). Paroral membrane originates in and protrudes only slightly from buccal cavity, extends to undersurface of preoral dome (Figs. 7A, B, 8A, D, G, H). Cytopharyngeal fibers curve anteriorly from cytostome into

zone (black arrowhead). (I) Ventral view of probable proter post-divider showing the peripheral-most dome kinety (white arrow), the long paroral membrane (black arrowhead), and what appears to be a perizonal stripe comprised of five rows (black arrow). It is unclear whether the fifth row migrates rightward to become dome kinety 1 or is resorbed. The tail region has not yet formed. (J) Dorsal view of same specimen showing dome kineties (black arrows), the anterior part of the adoral zone (black arrowhead), and the anterior part of the perizonal stripe (white arrowhead). (K) True ventral view showing lateral body compression and the posterior buccal margin (black arrowhead), the paroral membrane (white arrowhead), and the adoral membranelles (black arrow). (L) Right lateral view showing dome kineties (black arrowheads), adoral membranelles (white arrow), and the protuberant pellicular keel (black arrow). (M) Right ventrolateral view showing perizonal stripe cilia (black arrowhead), adoral membranelles (white arrow), and the protuberant pellicular keel (black arrow). Ma, macronucleus. Scale bars 25  $\mu\text{m}$  (A–D, F–M), 2.5  $\mu\text{m}$  (E).

**Table 4.** Morphometric data *Urostomides darwini*, Idaho population ADARBOT.

Characteristic <sup>a</sup>	Method <sup>b</sup>	Mean	M	SD	CV	Min	Max	n
Body, length	in vivo	112.5	120.5	19.9	17.7	81.0	132.0	10
	P	94.4	99.5	13.3	14.1	71.0	116.0	22
Body, width <sup>c</sup>	in vivo	44.7	46.0	4.37	9.8	35.0	50.0	10
	P	39.4	38.0	8.00	20.3	20.0	53.0	22
Body, length-width, ratio	in vivo	2.5	2.6	0.09	12.2	2.0	3.0	10
	P	2.4	2.3	0.37	15.0	2.0	3.6	22
Posterior spine, length	in vivo	34.8	40.5	14.32	41.2	15.0	54.0	10
	P	30.0	30.0	5.74	19.1	20.0	41.0	22
Posterior spine length-body length ratio (%)	in vivo	30.0	31.0	9.11	30.5	15.0	43.0	10
	P	31.7	32.0	4.0	12.6	25.0	39.0	22
Base of spine, width	in vivo <sup>c</sup>	12.6	12.0	1.65	13.1	10.0	15.0	10
	P <sup>c</sup>	8.4	8.0	1.05	12.5	6.0	10.0	22
Anterior pole to posterior end of adoral zone, distance	in vivo	65.0	64.0	7.57	11.6	54.0	76.0	10
	P	47.4	48.0	7.67	16.2	35.0	59.0	22
Distance anterior pole to posterior end adoral zone-body length, %	in vivo	59.0	58.0	7.22	12.3	50.0	69.0	10
	P	50.3	50.5	4.67	9.3	37.0	58.0	22
Anterior pole to posterior end of macronucleus, distance	in vivo	49.7	50.5	3.4	6.8	45.0	54.0	10
	P	43.3	43.0	6.38	14.7	31.0	55.0	22
Distance anterior pole to posterior end of macronucleus:body length, %	in vivo	45.1	42.0	6.66	14.8	39.0	58.0	10
	P	46.2	47.0	5.76	12.5	36.0	54.0	22
Anterior pole to anterior end of adoral zone, distance	P	15.8	15.0	2.94	18.6	10.0	22.0	22
	P	16.7	16.0	2.0	11.8	14.0	22.0	22
Macronucleus, length	in vivo	19.5	19.5	4.5	10.9	16.0	23.0	10
	P	17.3	17.0	2.49	14.4	13.5	22.0	22
Macronucleus, width	in vivo	17.2	17.0	2.25	13.1	14.0	22.0	10
	P	16.1	15.0	2.71	16.8	12.0	21.0	22
Micronucleus, length	P	5.0	5.0	0.38	7.6	4.0	6.0	20
	P	54.0	53.0	3.49	6.4	50.0	63.0	19
Somatic kinetics, number <sup>d</sup>	P	25.1	26.0	1.42	5.7	22.0	27.0	21
	P	10.8	11.0	0.40	3.7	10.0	11.0	21
Preoral dome kinetics, number	P	22.7	23.0	3.76	16.6	16.0	29.0	18
	P	4.0	4.0	0.00	0.0	4.0	4.0	22
Perizonal ciliary stripe rows, number	P	5.5	5.0	0.54	9.9	5.0	6.5	17

<sup>a</sup>All distances in  $\mu\text{m}$ .<sup>b</sup>Measurements and counts (in vivo) made from digital images using calibrated software, (P) made from formalin-fixed protargol-impregnated permanent preparations using ocular micrometer.<sup>c</sup>Measured from right cell margin to left edge of preoral dome.<sup>d</sup>Posterior body kinetics plus dome kinetics, excluding perizonal stripe rows.<sup>e</sup>Measured as the chord. CV, coefficient of variation (%); M, median; Max, maximum value; Min, minimum value; n, number of cells studied; P, protargol; SD, standard deviation of the mean.

preoral dome (Figs. 7B; 8E). Resting cysts, conjugants and dividers not observed.

**Description of population STAN5 (Table 5).** Since this population closely matches the ABACBLUFF population in general appearance, only noteworthy differences are included here: The STAN5 population is smaller than the ABACBLUFF population ( $50\text{--}81 \times 37\text{--}53 \mu\text{m}$

in vivo,  $50\text{--}76 \times 31\text{--}48 \mu\text{m}$  in protargol-impregnated specimens). It also has fewer adoral membranelles (32 vs. 42 on average), fewer somatic kinetics (18 vs. 23 on average), one less dome kinety (7 vs. 8), and a shorter paroral membrane (10 vs. 18  $\mu\text{m}$  long on average). There is overlap in most measurements and meristics except for length and width.

**Table 5.** Morphometric data for *Urostomides bacillatus*, Idaho strain ABACBLUFF and Canadian strain STAN5.

Characteristic <sup>a</sup>	Strain	Method <sup>b</sup>	Mean	M	SD	CV	Min	Max	n
Body, length	ABACBLUFF	in vivo	90.9	91.0	5.09	5.6	84.0	98.0	10
		P	76.0	75.0	7.27	9.6	65.0	95.0	41
	STAN5	in vivo	66.4	67.9	8.23	12.4	49.9	81.2	23
		P	62.6	61.8	7.14	11.4	50.2	75.7	15
Body, total width <sup>c</sup>	ABACBLUFF	in vivo	56.1	55.5	4.04	7.2	50.0	64.0	10
		P	51.1	50.0	5.76	11.3	42.0	66.0	41
	STAN5	in vivo	46.0	47.2	4.28	9.3	37.0	53.1	23
		P	40.2	39.9	5.30	13.2	30.6	47.6	15
Body, length-width, ratio	ABACBLUFF	in vivo	1.6	1.6	0.11	7.0	1.4	1.8	10
		P	1.5	1.5	0.13	8.6	1.3	1.8	41
	STAN5	in vivo	1.4	1.5	0.11	7.8	1.2	1.7	23
		P	1.6	1.6	0.11	7.3	1.4	1.8	15
Anterior BE to posterior end of adoral zone, distance	ABACBLUFF	in vivo	58.7	57.0	3.87	6.6	52.0	64.0	9
		P	50.1	49.0	5.24	10.5	43.0	63.0	41
	STAN5	in vivo	50.9	51.7	7.53	14.8	29.4	65.8	23
		P	44.0	43.3	5.14	11.7	34.7	54.8	15
Distance anterior BE to posterior end adoral zone-body length, ratio in %	ABACBLUFF	in vivo	64.0	63.0	5.00	7.2	57.0	64.2	9
		P	66.0	65.0	4.23	6.4	60.0	80.0	41
	STAN5	in vivo	76.5	76.9	5.75	7.5	58.9	85.9	23
		P	70.4	71.8	4.32	6.1	56.7	76.1	15
Anterior BE to posterior end of macronucleus, distance	ABACBLUFF	in vivo	46.7	47.0	2.54	5.4	44.0	52.0	10
		P	41.0	40.0	5.08	12.4	33.0	55.0	41
	STAN5	in vivo	40.4	39.9	5.93	14.7	29.4	53.5	23
		P	37.8	37.6	4.03	10.7	32.1	45.2	15
Distance anterior BE to posterior end macronucleus:body length, ratio in %	ABACBLUFF	in vivo	51.2	50.5	3.00	5.9	48.0	56.0	10
		P	53.9	54.0	4.04	7.5	46.0	65.0	41
	STAN5	in vivo	61.1	58.7	6.34	10.4	50.5	77.8	23
		P	60.5	60.6	2.20	3.6	57.0	64.9	15
Anterior BE to anterior end of adoral zone, distance	ABACBLUFF	in vivo	26.3	26.0	3.57	13.6	19.0	31.0	9
		P	29.2	30.0	3.54	12.1	20.0	36.0	41
	STAN5	in vivo	32.0	31.6	4.44	13.9	21.0	41.1	23
		P	34.5	34.1	4.88	14.1	26.3	43.0	15
Distance anterior BE to anterior end of adoral zone:body length, ratio in %	ABACBLUFF	in vivo	29.1	31.0	4.00	13.5	22.0	35.0	9
		P	38.8	39.0	3.40	8.8	27.0	47.0	41
	STAN5	in vivo	48.4	47.4	5.72	11.8	41.7	70.6	23
		P	55.2	55.0	5.12	9.3	47.6	70.3	15
Macronucleus, length	ABACBLUFF	in vivo	24.3	24.0	1.49	6.2	22.0	27.0	10
		P	19.5	19.0	2.22	11.4	15.0	27.0	41
	STAN5	in vivo	15.0	14.9	1.95	13.0	10.8	20.1	23
		P	15.5	15.2	1.60	10.3	12.8	18.4	15
Macronucleus, width	ABACBLUFF	in vivo	21.3	20.5	2.31	10.8	18.0	26.0	10
		P	18.6	19.0	2.15	11.6	15.0	27.0	41
	STAN5	in vivo	15.5	15.3	3.12	20.1	10.4	23.0	23
		P	15.5	15.2	1.32	8.5	13.5	18.2	15
Micronucleus, length	ABACBLUFF	in vivo	6.2	6.2	0.43	7.0	5.6	6.8	8
		P	4.5	4.5	0.61	13.6	3.0	6.5	40
	STAN5	in vivo	5.7	5.4	0.67	11.9	4.8	7.2	23
		P	4.3	4.2	0.67	15.6	3.2	6.2	15
Adoral membranelles, number	ABACBLUFF	P	42.3	42.0	3.16	7.5	32.0	47.0	33
		STAN5	P	32.5	33.0	3.48	10.7	28	39

Table 5 (Continued)

Characteristic <sup>a</sup>	Strain	Method <sup>b</sup>	Mean	M	SD	CV	Min	Max	n
Length of longest adoral membranelle base	ABACBLUFF	P	5.8	6.0	0.70	11.9	5.0	7.0	32
	STAN5	P	3.9	4	0.37	9.4	3	4.4	15
Somatic kinetics, number <sup>d</sup>	ABACBLUFF	P	23.4	24.0	1.12	4.8	21.0	25.0	41
	STAN5	P	18.2	18	1.83	10.1	15	21	15
Preoral dome kinetics, number	ABACBLUFF	P	8.0	8.0	0.00	0.0	8.0	8.0	40
	STAN5	P	7.0	7.0	0.00	0.0	7.0	7.0	15
Paroral membrane, length <sup>e</sup>	ABACBLUFF	P	18.3	18.0	2.15	11.7	14.0	23.0	41
	STAN5	P	9.7	9.5	2.92	30.1	4.3	15.3	15
Perizonal ciliary stripe rows, number	ABACBLUFF	P	4.0	4.0	0.00	0.0	4.0	4.0	41
	STAN5	P	4.0	4	0.00	0.0	4	4	15
Caudal cilia, length	ABACBLUFF	in vivo	28.1	28.5	3.6	12.8	24.0	33.0	8
	STAN5	in vivo	18.2	17.4	5.94	32.6	8.1	28.6	15

<sup>a</sup>All distances in µm.<sup>b</sup>Measurements and counts (in vivo) made from digital images using calibrated software, (P) made from formalin-fixed protargol-impregnated permanent preparations using ocular micrometer or QuickPhoto software, Promicra, CZ.<sup>c</sup>Measured from right cell margin to left edge of preoral dome.<sup>d</sup>Includes dome kinetics but excludes perizonal ciliary stripe rows.<sup>e</sup>Measured as the chord. BE, body end; CV, coefficient of variation; (%); Max, maximum value; M, median; Min, minimum value; n, number of cells studied; P, protargol; SD, standard deviation of the mean.

**Occurrence and ecology.** *Urostomides bacillatus* was collected from bottom sediments at the same site as *U. caducus* and also from sediments from Beaver Lake in Vancouver, Canada during August, 2015 (STAN5). Our populations fed on purple sulfur bacteria and small green algae.

**Voucher material.** One slide with protargol-impregnated specimens is deposited in the Biology Centre of the Upper Austrian Museum in Linz, Austria (accession no. 2017263). Relevant specimens are marked on the slide with black ink circles.

***Urostomides striatus* (McMurrich, 1884) Jankowski, 1964** (original combination *Metopus striatus* McMurrich, 1884) (Figs. 9A–G, 10A–J, Tables 1 and 6)

**Improved diagnosis based on Idaho strain ASTRTUB, Czech Republic strain RAJ2AN and the original description (McMurrich 1884):** Body size about 80–90 × 40–50 µm in vivo, more or less clavate. Preoral dome broadly rounded, slightly overhangs left margin. Posterior body tapers into narrow tail. About 16 ciliary rows on average, five to seven of which are widely spaced on preoral dome, none obviously specialized, inconspicuous elongated caudal cilia. Perizonal ciliary stripe never arranged in false kinetics. Adoral zone oblique, makes <180° turn around long axis, begins at posterior preoral dome, ends on left dorsal surface about 30 µm anterior to proximal end of adoral zone, usually about 40 adoral membranelles.

**Remarks.** Jankowski (1964a) created the subgenus *Metopus* (*Urostomides*) and later (Jankowski 2007) elevated it to genus rank with *Metopus striatus* McMurrich, 1884 as type species. The confusing circumstances of McMurrich's identification of *Metopus striatus* must be mentioned here in that

he refers in the formal description of *M. striatus* (McMurrich 1884) to an earlier description of an unnamed “normal form” (McMurrich 1883), and, inexplicably, represents it (Plate 1, Fig. 1) with a drawing of what is obviously a *Paramecium* species. Whether the illustration was provided in error or whether McMurrich actually mistook a *Paramecium* species for a “form” of the species he subsequently illustrated and described as a “shortened form” and named as *Metopus striatus* (McMurrich 1884) is unclear. His reference (McMurrich 1883) to an “anterior (contractile) vesicle” supports the latter possibility.

**Description of Idaho strain ASTRTUB (listed as *Metopus striatus* Acc. No. KF607085 in GenBank) and Czech Republic strain RAJ2AN and the original description (McMurrich 1884).**

Size in vivo 80 × 50 µm, in protargol-impregnated specimens 60–90 × 21–59 µm in vivo and about 77 × 43 µm after protargol impregnation. Cells hyaline. Shape broadly clavate, posterior end tapers to slender rounded tail, body laterally compressed 2:1. Length:width ratio including preoral dome about 1.8:1 in lateral view. Preoral dome broadly rounded, right margin convex, left anterior margin projects beyond left margin, dome occupies about two-thirds of body length, dome brim narrow, rounded, preoral dome overhangs entire adoral zone. Body posterior to preoral dome slender, tapered, right margin slightly concave, left margin flat to slightly convex (Figs. 9A–C, 10A–J). Macronucleus 16 × 14 µm in diameter in protargol preparations, globular to slightly ovoid, located in anterior half of body, chromatin coarsely granular, many 1–2 µm diameter nucleoli in protargol preparations. Micronucleus 4 µm in diameter on average in protargol-impregnated specimens, ellipsoidal to planocon-

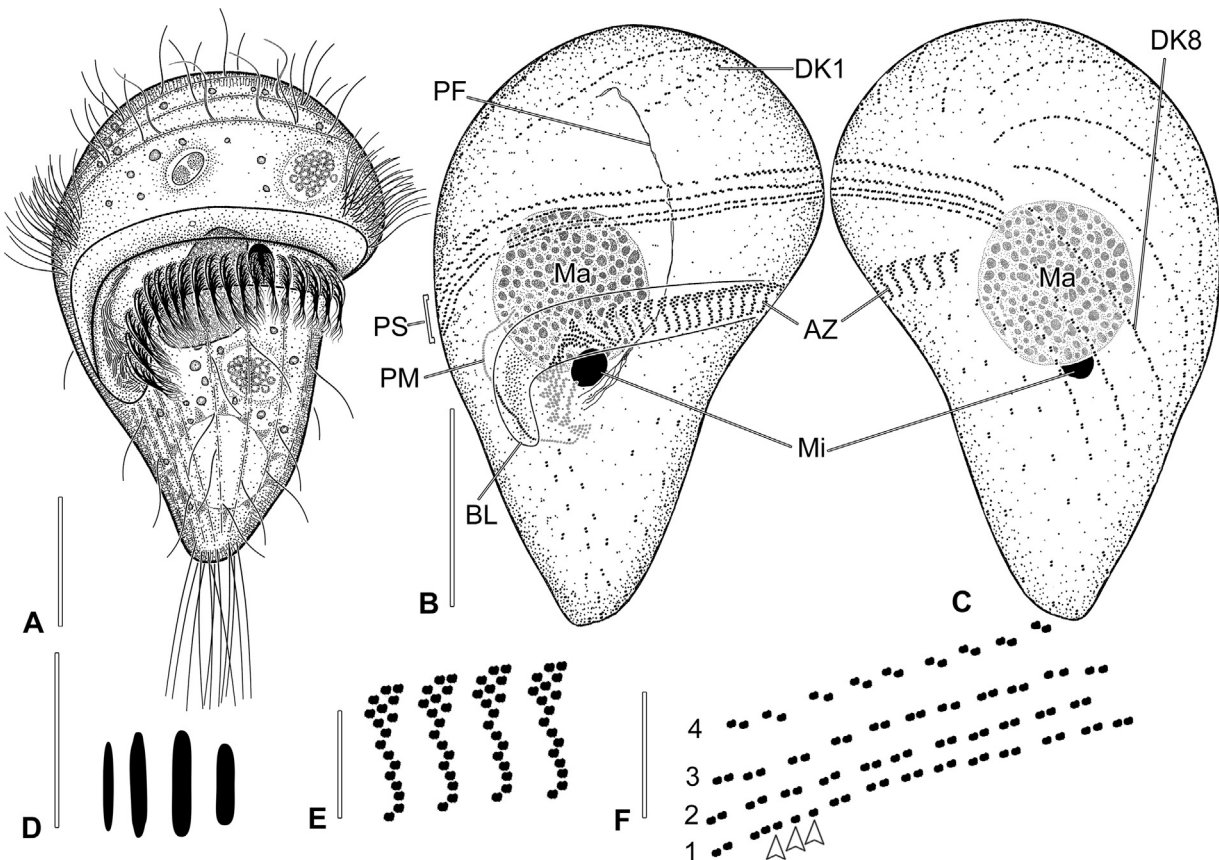


**Fig. 7.** (A–F) *Urostomides bacillatus*, comb. nov., Idaho population (ABACBLUFF) from life (A) and after protargol impregnation (B–F). (A) Ventral view of a representative specimen. (B, C) Ventral (B) and dorsal (C) view of same specimen. (D) Extrusomes. (E) Structure of membranelles from mid-portion of the adoral zone. (F) Structure of the four-rowed perizonal ciliary stripe. Row 1 lies along the margin of the preoral dome, row 4 lies between row 3 and dome kinety 1. Single basal bodies (arrowheads) are sometimes found in row 1. AZ, adoral zone; BL, buccal lip; DK1 and 8, preoral dome kineties 1 and 8; Ma, macronucleus; Mi, micronucleus; PF, pharyngeal fibers; PM, paroral membrane; PS, perizonal ciliary stripe. Scale bars: 25 µm (A–C), 5 µm (D–F).

vex, usually adjacent to macronucleus (Figs. 9A–C, 10A, C–G). Cytopype not observed. Contractile vacuole in mid-region of posterior body portion, excretory pore not observed (Figs. 9A, 10A, C, D). Cytoplasm colorless, contains scattered refractive 2 µm diameter globules (Fig. 10A). Cortex slightly flexible, kinetal furrows only in dome. Extrusomes oblong rods, 2–3 µm long, colorless in vivo, form distinct, dense, refractive peripheral fringe in vivo, appear as densely spaced 0.5 µm granules when cortex viewed en face, do not stain with methyl green–rhodamine B, stain inconsistently with protargol, but intensely with silver carbonate, ejection with mucus coat formation not observed (Figs. 9A, D, 10A, B). Food vacuoles up to 15 µm in diameter. (Fig. 9A). Swims at moderate pace; rotates on long axis.

Ordinary somatic cilia and preoral dome cilia about 10 µm long in vivo, perizonal stripe cilia about 15 µm in vivo, inconspicuous elongated posterior cilia. Sixteen somatic kineties on average (range 13–20); about eight posterior body kineties converge at posterior end, posterior-most dikinetids bear elongated cilia, five to seven widely-spaced dome kineties, none obviously specialized (Figs. 9A–C, 10B, E–J). Peri-

zonial stripe invariably composed of dikinetids arranged in four rows, about same length as adoral zone, dikinetids sometimes disorganized in proximal part, rows 1–4 more or less equidistant, dikinetids of rows 1, 2 oriented in axis of kineties, row 3, 4 dikinetids inclined, perizonal stripe dikinetids never form “false kineties”. Dikinetids of perizonal stripe and most dome kineties have both basal bodies ciliated. Dikinetids of dome kineties ordinarily spaced. Dome kineties often bear syncilia (Figs. 9A–C, F, 10E–G).

Adoral zone comprises about 39 membranelles (range 33–42), begins on ventral surface, extends obliquely about 28 µm more anteriorly to dorsal surface (i.e. makes <180° turn around long axis), only the first few membranelles enclosed in buccal cavity, membranelles composed of three rows of steeply inclined basal bodies with three basal bodies in triangular array to the left of anterior end of membranelle (Figs. 9A–C, E, G, 10A, C, E, H, I). Proximal part of adoral zone makes 180° anticlockwise rotation as it descends into buccal cavity as in *U. bacillatus* (Fig. 9G). Paroral membrane stichomonad, originates in and protrudes only slightly from buccal cavity, extends to undersurface of preoral dome

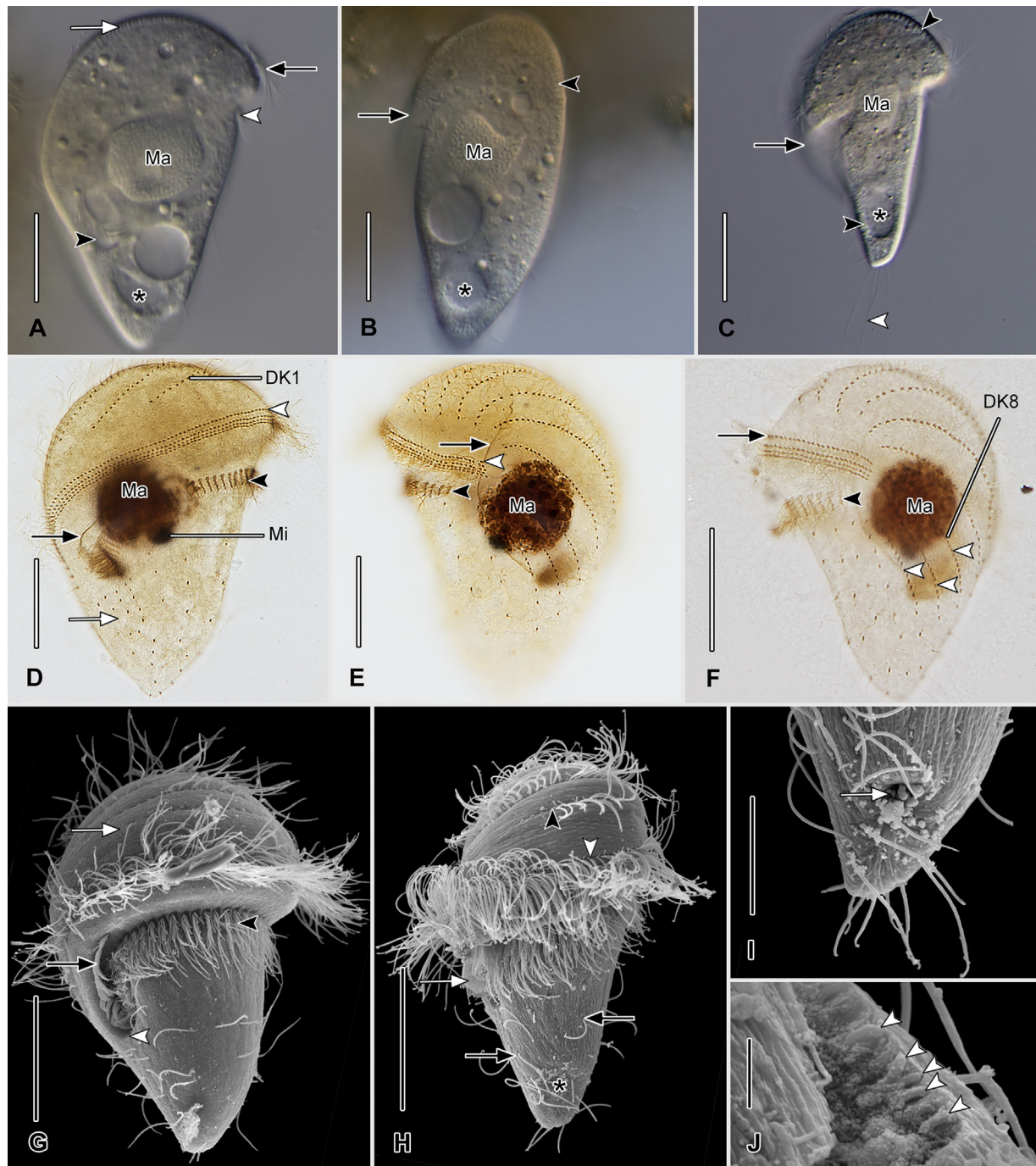


**Fig. 8.** (A–J) *Urostomides bacillatus* comb. nov., Idaho population (ABACBLUFF) from life (A–C, differential interference contrast), after protargol impregnation (D–F, brightfield), and in scanning electron microscope (G–J). (A) Optical section showing densely-spaced rod-shaped to slightly fusiform extrusomes (white arrow), perizonal stripe cilia (black arrow), adoral membranelle cilia (white arrowhead), the buccal cavity (black arrowhead), and the contractile vacuole (asterisk). (B) Optical section showing dorsoventral flattening, ventral margin of preoral dome (arrow), extrusome layer (black arrowhead), and the contractile vacuole (asterisk). (C) left ventrolateral view showing margin of preoral dome (arrow), extrusome layer (black arrowheads), and caudal cilia (white arrowhead). (D) Ventral view showing perizonal ciliary stripe row 4 (white arrowhead), the paroral membrane (black arrow), adoral membranelles (black arrowhead), and slightly disorganized, more closely spaced basal bodies of right postoral field (white arrow). (E) Dorsal view of same cell as (D) showing extra basal body near distal perizonal ciliary stripe (white arrowhead), pharyngeal fibers extending into preoral dome (black arrow) and distal end of adoral zone (black arrowhead). (F) Dorsal view showing perizonal ciliary stripe row 4 (black arrow), the distal end of the adoral zone (black arrowhead), and condensed kinetics to left of postoral field. The distal end of dome kinety 8 (DK8) is obscured by the macronucleus (Ma). (G) Ventral view showing dome kinety 8 (white arrow), paroral membrane (black arrow), posterior margin of buccal cavity (white arrowhead), and adoral membranelles

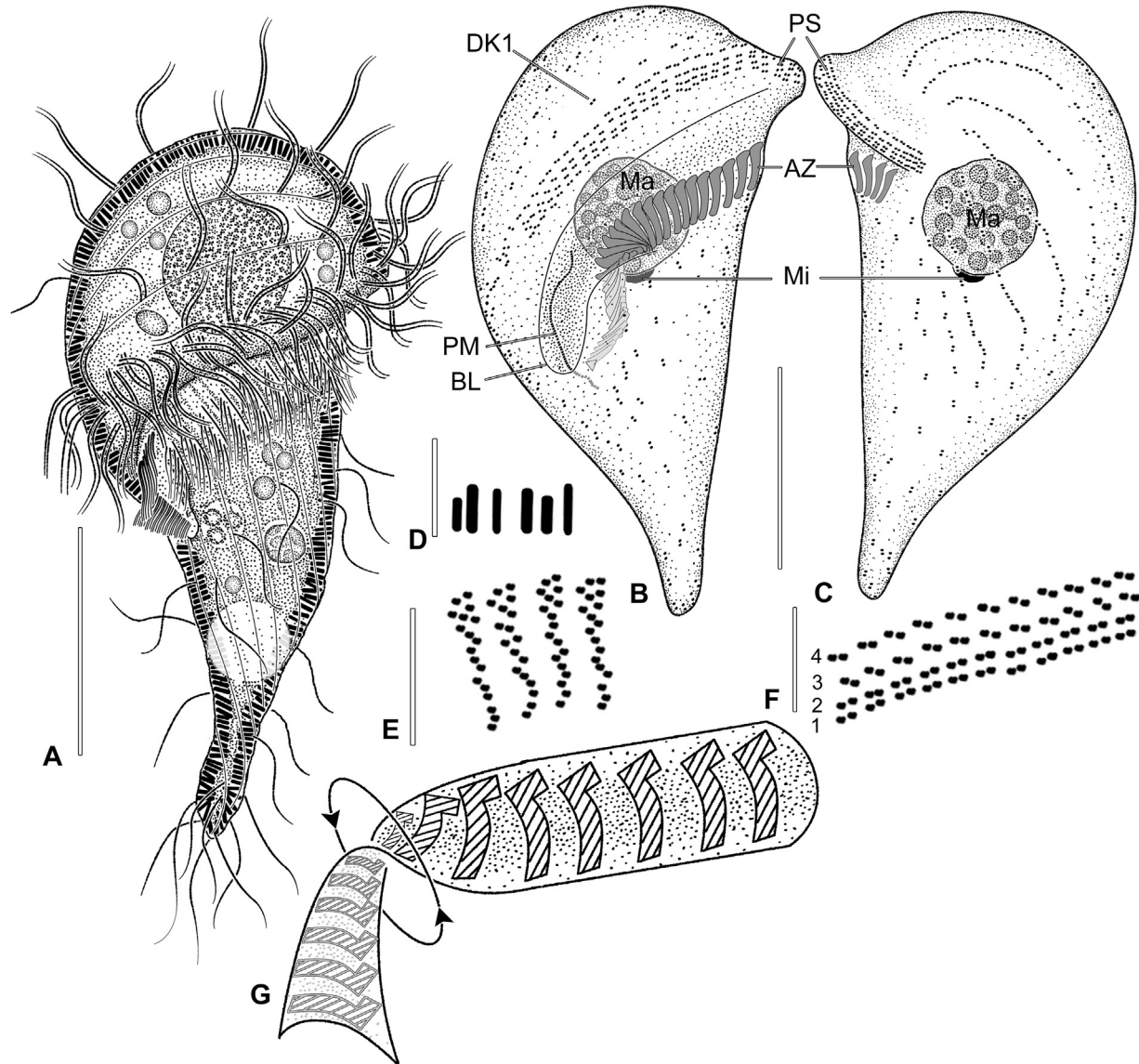


**Fig. 9.** (A–G) *Urostomides striatus*, Idaho population (ASTRTUB) from life (A) and after protargol impregnation (B–G). (A) Ventral view of a representative specimen. (B, C) Ventral (B) and dorsal (C) view of same specimen. (D) Extrusomes. (E) Structure of membranelles from mid-portion of the adoral zone. (F) Structure of the four-rowed perizonal ciliary stripe. Row 1 lies along the margin of the preoral dome, row 4 lies between row 3 and the most peripheral preoral dome kinety, e.g. DK1 (B). (G) Posterior part of adoral zone showing 180° anti-clockwise rotation (arrows) of the plane of the adoral zone as it enters the cell and deviates toward the dorsal surface. AZ, adoral zone; BL, buccal lip; DK1, preoral dome kinety 1; Ma, macronucleus; Mi, micronucleus; PM, paroral membrane; PS, perizonal ciliary stripe. Scale bars: 25 µm (A–C), 5 µm (D–F).

(Figs. 9A, B, 10A, E, H–J). Cytopharyngeal fibers curve anteriorly from cytostome into preoral dome, visible inconsistently in protargol preparations. Resting cysts, conjugants, and dividers not observed.

**Occurrence and ecology.** *Urostomides striatus* was collected from various sediments from ponds or streams in Europe, South and North America, as well as from bot-

tom sediments of a garden mesocosm described previously (Bourland et al. 2014), where the water is circumneutral (pH 6.53) and nonsaline (conductivity 117 µS/cm). The water level is maintained by tap water drip lines. The tub is exposed year-round to ambient conditions including precipitation, high summer temperatures (up to 43 °C), and winter freezing. Food includes purple sulfur bacteria and small green algae.

(black arrowhead). (H) Left lateral view showing dome kinety 8 (black arrowhead), perizonal stripe row 5 (white arrowhead), the paroral membrane (white arrow), singly ciliated postoral dikinetids (black arrows), site of the cytophyge (asterisk, cf. I). (I) Ventral view showing subterminal cytophyge (white arrow). (J) Fractured cell cortex revealing docked extrusomes (arrowheads). DK1, and 8, preoral dome kineties 1 and 8; Ma, macronucleus; Mi, micronucleus. Scale bars: 25 µm (A–H), 10 µm (I), 2 µm (J).

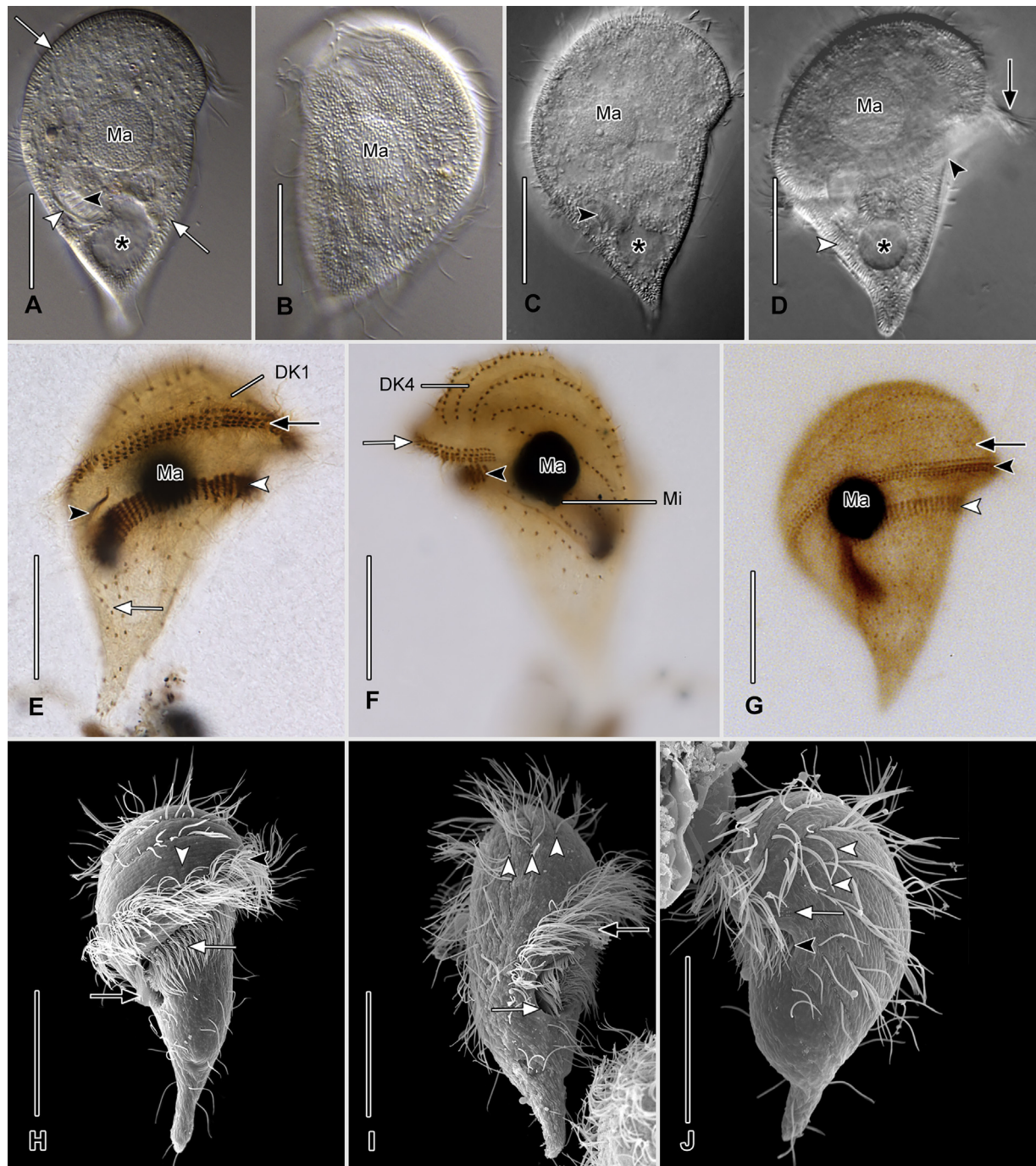


**Fig. 10. (A–J).** *Urostomides striatus*, Idaho population (ASTRTUB) (A, B, E–J), Czech Republic population (RADUŇ, C, D), and Croatian population (RAJ2AN, G) from life (A–D, differential interference contrast), after protargol impregnation (E–G, brightfield), and in scanning electron microscope (H–J). (A) Optical section showing subcortical layer of tightly-packed rod-shaped extrusomes (white arrows), proximal adoral membranelles (black arrowhead), paroral membrane (white arrowhead) and contractile vacuole (asterisk). (B) Surface view showing extrusomes. (C) Optical section showing contractile vacuole (asterisk) and buccal cavity (black arrowhead). (D) Ventral aspect showing extrusome layer (white arrowhead), cilia of perizonal stripe rows (black arrow), margin of preoral dome (black arrowhead), and contractile vacuole (asterisk). (E) Ventral view showing four-rowed perizonal ciliary stripe (black arrow), adoral zone (white arrowhead), paroral membrane, (black arrowhead), and slightly disorganized group of basal bodies in the right portion of the postoral field (white arrow). (F) Dorsal view showing distal end of adoral zone and the perizonal ciliary stripe (white arrow). (G) Left ventrolateral view showing peripheral-most preoral dome kinety (black arrow), perizonal ciliary stripe (black arrowhead), and adoral zone (white arrowhead). (H) Ventral view showing dome kinety 1 (white arrowhead), adoral membranelles (white arrow), and the paroral membrane (black arrow). (I) Right ventrolateral view showing dorsoventral flattening, preoral dome kineties (white arrowheads) and the proximal buccal margin or lip (white arrow).

**Brief description of Czech Republic strain RAJ2AN** (**Table 6**). Shape highly similar to the North American population, broadly clavate with tapered posterior tail region. Size about  $86 \times 42 \mu\text{m}$  in vivo,  $69 \times 38 \mu\text{m}$  after protargol impregnation. Cytostome located more anteriorly than in ASTRUB population (i.e. almost equatorial vs. between the middle and posterior one-third of the cell), but there is considerable overlap. The populations match well in terms of somatic kinety number (19 vs. 16), number of adoral membranelles (34 vs. 39), and number of dome kineties (7 in both populations on average).

**Voucher material.** One slide with protargol-impregnated specimens of strains ASTRUB is deposited in the Biology Centre of the Upper Austrian Museum in Linz, Austria (accession no. 2017268). Relevant specimens are marked on the slide with black ink.

***Urostomides denarius* (Kahl, 1927) comb. nov.** (original combination *Metopus bacillatus* var. *denarius* Kahl, 1927) (Figs. 11A–F, 12A–J, Tables 1 and 7)

**Remarks.** We studied the morphometry of population SUSBARB in vivo and in protargol impregnated specimens but the scanning electron microscopy (SEM) preparations of this strain were of mediocre quality (Tables 1 and 7). There was not enough protargol-impregnated material of strain MOLUKY4 for detailed morphometry, however the SEM preparations of this strain were of better quality (Fig. 12H–J). The 18S rRNA gene sequence was obtained from all eight cultured populations. Because both strains are from similar latitudes and habitat (i.e. fresh water) in the Paleotropis, and have 99.8% 18SrRNA gene sequence similarity we combine observations of the two populations.

**Improved diagnosis based on Malaysian strain SUSBARB, Indonesian strain MOLUKY4, and original description (Kahl 1927) and redescription by Kahl (1932):** Body size about  $35\text{--}57 \times 30\text{--}41 \mu\text{m}$  in vivo. Body shape round to almost *Maryna*-like. Preoral dome massive, slightly overhangs left margin. Posterior body obconical, posterior end rounded to truncate. Preoral dome granule aggregate absent. About 17 somatic kineties, five to seven usually six, extending onto preoral dome. Eccentric, elongated caudal cilia at right dorsolateral margin of posterior end. Perizonal ciliary stripe arranged in false kineties, longer than adoral zone anteriorly. Paroral stichomonad, proximal part parallel to long axis of cell. Adoral zone makes approximately  $220^\circ$  turn around long axis, composed of about 26 adoral membranelles. Smooth, flask-shaped resting cysts with neck like excystment apparatus.

**Description based on strains SUSBARB and MOLUKY4.** Body size about  $35\text{--}57 \times 25\text{--}40 \mu\text{m}$  in vivo, protargol-impregnated specimens  $35\text{--}50 \times 25\text{--}40 \mu\text{m}$ ; length:total width ratio 1.2:1 in protargol impregnations. Outline from round to almost *Maryna*-like. Preoral dome

broad, thick glabrous dome margin (Figs. 11A–C, 12A–I). Posterior body part rounded to obconical, depending on phase of contractile vacuole cycle. Macronucleus round, located in middle third of cell. Micronucleus round, to ellipsoidal, adjacent to macronucleus (Figs. 11A–C, 12A–I). Cytopype not observed. Contractile vacuole terminal, excretory pore appears as terminal crease (Fig. 12G–I). Cytoplasm colorless; anterior granule aggregate absent. Extrusomes tiny, about  $1 \mu\text{m}$ -long rounded rods, form less conspicuous subcortical fringe than in *U. striatus*, appear as tiny, densely packed granules when viewed en face (Figs. 11A–C, 12A–I). All populations form mucous sheath before dying. Food vacuoles up to  $7 \mu\text{m}$  in diameter. Swimming motion rapid.

About 17 somatic kineties composed of dikinetids, four to seven, usually six, extend onto preoral dome. Dome kinety 1 nearly transverse, sparsely ciliated, composed of four to ten, usually seven dikinetids (Fig. 12E). Dome kinety 2 nearly sagittal, densely ciliated especially anteriorly (Fig. 12F). Kineties slightly shortened posteriorly leaving small bare area (Fig. 11B). Right postoral kineties difficult to enumerate because somewhat disordered with occasional single dikinetids (Fig. 12E). Somatic cilia about  $7 \mu\text{m}$  long. Four to six caudal cilia from 17 to  $35 \mu\text{m}$  long. Perizonal ciliary stripe separated from peristomial groove by wide glabrous preoral dome brim composed of dikinetids arranged in about 50 false kineties (Fig. 11B). Perizonal stripe row 4 shortened by about six dikinetids at posterior end and two at anterior end (Fig. 12F). Perizonal ciliary stripe longer than adoral zone anteriorly (Fig. 12I).

Proximal part of adoral zone almost parallel to long axis of cell, distal three quarters nearly horizontal (Fig. 12A, E). Adoral zone originates in posterior one-fifth of the cell, makes  $<360^\circ$  turn around long axis, ends subapically, composed of 23–26 membranelles, proximal membranelles narrow triangular shape, enclosed in buccal cavity. (Figs. 11A–C, 12A–I). Midventral membranelles composed of four steeply inclined rows of three basal bodies with two shortened rows of two and one basal body at left anterior ends (Fig. 11B), separated by high intermembranellar ridges in SEM preparations (Fig. 12H). Cilia of adoral membranelles decrease from about  $8 \mu\text{m}$  to  $3 \mu\text{m}$  in length from posterior to anterior end of adoral zone in SEM preparations. Paroral J-shaped, stichomonad, about  $11 \mu\text{m}$  long, partially obscures buccal part of adoral zone (Fig. 12H–J). Resting cysts flask-shaped with distinct neck-like excystment apparatus (Fig. 12C, D).

**Occurrence and ecology** (**Table 1**). All populations of this species come from sediments of freshwater ponds, streams or rivers in Africa, Asia, and Europe. In the original description, Kahl (1932) mentions this species was found infrequently in Germany. This species is relatively frequent in tropical localities, where five of our seven strains were collected.

(J) Dorsal view showing syncilia (white arrowheads) of preoral dome kineties, basal bodies of the distal perizonal ciliary stripe (white arrow) and the distal margin of the peristomial area (black arrowhead). DK 1, 4 preoral dome kinety 1 and 4; Ma, macronucleus; Mi, micronucleus. Scale bars:  $25 \mu\text{m}$  (A–J).

All populations were observed to ingest bacteria. Strain SUSBARB contains fine rod-shaped endobionts that autofluoresce with UV light consistent with archaeal methanogens (Fig. 12G)

**Voucher material.** One slide with protargol-impregnated specimens of strain SUSBARB is deposited in the Biology Centre of the Upper Austrian Museum in Linz, Austria

(accession no. 2017269). Relevant specimens are marked on the slide with black ink.

***Urostomides pullus* (Kahl, 1927) comb. nov.** (original combination *Metopus bacillus* var. *pullus* Kahl, 1927) (Figs. 13A–E, 14A–J, Tables 1 and 8)

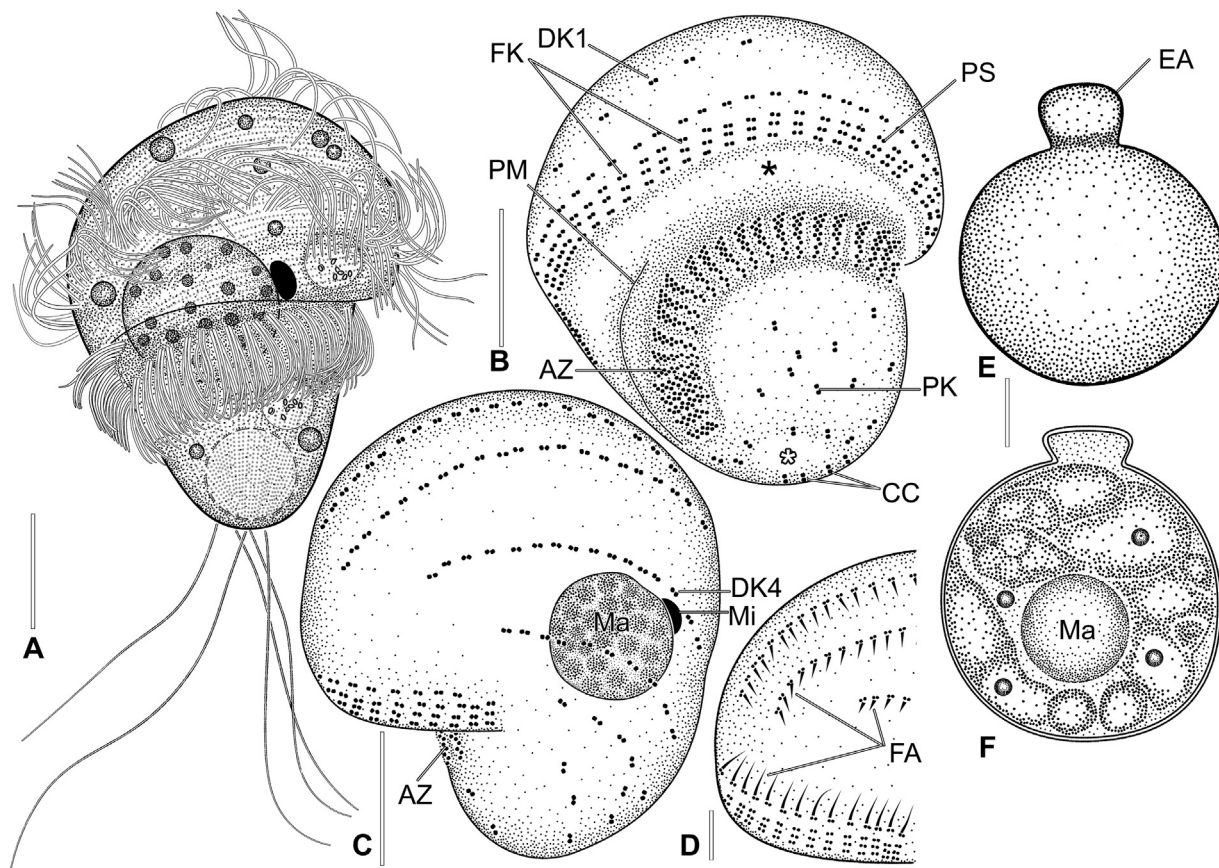
**Improved diagnosis based on Czech Republic strain KLAN2BC and original description (Kahl 1927)**

**Table 6.** Morphometric data for *Urostomides striatus*, Idaho strain ASTRTUB and Czech Republic strain RAJ2AN.

Characteristic <sup>a</sup>	Isolate	Method <sup>b</sup>	Mean	M	SD	CV	Min	Max	n
Body, length	ASTRTUB	P	76.9	75.0	9.00	11.6	60.0	90.0	15
	RAJN2AN	in vivo	86.4	85.9	8.41	9.7	74.8	106.7	17
		P	68.7	67.0	5.30	7.7	62.3	75.1	7
Body, total width <sup>c</sup>	ASTRTUB	P	43.4	45.0	8.21	18.9	21.0	59.0	15
	RAJN2AN	in vivo	42.1	43.0	7.02	16.7	31.0	53.6	10
		P	37.7	38.2	3.27	8.7	32.9	41.8	7
Body, length-width, ratio	ASTRTUB	P	1.8	1.7	0.38	21.0	1.6	3.1	15
	RAJN2AN	in vivo	2.1	2.1	0.46	21.7	1.5	2.9	17
		P	1.8	1.8	0.10	5.4	1.7	2.0	7
Anterior BE to posterior end of adoral zone, distance	ASTRTUB	P	49.6	48.0	4.48	9.0	45.0	60.0	15
	RAJN2AN	in vivo	34.6	34.8	4.74	13.7	26.7	47.2	17
		P	27.7	27.0	2.58	9.3	25.3	33.5	7
Distance anterior BE to posterior end adoral zone:body length, ratio in %	ASTRTUB	P	64.9	63.0	5.82	9.0	57.0	77.0	15
	RAJN2AN	in vivo	40.4	39.4	6.71	16.6	29.9	51.1	17
		P	40.4	40.0	2.64	6.5	37.2	44.6	7
Anterior BE to posterior end of macronucleus, distance	ASTRTUB	P	34.8	34.0	4.30	12.4	28.0	42.0	15
	RAJN2AN	in vivo	47.4	45.4	7.19	15.2	36.0	66.5	17
		P	35.3	35.7	3.40	9.6	29.6	39.1	7
Distance anterior BE to posterior end macronucleus:body length, ratio in %	ASTRTUB	P	45.4	43.0	4.61	10.2	40.0	55.0	15
	RAJN2AN	in vivo	54.7	53.9	5.98	10.9	46.0	74.6	17
		P	51.5	52.1	4.24	8.2	44.2	59.3	7
Anterior BE to anterior end of adoral zone, distance	ASTRTUB	P	21.6	22.0	5.00	23.0	13.0	30.0	15
	RAJN2AN	in vivo	63.1	61.7	7.13	11.3	50.3	74.6	17
		P	45.4	45.7	3.29	7.2	40.6	50.1	7
Distance anterior BE to anterior end adoral zone:body length, ratio in %	ASTRTUB	P	27.7	28.0	4.08	14.7	20.0	34.0	15
	RAJN2AN	in vivo	73.1	72.4	4.52	6.2	64.2	83.6	17
		P	66.1	66.7	2.19	3.3	62.1	68.8	7
Macronucleus, length	ASTRTUB	P	16.3	15.0	2.37	14.6	13.0	21.0	15
	RAJN2AN	in vivo	17.9	17.9	2.34	13.1	12.7	23.2	15
		P	13.2	13.4	0.71	5.4	11.8	14.1	7
Macronucleus, width	ASTRTUB	P	13.9	14.0	1.95	14.0	11.5	18.0	15
	RAJN2AN	in vivo	17.8	17.6	3.41	19.2	10.4	23.8	15
		P	12.3	12.1	1.27	10.3	11.0	14.6	7
Micronucleus, length	ASTRTUB	P	3.9	4.0	0.36	9.4	3.0	4.5	14
	RAJN2AN	in vivo	4.1	4.0	0.28	6.8	3.9	4.9	10
		P	3.4	3.4	0.42	12.3	2.9	4.0	7
Adoral membranelles, number	ASTRTUB	P	38.8	39.5	2.91	7.5	33.0	42.0	14
	RAJN2AN	P	34.4	37.0	4.20	12.2	28.0	39.0	7
Length of longest adoral membranelle base	ASTRTUB	P	5.6	5.5	0.44	7.8	5.0	6.0	11
	RAJN2AN	P	4.2	4.2	0.62	14.8	2.8	4.8	7
Somatic kineties, number <sup>d</sup>	ASTRTUB	P	16.5	16	1.73	10.5	13.0	20.0	12
	RAJN2AN	P	19.3	19.0	0.43	2.2	19.0	20.0	4

Table 6 (Continued)

Characteristic <sup>a</sup>	Isolate	Method <sup>b</sup>	Mean	M	SD	CV	Min	Max	n
Preoral dome kineties, number	ASTRTUB	P	6.8	7	0.58	8.5	5.0	7.0	14
	RAJN2AN	P	7.0	7	0.00	0.0	7.0	7.0	4
Paroral membrane, length <sup>c</sup>	ASTRTUB	P	15.9	15.0	2.36	14.8	12.0	22.0	15
	RAJN2AN	P	12.1	12.6	2.41	20.0	8.7	15.6	7
Perizonal ciliary stripe rows, number	ASTRTUB	P	4.0	4.0	0.00	0.0	4.0	4.0	15
	RAJN2AN	P	4.0	4.0	0.00	0.0	4.0	4.0	7

<sup>a</sup>All distances in μm.<sup>b</sup>Measurements and counts (in vivo) made from digital images using calibrated software, (P) made from formalin-fixed protargol-impregnated permanent preparations using ocular micrometer or QuickPhoto software.<sup>c</sup>Measured from right cell margin to left edge of preoral dome.<sup>d</sup>Includes dome kineties but excludes perizonal ciliary stripe rows.<sup>e</sup>Measured as the chord. BE, body end; CV, coefficient of variation; (%); Max, maximum value; M, median; Min, minimum value; n, number of cells studied; P, protargol; SD, standard deviation of the mean.

**Fig. 11. (A–F).** *Urostomides denarius* comb. nov., Malaysian strain SUSBARB and resting cysts from life (A, E, F) and after protargol impregnation (B–D). (A) Left ventrolateral view of typical specimen. (B) Posteroventral view. (C) Anterodorsal view. (D) Detail of fibrillar associates of dome kineties and perizonal stripe. (E) Surface view of resting cyst. (F) Optical section through center of resting cyst. AZ, adoral zone; CC, dikinetids of caudal cilia; DK1, 4, dome kineties 1 and 4; FA, fibrillar associates; FK, false kineties; EA, excystment aperture; Ma, macronucleus; Mi, micronucleus; PK, postoral kinety; PM, paroral membrane. Scale bars: 10 μm (A–C, E, F), 5 μm (D).

and redescriptions by Kahl (1932): Body size about 50–80 × 30–60 μm in vivo, obpyriform, dorsoventrally flattened. Preoral dome broadly rounded, wider than posterior body, slightly overhangs left margin. Posterior body

obconical, posterior end rounded. Eight to ten very widely spaced ciliary rows, four to five of which extend onto preoral dome. Perizonal ciliary stripe arranged in false kineties, makes about 220° turn around long axis, separated from

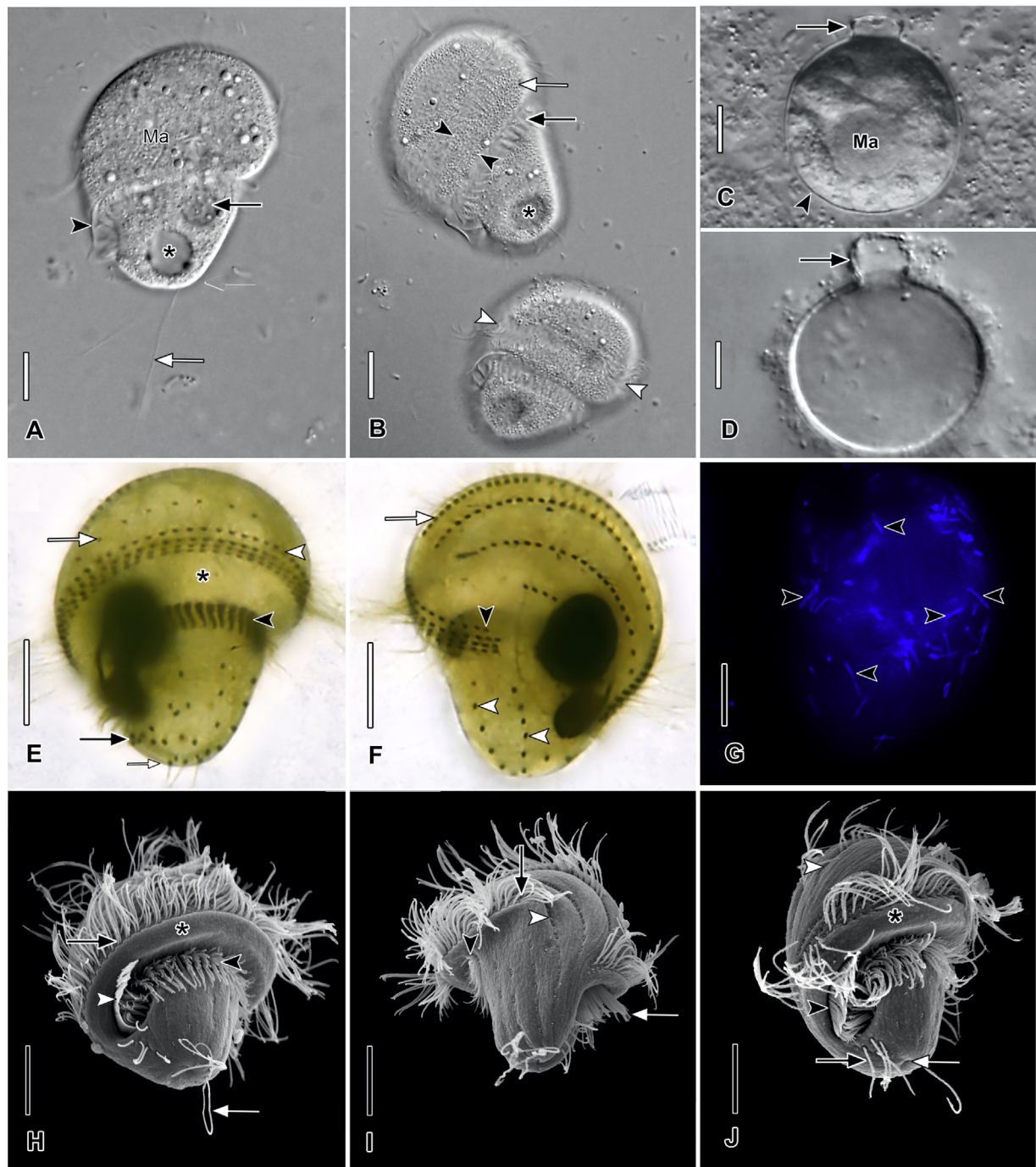


**Fig. 12. (A–J)** *Urostomides denarius* comb. nov., Malaysian strain SUSBARB from life (A–D, differential interference contrast), protargol impregnation (E–F, brightfield, stacked), UV autofluorescence (G), and MOLUKY4 in scanning electron microscope (H–J). (A) Ventral view showing paroral membrane (black arrowhead), caudal cilia (white arrow), food vacuole (black arrow), and contractile vacuole (asterisk). (B) Two individuals showing adoral zone (black arrow), perizonal stripe (white arrowheads), the wide glabrous brim of the preoral dome (black arrowheads), surface view of extrusomes (white arrow), and contractile vacuole (asterisk). (C, D) Optical section (C) of resting cysts showing thin cyst wall (black arrowhead) and excystment aperture (black arrow) and surface view (D) showing smooth cyst wall and excystment aperture (black arrow). (E) Ventral view showing crowded, disorganized right postoral dikinetids (black arrow), horizontal part of adoral zone (black arrowhead), perizonal stripe row 4 (white arrowhead), widely-spaced dikinetids of dome kinety 1 (white arrow), dikinetids of caudal cilia (small arrow), and wide glabrous preoral dome brim (asterisk). (F) Dorsal view showing shortened perizonal stripe row 4 (black arrowhead), postoral kinetics (white arrowheads), and closely spaced dikinetids at anterior end of dome kinety 2 (white arrow). (G) UV autofluorescence of fine rod-shaped cytoplasmic endobionts (arrowheads). (H) Right dorsolateral view showing 4th dome kinety (white arrowhead), paroral membrane (white arrow), and distal ends of the perizonal stipe (black arrow) and adoral zone (black arrowhead). (J) Ventral view showing dome kinety 1 (white arrowhead), paroral membrane (black arrowhead), postoral cilia (black arrow), cytopype/excretory pore (white arrow), and wide glabrous brim of preoral dome (asterisk). Ma, macronucleus. Scale bars: 10 µm.

**Table 7.** Morphometric data for *Urostomides denarius*, Malaysian strain SUSBARB.

Characteristic <sup>a</sup>	Method <sup>b</sup>	Mean	M	SD	CV	Min	Max	n
Body, length	in vivo	46.9	47.4	5.30	11.3	35.4	56.6	20
	P	37.3	37.0	3.87	10.4	30.0	47.0	25
Body, total width <sup>c</sup>	in vivo	37.0	37.7	2.70	7.3	30.3	40.8	20
	P	31.2	31.0	2.99	9.6	25.0	40.0	25
Body, length-width, ratio	in vivo	1.3	1.3	0.05	4.0	1.2	1.4	20
	P	1.2	1.2	0.09	7.8	1.0	1.4	25
Anterior cell end to posterior end of adoral zone, distance	in vivo	40.3	41.6	7.46	18.5	15.1	51.1	20
	P	30.1	30.0	2.32	7.7	26.0	36.0	25
Distance anterior cell end to posterior end of adoral zone-body length, %	in vivo	86.3	88.8	13.78	16.0	28.3	96.2	20
	P	81.0	82.0	5.41	6.7	67.0	90.0	25
Anterior cell end to posterior end of macronucleus, distance	in vivo	30.4	30.2	3.48	11.5	25.1	37.9	18
	P	24.1	24.5	2.95	12.2	17.0	30.0	24
Distance anterior cell end to posterior end of macronucleus:body length, %	in vivo	65.0	65.1	7.61	11.7	53.5	78.2	18
	P	64.7	64.5	5.10	7.9	52.0	73.0	24
Macronucleus, length	in vivo	14.1	15.1	2.64	18.6	9.5	17.4	9
	P	10.1	10.0	0.70	6.9	9.0	11.5	25
Macronucleus, width	in vivo	13.2	13.5	2.36	17.8	9.3	16.7	9
	P	9.7	10.0	0.62	6.5	9.0	11.0	25
Micronucleus, length	in vivo	3.6	3.6	0.00	0.0	3.6	3.6	1
	P	2.4	2.5	0.43	18.0	2.0	3.0	15
Adoral membranelles, number	P	26.1	26.0	1.50	5.8	23.0	26.0	24
Length of midventral adoral membranelle base	P	3.2	3.0	0.46	14.2	2.5	4.5	25
Somatic kinetics, number <sup>d</sup>	P	16.9	17.0	1.68	9.9	13.0	19.0	25
Preoral dome kinetics, number	P	6.1	6.0	0.40	6.6	5.0	7.0	25
Dikinetids in dome kinety 1, number	P	7.0	7.0	1.57	22.2	4.0	10.0	25
Paroral membrane, length <sup>e</sup>	P	11.4	11.5	1.15	10.1	10.0	13.0	16
Perizonal ciliary stripe rows, number	P	4.0	4.0	0.00	0.0	4.0	4.0	25
False kinetics, number	P	48.8	49.0	3.40	7.0	44.0	55.0	25
Caudal ciliary dikinetids	P	5.0	5.0	0.69	13.9	4.0	6.0	24
Caudal cilia, length	in vivo	25.6	26.7	4.92	19.3	17.3	35.2	15

<sup>a</sup>All distances in µm.<sup>b</sup>Measurements and counts (in vivo) made from digital images using calibrated software, (P) made from formalin-fixed protargol-impregnated permanent preparations using ocular micrometer.<sup>c</sup>Measured from right cell margin to left edge of preoral dome.<sup>d</sup>Posterior body kinetics plus dome kinetics, excluding perizonal stripe rows.<sup>e</sup>Measured as the chord. CV, coefficient of variation (%); M, median; Max, maximum value; Min, minimum value; n, number of cells studied.

adoral zone by wide gap. Adoral zone composed of about 20 membranelles, posterior part of adoral zone nearly parallel to long axis of cell, anterior three quarters of adoral zone nearly horizontal. Adoral zone approximately same length as perizonal stripe anteriorly.

**Description of strain KLAN2BC.** Body size about 47–82 × 31–59 µm in vivo, 42–57 × 21–39 µm in protargol-impregnated specimens; length:total width ratio 1.3:1. Outline broadly obpyriform with posterior end usually wider than in *Urostomides striatus* or *U. bacillatus*, dis-

tinctively dorsoventrally flattened. Preoral dome broad with thick margin, anterior part wider than mid-body, posterior part obconical to oval (Figs. 13A–C, 14A–J). Macronucleus globular to ovoid, located at junction of preoral dome and posterior body part. Micronucleus globular, adjacent to macronucleus (Figs. 13A–C, 14A–J). Cytopype not observed. Contractile vacuole terminal. Cytoplasm colorless to faint golden-yellow. Many ovoid 2.5 × 1.3 µm cytoplasmic inclusions, possibly endosymbionts. Anterior granule aggregate absent. Extrosomes rod-shaped, about 1.5–2.0 µm

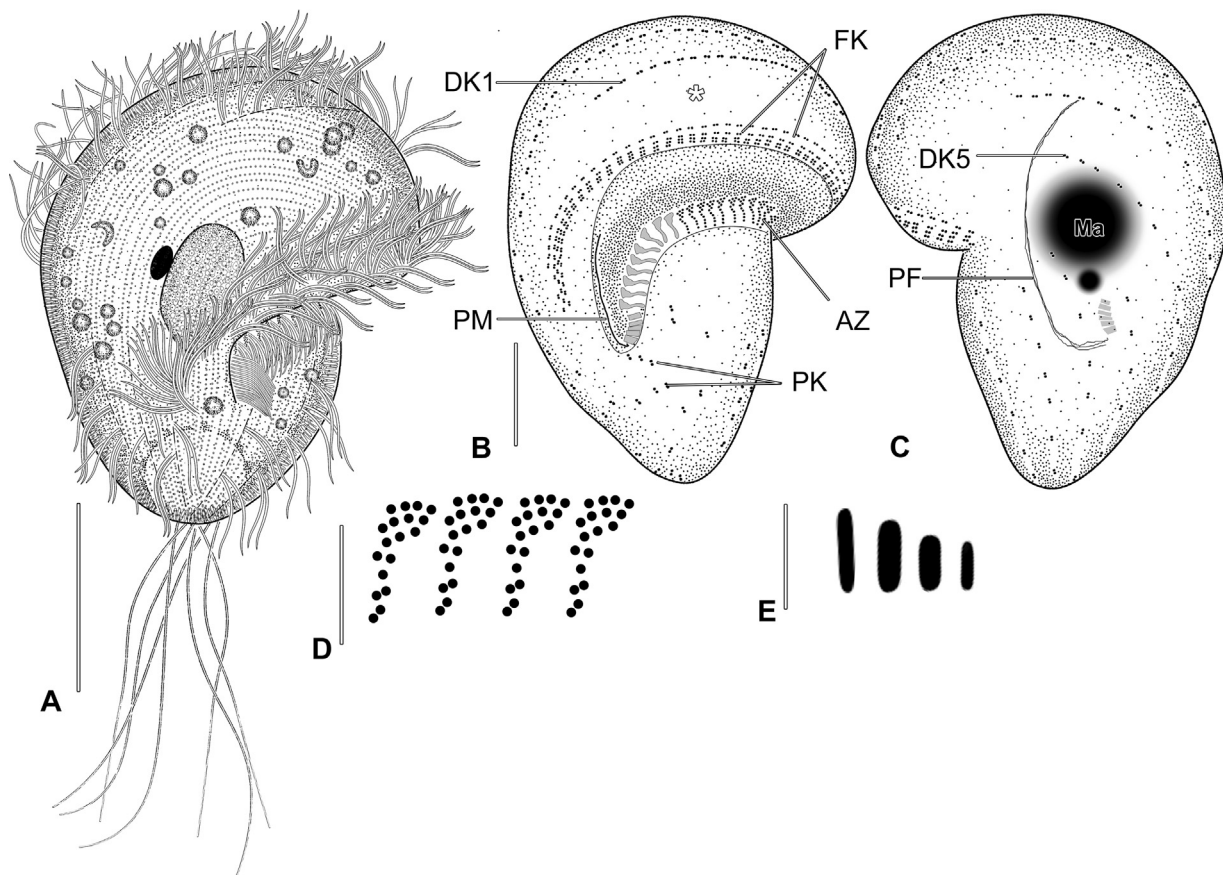


**Fig. 13.** (A–E). *Urostomides pullus* comb. nov., Czech strain KLAN2BC from life (A), and after protargol impregnation (B–E). (A) Right ventrolateral view of representative specimen from life. (B, C) Same specimen. Ventral (B) and dorsal (C) views. (D) Adoral membranelles from mid-portion of adoral zone. (E) Extrusomes. AZ, adoral zone; DK1, 5, dome kineties 1 and 5; FK, false kineties of the perizonal stripe; PF, pharyngeal fibers; PK, posterior body kineties; PM, paroral membrane. Scale bars: 25 µm (A), 10 µm (B, C), 2.5 µm (D, E).

long, densely packed in subcortical layer forming prominent fringe as in *U. striatus* (Figs. 13A, 14A, D). Food vacuoles up to 9 µm in diameter, sparse, inconspicuous (Figs. 13A–C, 14A–J).

About 8–10 somatic kineties composed of dikinetids, four or five extend onto preoral dome (Figs. 13A–C, 14A–J). Somatic kineties converge at posterior end. Somatic cilia about 7 µm long. Perizonal ciliary stripe on preoral dome margin composed of four rows of dikinetids arranged in false kineties, third and fourth row shortened proximally. Perizonal ciliary stripe makes 190° turn around long axis parallel with adoral zone, perizonal stripe kineties lie on edge of preoral dome brim (i.e. no glabrous stripe between it and rook of peristomial area). Approximately seven caudal cilia about 10 µm long and ten shorter (about 5 µm long) cilia below paroral membrane.

Proximal margin of the buccal cavity and steeply oblique adoral zone begin about 15 µm above the posterior end of the cell. Adoral zone composed of 12–25 membranelles. Paroral membrane stichomonad, about 6-µm long, J-shaped, covers buccal part of adoral zone. Swimming slower than other species of genus. Dividers frequently observed (Fig. 14J). Division occurs in free-swimming state. Some cells have a

narrowed elongated morphotype (excluded from morphometrics).

**Occurrence and ecology** (Table 1). The species was first collected by Kahl (1927) under a layer of decaying leaves, shortly after the spring ice melt. Our strain (KLANBC) was isolated in Czech Republic, also from sediments under a layer of decaying leaves in a freshwater forest stream during late fall. Bactivorous.

**Voucher material.** One slide with protargol-impregnated specimens is deposited in the Biology Centre of the Upper Austrian Museum in Linz, Austria (accession no. 2017266). Relevant specimens are marked on the slide with black ink circles.

#### Assignment of the redescribed taxa at the family level

The order Metopida Jankowski, 1980 now comprises two families, Metopidae Kahl, 1927 and Apometopidae Foissner, 2016. Although Lynn (2008) includes the Caenomorphidae Poche, 1913 together with Metopidae in order Armophoridae Jankowski, 1964, a sister relationship between Metopidae

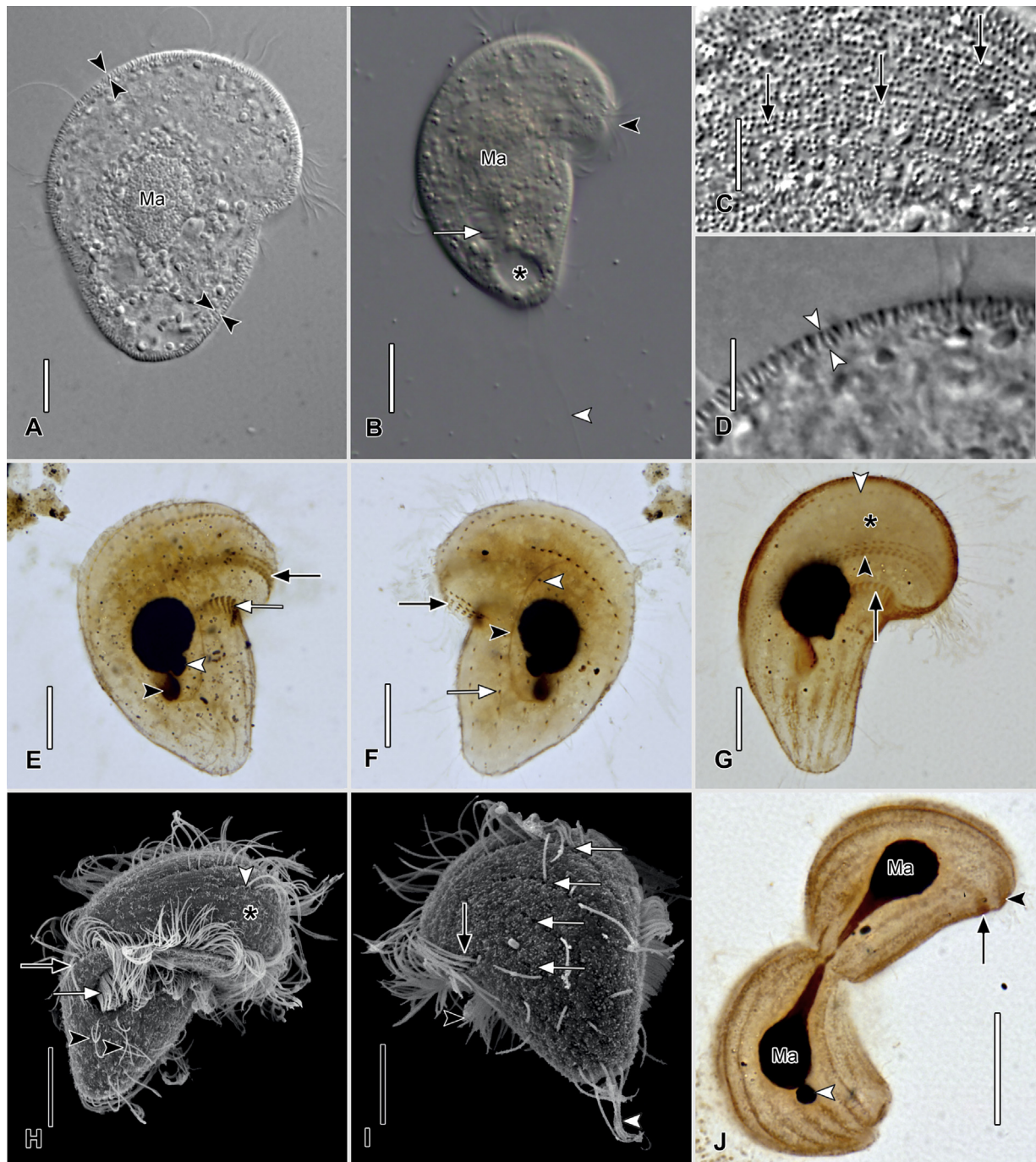


**Fig. 14.** (A–J) *Urostomides pullus* comb. nov., Czech strain KLAN2BC from life (A–D differential interference contrast), after protargol impregnation (E–G, J, brightfield), and in scanning electron microscope (H, I). (A) Optical section showing extrusome layer (black arrowheads). (B) Ventral view showing proximal part of adoral zone (white arrow), cilia of perizonal stripe (black arrowhead), and contractile vacuole (asterisk). (C) Image of cell surface showing extrusomes (black arrows). (D) Detail showing extrusome layer (white arrowheads). (E) Ventral view showing micromacronucleus (white arrowhead), perizonal stripe (black arrow), and proximal (black arrowhead) and mid-portion (white arrow) of adoral zone. (F) Dorsal view showing posterior body somatic kinety (white arrow), distal end of dome kinety 5 (white arrowhead), four-rowed perizonal stripe (black arrow), and pharyngeal fibers (black arrowhead). (G) Ventral view of slender morphotype, showing wide glabrous area (asterisk) between dome kinety 1 and perizonal stripe, and ventral part of adoral zone (black arrow). The perizonal stripe dikanetids are arranged in false kineties (black arrowhead). (H) Ventral view showing cilia of posterior somatic kineties (black arrowheads), paroral membrane (white arrow), proximal end of perizonal stripe (black arrow), and wide glabrous area (asterisk) between dome kinety 1 and perizonal stripe. (I) Dorsal view showing dome kineties (white arrows), distal end of perizonal stripe (black arrow), and caudal cilia (white arrowhead). (J) Late divider showing adoral zone (black arrow) and perizonal stripe (black arrowhead) of proter and micronucleus of opisthe (white arrowhead). Ma, macronucleus. Scale bars: 25 µm (J), 10 µm (A, B, E–I), 5 µm (C, D).

**Table 8.** Morphometric data for *Urostomides pullus*, Czech Republic strain KLAN2BC.

Characteristic <sup>a</sup>	Method	Mean	M	SD	CV	Min	Max	n
Body, length	in vivo	61.3	60.5	9.12	14.8	46.5	82.1	11
	P	47.6	45.5	4.54	9.5	42.2	56.6	20
Body, total width <sup>b</sup>	in vivo	43.7	47.7	11.94	27.3	14.2	59.4	11
	P	28.4	28.8	6.14	21.6	18.1	39.3	20
Body, length-width, ratio	in vivo	1.6	1.4	0.81	51.0	1.2	4.1	11
	P	1.7	1.6	0.30	17.5	1.4	2.5	20
Posterior end width	in vivo	10.1	10.0	1.98	19.7	7.5	14.5	11
	P	10.3	9.8	3.56	34.5	6.4	18.2	20
Anterior cell end to posterior end of adoral zone, distance	in vivo	41.1	46.9	9.62	23.4	25.0	54.5	11
	P	33.3	33.0	2.60	7.8	29.7	37.3	19
Distance anterior cell end to posterior end of adoral zone:body length, %	in vivo	67.1	72.0	12.55	18.7	41.5	80.5	11
	P	70.1	70.3	4.00	5.7	60.0	78.3	19
Anterior cell end to posterior end of macronucleus, distance	in vivo	39.5	39.1	8.75	22.1	28.1	54.0	11
	P	29.2	28.0	3.08	10.6	25.0	35.7	20
Distance anterior cell end to posterior end of macronucleus:body length, %	in vivo	64.8	60.5	12.78	19.7	44.2	85.6	11
	P	61.3	61.1	1.73	2.8	57.9	64.5	20
Anterior cell end to anterior end of adoral zone, distance	in vivo	30.9	31.3	6.64	21.5	19.2	39.5	11
	P	22.1	20.8	3.12	14.1	18.4	28.5	19
Distance anterior cell end to anterior end of adoral zone:body length, %	in vivo	50.1	52.0	6.77	13.5	37.9	60.0	11
	P	46.2	46.2	3.27	7.1	38.9	52.0	19
Macronucleus, length	in vivo	16.9	17.1	3.03	17.9	12.2	23.4	11
	P	13.8	13.9	1.16	8.4	11.7	16.3	20
Macronucleus, width	in vivo	14.7	13.0	4.28	29.2	9.0	24.5	11
	P	10.1	10.2	0.99	9.8	7.7	12.5	20
Micronucleus, length	in vivo	5.3	5.4	0.57	10.7	4.1	6.0	7
	P	3.6	3.8	0.51	14.3	2.5	4.4	18
Adoral membranelles, number	P	21.3	21.0	3.23	15.2	12.0	25.0	17
Length of midventral adoral membranelle base	P	3.1	2.9	0.39	12.6	2.5	3.8	17
Somatic kinetics, number <sup>d</sup>	P	9.5	10.0	0.71	7.4	8.0	10.0	8
Preoral dome kinetics, number	P	4.2	4.0	0.40	9.5	4.0	5.0	10
Paroral membrane, length <sup>e</sup>	P	6.4	6.5	0.42	6.5	5.4	7.1	18
Perizonal ciliary stripe rows, number	P	4.0	4.0	0.00	0.0	4.0	4.0	20
Caudal ciliary dikinetids	in vivo	4.2	4.0	0.98	23.3	3.0	6.0	8
	P	5.4	5.0	1.15	21.4	4.0	8.0	11
Caudal cilia, length	in vivo	32.0	30.0	7.02	21.9	21.8	45.3	11
	P	27.3	26.9	6.44	23.6	13.7	38.0	12

<sup>a</sup>All distances in µm; <sup>b</sup>Measurements and counts (in vivo) made from digital images using calibrated software, (P) made from formalin-fixed protargol-impregnated permanent preparations using ocular micrometer; <sup>c</sup>Measured from right cell margin to left edge of preoral dome; <sup>d</sup>Posterior body kinetics plus dome kinetics, excluding perizonal stripe rows; <sup>e</sup>Measured as the chord. CV, coefficient of variation (%); M, median; Max, maximum value; Min, minimum value; n, number of cells studied.

(and now Apometopidae) and Caenomorphidae is increasingly doubtful based on morphologic and molecular data (Bourland et al. 2017; Paiva et al. 2013). Apometopidae was established for pyriform metopid ciliates having specialized dome kinetics and a nearly equatorial adoral zone (Foissner 2016b). The most notable character of the type

genus, *Urostomides* (new junior subjective synonym: *Apometopus* Foissner, 2016), is the four-rowed rather than the typical metopid five-rowed perizonal ciliary stripe. Foissner (2016b) split *Apometopus* into two monotypic subgenera, *Apometopus* (*Apometopus*) and *Apometopus* (*Apometopides*) based on the single character of cohering or non-cohering caudal cilia

respectively. Herein both subgenera are synonymized with *Urostomides* Jankowski, 1964.

During our study of free-living freshwater metopids, we characterized 24 populations, representing seven species and forming a well-supported clade in the 18S rRNA gene phylogeny, all of which had a four-rowed perizonal ciliary stripe (Table 1). The surprising level of morphologic diversity of these taxa invites further subdivision, at least at the genus level. However, at the present state of knowledge, we prefer to assign the taxa redescribed in this report to the genus *Urostomides* in the family Apometopidae until more extensive morphologic, morphogenetic, and molecular data are available. This placement requires an emended family diagnosis to accommodate taxa lacking obviously “specialized” (possibly thigmotactic) dome kineties (referred to by Foissner [2016b] as “specific”, “special” or simply “ventral” kineties) and a horizontally oriented adoral zone, but included in the large well-supported molecular clade (e.g., *Urostomides bacillatus*, *U. caducus*, *U. darwini*, and *U. striatus*).

With the addition of more, well-characterized taxa, it is likely that the morphologically diverse Apometopidae will require subdivision into multiple genera. *Cirranter mobilis* (Penard, 1922) Jankowski, 1964 was previously assigned to Caenomorphidae, mainly on the basis of the single bell kinety and body shape (also see Sola et al. 1992), however Foissner (2016b) transferred it to *Apometopus*. We concur with this decision since Sola et al. (1992) demonstrated a four-rowed perizonal stripe in *C. mobilis*. The Caenomorphidae have been recently shown to form an independent lineage to Armophorea (Bourland et al. 2017; Paiva et al. 2013), further stressing the obvious inconsistency in the morphologic determination of many armophorean taxa. Such inconsistencies include methodologically limited and sometimes ambiguous descriptions and depictions in the older literature and mistaking analogy for homology in the metopid and caenomorphid perizonal ciliary stripe and, of course, the lack of molecular sequence data for the majority of known taxa.

### Assignment at the genus and species level and synonymization of *Urostomides* Jankowski, 1964 and *Apometopus* Foissner, 2016

We assign seven additional species to genus *Urostomides*. There are several reasons we avoid further subdivision of the genus at present. Firstly, a reliable description of the ciliature for many metopid taxa is still lacking, increasing the likelihood of misassignment. For example, the perizonal stripe of *Metopus contortus* (Quennerstedt, 1861) Kahl, 1932 is described by Dragesco (1996) as three-rowed, and by others (Esteban et al. 1995; Foissner et al. 2002) as five-rowed; Jankowski (1964) describes the structure as five-rowed but illustrates only four. *Metopus entorhipediooides* Jankowski, 1964 is described as having a five-rowed perizonal stripe but illustrated with only three and *Metopus trichocystiferus* Jankowski, 1964 is illustrated without a perizonal stripe

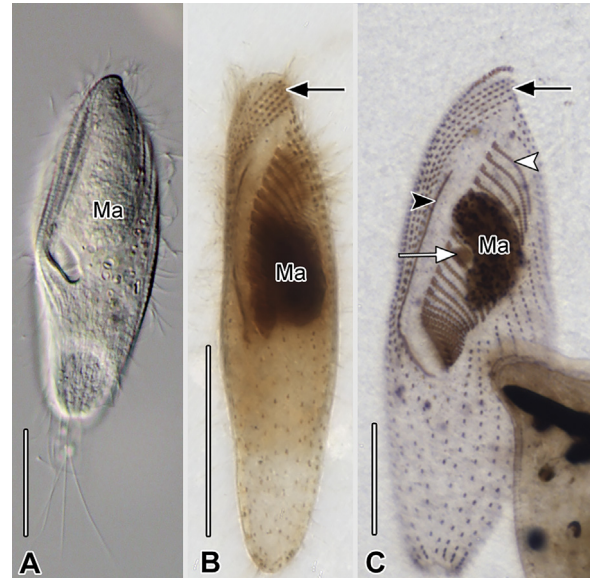


**Fig. 15.** (A–C). *Bothrostoma undulans*, Idaho population from life (A, differential interference contrast) and after protargol impregnation (B, C brightfield). (A) Ventral view. (B, C) Ventral views showing five-rowed perizonal ciliary stripe (black arrows), stichomonad paroral membrane (black arrowhead), anterior end of adoral zone (white arrowhead), and micronucleus (white arrow). Ma, macronucleus. Scale bars: 25 µm (A–C).

at all (Jankowski 1964b). The unreliability of many older reports is underscored by the example of genus *Bothrostoma* Stokes, 1887. Jankowski (1964b) describes five perizonal stripe kineties in the type species, *B. undulans* Stokes, 1887 but illustrates two specimens, one with four rows and one with three (his Fig. 16a, b). A four-rowed perizonal stripe has since been listed as a genus character for *Bothrostoma* (Lynn and Small 2002; Small and Lynn 1985). However, our protargol impregnations of two strains of *B. undulans*, one Malaysian and the other North American, show, unequivocally, a five-rowed perizonal stripe (Fig. 15A–C, redescription and molecular phylogeny of this genus is in preparation). The species described as *Cirranter mobilis* by Jankowski (1964) matches that described by Sola et al. (1992) very closely, except that the former author describes and depicts a five-rowed perizonal stripe, whereas Sola et al. (1992) found a four-rowed stripe in silver carbonate preparations. All genera of Metopida we have thus far studied, and those recently reported by others, have either a five-rowed (Metopidae) or four-rowed (Apometopidae) perizonal ciliary stripe. Secondly, molecular data is lacking for most of this group as yet, including the type species of *Heterometopus*, *Palmarella*, *Bothrostoma*, *Eometopus*, *Tropidoactractus*, and for five new *Metopus* species (Foissner 2016a,b; Vd'ácný and Foissner 2017). Based on the four-rowed perizonal stripe we consider the genus *Urostomides* Jankowski, 1964 a senior synonym of *Apometopus* (Foissner, 2016) and place it in family Apometopidae Foissner, 2016.

All *Urostomides* species described to date, including those redescribed in the current report, have elongated caudal cilia often, but not always, eccentrically grouped. Although the caudal cilia of *U. pelobius* (Foissner, 2016) comb. nov. (original combination *Apometopus* (*Apometopus*) *pelobius* Foissner, 2016) cohere in a single bundle in protargol preparations and those of *U. pyriformis* (Levander, 1894) comb. nov. (original combination *Metopus pyriformis* Levander, 1894) do not, in our opinion, this feature does not rise to the level of a subgeneric character. Unfortunately, although Foissner remarks on some *in vivo* observations, *in vivo* images of *U. pelobius* and *U. pyriformis* were not included in the original descriptions (Foissner 2016b).

We omit the description of the adoral zone as comprising “paramembranelles” in *Urostomides* since there is currently no ultrastructural evidence to support this designation. Interestingly, perizonal stripe false kineties were observed in two of the species redescribed herein (*U. pullus*, *U. denarius*), with no significant correlation of their phylogenetic positions. It appears that the morphologic character of false kineties (Foissner and Agatha 1999) occurs in many taxa that are only distantly related in the metopid molecular phylogeny, for example in *Urostomides denarius*, *U. pullus*, *Atopospira* spp., *Metopus laminarius*, *M. hasei*, and *Heterometopus palaeformis* (Bourland and Wendell 2014; Foissner 2016a,b; Foissner and Agatha 1999; authors' own observations).

The phylogenetic importance, if any, of paroral membrane morphology in the Metopida remains unclear and has recently become more confused. The structure of the paroral membrane was not included by Foissner (2016b) as a diagnostic feature at the family or genus level. However, the paroral of *Urostomides pelobius* and *U. pyriformis* is described as “dikinetid” and depicted as dikinetids in a distinct zigzag (i.e. stichodyad) configuration for both species. In metopid species described prior to 2016, a paroral consisting of a single row of basal bodies is described and depicted by most authors (Dragesco and Dragesco-Kernéis 1986; Foissner 1980; Foissner and Agatha 1999; Foissner et al. 2002). In many metopids described subsequently the paroral has been described as “dikinetid” and usually depicted in a stichodyad-like zigzag configuration (Foissner 2016a,b; Vd'ačný and Foissner 2017). To our knowledge a “dikinetid paroral” has not been previously described. The term “dikinetid” means “composed of two kineties”, it is possible that the intended term was “dikinetidal” i.e. “composed of dikinetids”. In any event, based on protargol impregnation and scanning electron microscopy, we have been able to confirm only two paroral morphologies (i.e. diplostichomonad in *Atopospira* and stichomonad in all other metopid species we have studied) among the Metopida. Silva-Neto et al. (2016) also found a diplostichomonad paroral membrane in *Parametopidium circumlabens*, which, interestingly, is sister to a larger clade containing, among others, *Atopospira* in the molecular phylogeny (Fig. 16). A diplostichomonad paroral also occurs in the clevelandellid, *Nyctotherus ovalis* (Santos et al. 1986). Our examination of the type material of *Urostomides*

*pelobius* (original combination *Apometopus pelobius*) and voucher material for *U. pyriformis* (original combination *Metopus pyriformis* Levander, 1894) and *Heterometopus meisterfeldi* was consistent with previous interpretations of the metopid paroral as comprising a single file of basal bodies (Bourland et al. 2014, 2017; Bourland and Wendell 2014; Dragesco and Dragesco-Kernéis 1986; Foissner et al. 2002; Foissner and Agatha 1999). Misinterpretation of this feature, due to confounding fibrillar associates in protargol preparations, is likely. Transmission electron microscopy will resolve this question definitively (Grain 1984).

We did find one “special kinety” (DK3) in *Urostomides campanula* but in the other six taxa, especially *U. denarius* and *U. pullus*, the situation is more ambiguous. Whether DK2 in the latter two species correspond to Foissner's “special” kineties is unclear. They conform in having more closely spaced dikinetids than the other dome rows, are similarly curved and correspondingly located. However, their dikinetids are either not inclined or only slightly so, thus we hesitate to equate them with the “special” kineties depicted in *U. pelobius* and *U. pyriformis* (Foissner 2016b). By the same token, the taxonomic value of these structures is unclear.

## Phylogenetic relationships within Metopida with emphasis on genus *Urostomides*.

The unrooted phylogenetic tree of the SAL (Spirotrichea, Armophorea, and Litostomatea) clade (see Gentekaki et al. 2014) as inferred from the 18S rRNA gene sequences is shown in Fig. 16. Of the classes comprising SAL, only Litostomatea and Spirotrichea appeared to be robustly monophyletic (bootstrap support (BS)  $\geq 93$ , Bayesian posterior probability (BPP) 1). Armophorea split into two robustly supported clades (BS  $\geq 93$ , BPP 1), Armophorida and Metopida/Clevelandellida. The Metopida/Clevelandellida clade is closely related with maximum support to a clade formed by environmental sequences from hypoxic/anoxic, marine/saline habitats, possibly belonging to unidentified metopids. However, the monophyly of the latter clade received only moderate support (BS 86, BPP 0.98). The Metopida/Clevelandellida clade split into four lineages whose interrelationships remained unresolved: (1) *Metopus es* and *Brachonella contorta* with medium support (BS 71, BPP 0.98), (2) a marine clade composed of environmental sequences and *M. contortus* with maximum support, (3) family Apometopidae including all available *Urostomides* spp. sequences with strong support (BS 97, BPP 1), (4) *Metopus fuscus*, *M. setosus*, *M. laminarius*, *Heterometopus palaeformis*, *Atopospira* spp., *Parametopidium circumlabens*, and the entire Clevelandellida with strong support (BS 92, BPP 1). The relationships within the latter clade were generally unresolved, though Clevelandellida was recovered monophyletic with maximum support.

*Urostomides* split into three clades: (A) *U. campanula*, *U. caducus*; (B) *U. darwini*; (C) *U. denarius*, *U. pullus*,

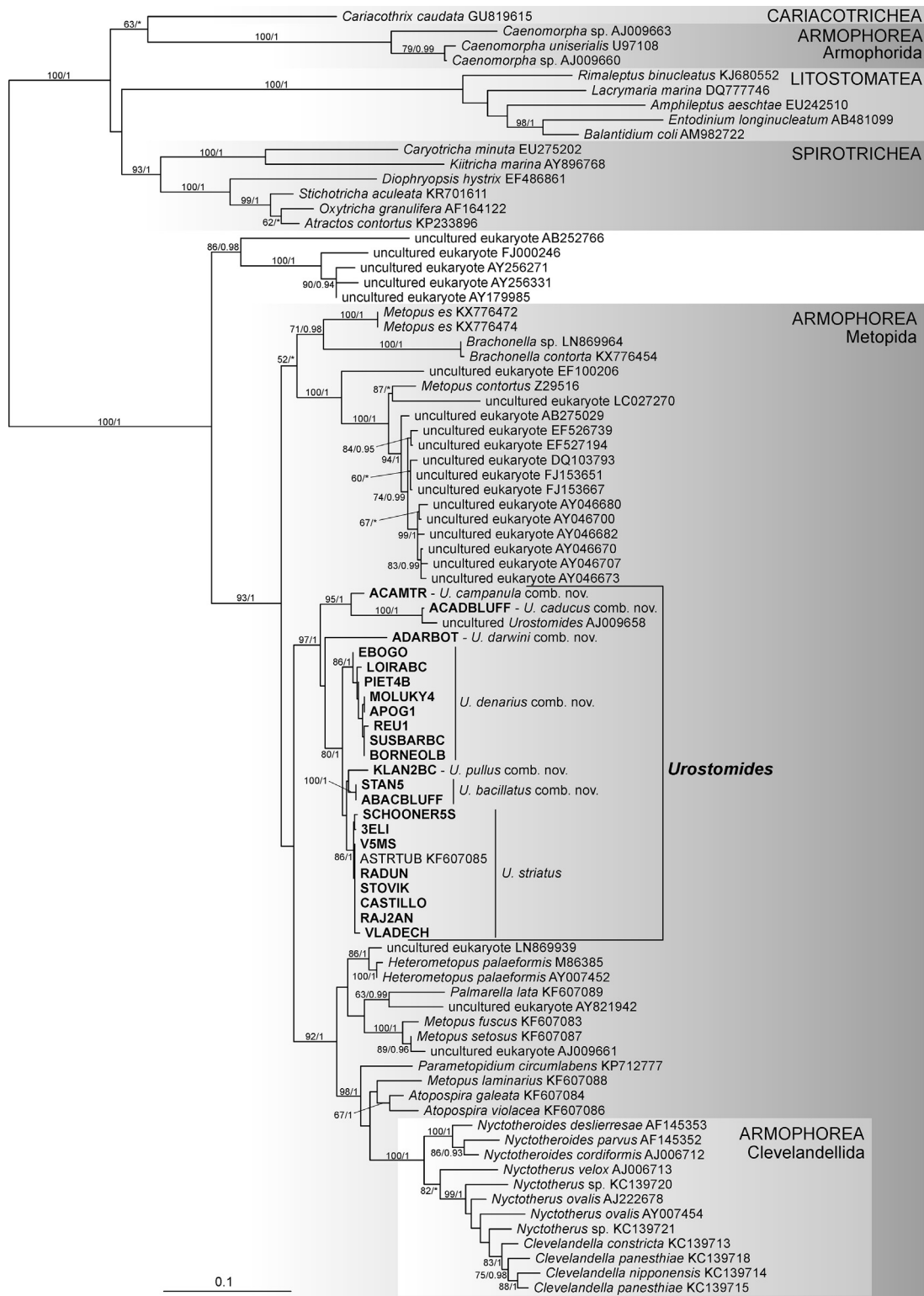


**Fig. 16.** Unrooted phylogenetic tree of the SAL superclade based on the 18S rRNA gene sequences. The tree was constructed by the maximum likelihood method in RAxML (GTRGAMMA1 model). The values at branches represent statistical support in bootstrap values (RAxML)/posterior probabilities (MrBayes). Support values below 50/0.90 are not shown or are represented by an asterisk (\*). New sequences in bold. The scale bar represents 10 changes per 100 positions.

*U. bacillus*, *U. striatus*. The intraspecies genetic distance (uncorrected p distance) within *Urostomides denarius* and *U. striatus* reached 0.009 and 0.006, respectively. Sequentially most similar species were *U. striatus* and *U. bacillus* (minimum genetic distance 0.014) and *U. bacillus* and *U. denarius* (0.017). The maximum genetic distance between *Urostomides* species reached 0.070 (*U. caducus* and *U. pullus*; *U. caducus* and *U. darwini*).

**Remarks.** Because no molecular characterization was associated with the morphologic descriptions of either *Urostomides pelobius* (Foissner, 2016) or *U. pyriformis* (Levander, 1894), their position in the molecular phylogeny is speculative at this point and it is unlikely that it will be forthcoming in the foreseeable future. This underscores the taxonomic and phylogenetic problems stemming from contemporary descriptions of new species without associated molecular data. If many such new species are described, it results in parallel and almost irreconcilable classification systems and phylogenies, one based purely on morphology (with or without morphogenetic data), and the other with these types of data together with molecular characterization.

### Comparisons of our strains with original descriptions and similar species

Genus *Cirranter* differs from genus *Urostomides* in the number of dome kineties (single vs. multiple) and the posterior body kineties (absent vs. present). Without further morphological and molecular data for this genus, we cannot resolve the significance of the variability in dome kineties. The single bell kinety and absence of posterior body kineties probably led to the previous classification of *Cirranter mobilis* within Caenomorphidae, however the structure of the perizonal stripe is clearly metopid rather than caenomorphid (Paiva et al. 2013; Sola et al. 1992). We could only speculate as to the identity of the environmental sequence (GenBank accession number AJ009658), probably misidentified by Hoek et al. (1999) as a ‘Caenomorphidae’ perhaps due to similar reasons as *Cirranter mobilis*.

Some cells in several populations of *Urostomides striatus* and *U. pullus* evince a distinct morphotype which resembles *Metopus convexus* Kahl, 1927 and *M. curvatus* Kahl, 1927 in most features but dissimilar with regard to the caudal cilia (several long cilia in the former two species vs. tuft of short dense cilia in *M. convexus* and no elongated caudal cilia in *M. curvatus*). These forms may reflect nutritional state or other environmental factors and possible synonymy of these two species with *U. striatus* or *U. pullus* cannot be excluded. Other species currently assigned to genus *Metopus* may, in fact belong to the genus *Urostomides*, namely *M. minimus* Kahl, 1927, in view of its general apometopid-like features (see below).

***Urostomides caducus*:** The Idaho populations match Kahl's (1927, 1932) description and illustrations so closely that conspecificity is beyond doubt. Both Kahl (1927, 1932)

and Wetzel (1928) noted the excretion of a mucus envelope by *U. caducus* in response to cover glass pressure, the “Gallerthülle” according to Kahl and the “Tekthülle” according to Wetzel (Fig. 2E). Wetzel also noted the four-rowed perizonal ciliary stripe. The Idaho populations also match Jankowski's (1964) description and illustrations closely.

*Urostomides caducus* is unlikely to be confused with many other species. Levander (1894) depicted two forms of *Metopus pyriformis* (his Taf. I, Figs. 10 and 11), one of which (his Taf. I, Fig. 11) was transferred by Foissner (2016b) to *Apometopus* (new junior synonym of *Urostomides*), and designated as type of the subgenus *Apometopus* (*Apometopides*). *Urostomides caducus* can be distinguished from *U. pyriformis* (Levander 1894) (Fig. I, 10, Kahl 1932, fig. 71, 11, p. 425) by: dorsoventral flattening (present vs. absent), eccentric caudal ciliary tuft (present vs. absent), and shape of posterior end (broadly vs. narrowly truncate). *Urostomides caducus* can be distinguished from *Brachonella cydonia* (Kahl, 1927) by: dorsoventral flattening (present vs. absent), eccentric caudal ciliary tuft (present vs. absent), shape of the posterior end (broadly truncate vs. narrowly tapered, circular in cross-section), and preoral dome granule aggregate (absent vs. present). *Urostomides caducus* is easily distinguished from *U. darwini* (Kahl, 1927) comb. nov. by the outline of the posterior end (broadly truncate vs. long, acute tail).

***Urostomides campanula*:** In 1932, Kahl described *Metopus campanula*, elevating his earlier (1927) variety “minor” of *Metopus intercedens* to species level. Kahl's descriptions are brief, but the Idaho population, although smaller, matches most features of the German populations presented by Kahl (e.g. overall shape, rod-shaped extrusomes in the preoral dome, and posterior part of the body). Kahl's population and the population of *U. campanula* described herein both differ from the Russian material (as *Brachonella campanula*) sensu Jankowski (1964b) in at least two important features: posterior body extrusomes (present in both vs. absent) and meridional dome kineties (absent vs. present). The spacing of dikinetids in Jankowski's drawings of metopids is almost certainly unreliable as nearly all are shown with identical dense spacing. Kahl (1932) found a population lacking extrusomes and speculated it might represent a separate species. *Urostomides campanula* bears an overall similarity to *U. pelobius* and *U. pyriformis* with regard to general shape. *Urostomides campanula* differs from *U. pelobius* in the number of dome kineties (5 vs. 6–7), number of “special” dome kineties (one vs. 4), adoral membranelle number (average of 33 vs. 38), and caudal cilia (noncohesive vs. cohesive bundle), and possibly extrusomes (present, conspicuous vs. not mentioned). *Urostomides campanula* differs from *U. pyriformis* in size (40 × 35 µm vs. 50 × 45 µm), number of posterior body or “cone” dikinetids (about 30 vs. up to 80), adoral membranelle number (33 on average vs. 46 on average), number of “special” kineties (one vs. four), and paroral membrane length (12 µm on average vs. 22 µm on average). The absence of 18S rRNA gene sequences for *U. pelobius* and *U. pyriformis*

do not allow us to define their relationship to *U. campanula* (or any of the other Apometopidae).

*Urostomides campanula* is easily distinguished from *Atopospira galeata* (Kahl, 1927) Bourland and Wendell, 2014 by: the preoral dome shape (broadly rounded vs. helmet-like with brim), number of perizonal ciliary stripe rows (four vs. five), the thigmotactic sagittal preoral dome kinety (present vs. absent), bipartite adoral zone (absent vs. present), and the 18S rRNA gene sequence (Fig. 16).

***Urostomides darwini*:** The Idaho population of *U. darwini* matches Kahl's (1927) original description and illustration so closely that conspecificity is beyond doubt. Although Kahl initially mistook *U. darwini* for a caenomorphid and even wondered whether it might be a transitional form between *Metopus* and *Caenomorpha*, he concluded this was doubtful (Kahl 1927). The unique shape of *U. darwini* makes confusion with other species highly unlikely and in this sense *U. darwini* qualifies as a “flagship” species (Foissner 2005, 2006). However, distinction from other “tailed” members of Metopida is appropriate. *Urostomides darwini* can be easily distinguished from *Metopus vestitus* Kahl, 1932 and *M. v. major* Tucolesco, 1962 by: overall shape (broad vs. slender), habitat (freshwater vs. marine), and pellicular ectosymbionts (absent vs. present). *Urostomides darwini* is distinguished from the freshwater *M. spinosus* Kahl, 1927 by: size (length about 110 µm vs. about 70 µm), shape (broad vs. slender), preoral dome granule aggregate (absent vs. present), and lack of macronuclear endobionts (Jankowski 1964b, Kahl 1932).

***Urostomides bacillatus*:** Levander (1894) classified *U. bacillatus* as a *Metopus* species based on observation of only three individuals and Kahl (1927) recognized no fewer than ten “varieties” of this species in his “Group IV” (later [Kahl 1932] elevating them to species status). The illustration designated as “*M. bacillatus* from Levander, 1894” in Jankowski's revision (1964, Fig. 11d) does not appear to represent either of Levander's two drawings (Taf I; 12, 13). Confident comparison of the Idaho population with Levander's or Kahl's species is difficult. Nevertheless, the Idaho population matches Levander's and Kahl's species in most features. The question of elongated caudal cilia is problematic. Levander noted their absence in the three individuals he found, but Kahl did not mention the caudal cilia and his illustration is somewhat ambiguous (1927, Fig. 17a, p. 152). The elongated caudal cilia in both the Idaho population and strain STAN5 are inconspicuous (Fig. 8C); also they are quite delicate and often lost during preparation (Fig. 8G–I). *Urostomides bacillatus* can be distinguished from *Metopus gibbus* Kahl, 1927, redescribed by Foissner et al. (2002), by the perizonal ciliary stripe row number (four vs. five). *Urostomides bacillatus* is distinguished from *U. striatus* comb. nov. and other Kahl's “Group IV” metopids (e.g. *Metopus acutus* Kahl, 1932; *M. dentatus* Kahl, 1927; *M. acuminatus* Kahl, 1932) by the shape of the posterior end, i.e. broadly tapered, rounded or truncate vs. narrowly tapered into a distinct “tail”, and by the 18S rRNA gene sequence (Fig. 16). *Urostomides bacillatus* also resembles another species in this group (*M. minimus*

Kahl, 1927). Although the possibility cannot be completely excluded, we prefer not to synonymize *U. bacillatus* and *M. minimus* at the present state of knowledge. The two populations (ACADBLUFF, STAN5) of *U. bacillatus* noticeably differed in body size, which may be caused by the long-term cultivation of the latter.

***Urostomides striatus*:** McMurrich (1884; Fig. 1, p. 831) provided only one illustration of *U. striatus* showing a short but tail-like posterior end with elongated caudal cilia. The reliability of his size measurements (80–170 µm) is questionable, but in most features the Idaho population is consistent with his original description. Esteban et al. (1995) synonymized *U. striatus* with 13 species (including *Metopus bacillatus*, here transferred to *Urostomides*) and one subspecies. Although synonymy of *U. striatus* with taxa such as *Metopus acuminatus* (Stokes, 1886) Kahl, 1932, *M. acutus* (Kahl, 1932), and *M. dentatus* (Kahl, 1932) is possible or even likely, we reject the wholesale synonymization of the *U. striatus*-like taxa at the present state of knowledge. This more conservative approach is supported by the present work that refutes the synonymy of *U. striatus* and *U. bacillatus* on the basis of morphology and molecular characterization. Further, recent reports also refute the synonymy of *U. striatus* with *Atopospira violacea* and *Metopus gibbus* (Bourland and Wendell 2014; Esteban et al. 1995; Foissner et al. 2002).

***Urostomides denarius*:** Kahl (1927) described *Metopus denarius* as a variety and later elevated the variety to species level (Kahl 1932). His description and drawing are both rather vague. The live specimens of our populations are slightly larger (35–57 µm) than Kahl's populations, 30–35 µm (Kahl 1927) and 35–45 µm (Kahl 1932). Kahl also observed some cells that had “only one-fourth of the usual size”. The overall shape of our population also agrees with that of Kahl's (length:width ratio 1.3 vs. 1.2). Extrusomes were not observed originally, but Kahl mentioned he “expected” them to exist, whereas they are easily seen in the populations described herein. Kahl's drawing neither shows caudal cilia nor are they mentioned in the text, while our populations do possess caudal cilia, however they are sparse (five on average) and inconspicuous. Also, Kahl's descriptions and depictions of caudal cilia can be inconsistent (Bourland et al. 2014). Our population and Kahl's both share similar posterior displacement of the cytostome to the posterior one-fifth of the body.

As is the case with many species described by Kahl, conspecificity can never be “proven” because descriptions and drawings are sometimes not sufficiently detailed and type material doesn't exist. This is particularly troublesome for species with a similar appearance (e.g. Kahl's varieties of *Metopus bacillus*, later elevated to species rank). However, taking these limitations and the minor differences noted into account, we prefer not to create a new species at our current state of knowledge.

*Urostomides denarius* can be distinguished from the similar *U. pyriformis* (Levander, 1894) and *U. pelobius* (Foissner, 2016b) mainly by the shape of the posterior part of the

adoral zone and the number of membranelles (vertical, 26 vs. horizontal, 46, 38 respectively), false kineties (present vs. absent in both), and caudal cilia (sparse vs. longer in both and as a bundle in *U. pelobius*), and from *Metopus dentatus* Kahl, 1927 by rounded vs. pointed posterior body end, and cell flattening (absent vs. present). Another similar species is *Metopus minimus* Kahl, 1927, with following features: 45–50 µm (Kahl 1927) or 50–60 µm (Kahl 1932) large, hyaline, with ‘narrowed but rounded’ posterior part and caudal cilia longer than in *U. denarius*. The original drawing depicts a smooth surface (no extrusomes) and oval macronucleus, conflicting with our observations. *Cirranter mobilis* differs from *U. denarius* in shape of posterior end (truncate with two short protrusions vs. rounded), but most significantly, in number of dome kineties (one bell kinety vs. five to seven dome kineties). The resting cysts of *U. denarius* have a unique flask-like morphology with a distinctive escape apparatus (Fig. 12C, D). The resting cysts of *Heterometopus palaformis* also have an escape aperture but are ovoidal in shape, resembling resting cysts of *Frontonia* (Esteban et al. 1995; Foissner et al. 1994). There is little known about cyst morphology in metopids and this subject is ripe for further morphologic, ultrastructural, and biochemical investigation. Resting cysts may prove to be of phylogenetic importance in Metopida as in other groups, such as Spirotrichea (Foissner et al. 2007).

*Urostomides pullus*: Kahl (1927) originally described this species as a variety of *U. bacillatus* with subsequent elevation to species level (Kahl 1932). Unlike the original description, our strain is not dark brown colored but varies from golden yellow to hyaline, however, this character may vary with the nutritional state and type of food vacuole content. Some cells of KLAN2BC are smaller than the originally described population (60–80 µm long). The original population was described with inconspicuous flattening, ratio 3:2 or 4:3 unlike our conspicuously flattened KLAN2BC (precise data unfortunately not recorded but extent of flattening approximates 2:1). Kahl (1927) suggested that this variety might belong to another species, *M. intercedens*, but we argue against this due to its larger body size and the originally described dense somatic kineties. Kahl does not mention the shape of macronucleus but Kahl (1932) depicts an ellipsoidal macronucleus rather than the round macronucleus in KLAN2BC. The adoral zone has a distinctive shape and orientation, the posterior part being almost vertical and the more anterior part horizontal (Figs. 13A, B, 14G, H). We reject the synonymy of *U. denarius* and *U. pullus* with *U. striatus* suggested by Esteban et al. (1995) on the basis of cell shape (rounded or truncate posterior in the former two vs. tail-like in the latter) and due their distinct molecular phylogenetic positions (Fig. 16). *Urostomides denarius* and *U. pullus* clearly differ in several important features: size (47 × 37 µm vs. 61 × 47 µm on average), glabrous broad preoral dome brim (present vs. absent), and distal shortening of the adoral zone relative to the perizonal stripe (present vs. absent).

## Phylogenetic relationships within Metopida and Urostomides and their correlation with morphology and lifestyle

The taxonomic reappraisal of Armophorea as a whole started recently with the transfer of *Metopus violaceus* Kahl, 1927 and *Brachonella galeata* (Kahl, 1927) Jankowski, 1964 into genus *Atopospira* Jankowski, 1964 on morphological and molecular grounds (Bourland and Wendell 2014). We now know that a large group of morphologically highly diverse metopids is more closely related to the endobiotic Clevelandellida than to the type species of the genus *Metopus*, *M. es* (Fig. 16 in this article; Bourland et al. 2017). This clade includes *Heterometopus*, *Atopospira*, *Palmarella*, *Parametopidium* and a number of species classified as *Metopus* that will require transfer to other genera. This underscores the need for detailed morphological descriptions and molecular characterization of the Metopida.

Although internal relations are not fully resolved in *Urostomides*, the well supported clade (A), uniting *U. campanula*, *U. caducus*, and an uncharacterized apometopid, includes two morphologically quite different species that share only a few features: a horizontally situated proximal part of the adoral zone, a truncate posterior end, and an eccentric tuft of long caudal cilia. Clade (B) comprises a single species, *U. darwini*, easily morphologically distinguished by typical pisciform shape, tapered tail and massive preoral dome. Clade (C) unites four species, more or less fist-shaped, with oblong extrusomes, a vertically oriented posterior part of the adoral zone that then winds horizontally around the body, a broad preoral dome overhanging left margin, and two species with perizonal stripe false kineties. In *U. denarius*, *U. pullus*, *U. striatus*, and *U. bacillatus*, the paroral membrane runs vertically together with posterior part of adoral zone as oppose horizontal arrangement of this portion in other *Urostomides* species and these species may be grouped in a separate genus in the future.

## Biogeography, ecology, and cultivability of Metopida

With few exceptions, most of the more than 70 nominal metopid species were originally described from Laurasian habitats (primarily Europe and Russia), which undoubtedly reflects sampling bias (Jankowski 1964b, Kahl 1927, 1932; Roskov et al. 2016). The current study is the first report of *Urostomides caducus*, *U. darwini*, *U. campanula*, and *U. bacillatus* from the U.S.A. In addition to Europe and North America, we collected *U. striatus* from Chile. *Urostomides denarius* was found in Asia, Africa, and Europe, and *U. pullus* has been found, to date, only in the Czech Republic. Foissner (2016b) found *U. pelobius* in the Dominican Republic and *U. pyriformis* in Australia. Rather than being endemic, it is likely that unmistakable “flagship” species such as *U. dar-*

*wini* are widely distributed but seldom encountered due to rarity and undersampling.

Interestingly, the only other observed strain of *U. pullus* after original description in 1927 by Kahl comes from a very similar habitat, that is sediment under a layer of decaying leaves both in temperate deciduous forests in Germany. Although eukaryovory has been confirmed in several metopid and apometopid species (Bourland et al. 2014; Esteban et al. 1995; current study), we have not observed it in *Urostomides denarius* or *U. pullus*, which may, however, reflect composition of sediment biota or reduction of other eukaryotes in our cultures. The smaller body size in the case of *U. denarius* may also be a factor.

Metopidae, although specialized to occupy microaerophilic and anoxic habitats, likely have a cosmopolitan distribution (Bourland et al. 2017). Although not yet reported from Antarctica, Petz et al. (2007) did find *Metopus es* in the Arctic.

In contrast to previous attempts to cultivate representatives of this anaerobic group of ciliates (Fenchel and Finlay 1990; Narayanan et al. 2007), the culture methods described herein are quite simple and enable routine and long-term cultivation of free-living Metopida, facilitating their study. No evidence of ectobiotic prokaryotes has yet been found in apometopids. Although we examined only *U. denarius* with fluorescence microscopy and found rod-shaped endobionts consistent with methanogenic archaea, it is quite likely that our other populations of Apometopidae also harbor archaeal endobionts.

## Taxonomic summary

Class Armophorea Lynn, 2003

Order Metopida Jankowski, 1980

### Family Apometopidae Foissner, 2016

**Emended diagnosis:** Obpyriform to clavate Metopida with perizonal ciliary stripe composed of four kineties.

**Nominotypical type genus:** *Apometopus* Foissner, 2016 (junior synonym of *Urostomides* Jankowski, 1964)

**Included genera:** *Urostomides* Jankowski, 1964; *Cirranter* Jankowski, 1964

### Genus *Urostomides* Jankowski, 1964

**New subjective junior synonym:** *Apometopus* Foissner, 2016

**Emended diagnosis:** Small to medium-sized Apometopidae with dominant preoral dome wider than posterior part of cell, conical or tail-like posterior end, 2–11 widely-spaced preoral dome kineties, with or without zigzag pattern, and elongated, sometimes inconspicuous, caudal cilia. Paroral stichomonad.

**Remarks:** Although *Apometopus* is a junior subjective syn-

onym of *Urostomides*, the validity of the family-group name (i.e. Apometopidae) is unaffected (ICZN 1999, Article 40.1). Although Jankowski (2007) included *Metopus turbo* Dragesco and Dragesco-Kernéis, 1986 in *Urostomides*, this species is described as having a five-rowed perizonal ciliary stripe, excluding it from the Apometopidae. Pending further molecular and morphologic data, we leave *M. turbo* in genus *Metopus*.

**Type species (by original designation by Jankowski 1964a):** *Urostomides striatus* (McMurrich, 1884) Jankowski, 2007 (original combination *Metopus striatus* McMurrich, 1884)

**Included species:** *Urostomides bacillatus* (Levander, 1894) comb. nov., *U. caducus* (Kahl, 1927) comb. nov., *U. campanula* (Kahl, 1932) comb. nov., *U. darwini* (Kahl, 1927) comb. nov., *U. denarius* (Kahl, 1932) comb. nov., *Urostomides pelobius* (Foissner, 2016) comb. nov., *U. pullus* (Kahl, 1932) comb. nov., *Urostomides pyriformis* (Levander, 1894) comb. nov. *U. striatus* (McMurrich, 1884) Jankowski, 1964.

**Remarks:** Jankowski (1964a) split the genus *Metopus* into several subgenera including *Metopus* (*Urostomides*). This was done explicitly, *Metopus striatus* McMurrich 1984 was designated as type, and a description was given thus meeting the requirements for availability under the ICZN Code (ICZN 1999, Articles 8, 10, 11). Jankowski (2007) elevated this subgenus to genus rank. Sequence data reported in this paper are available in GenBank under accession numbers KY025567-KY025588.

## Acknowledgements

The authors wish to thank the Idaho Botanical Garden and Aquatic Systems Shoakoi, both in Boise, Idaho for permitting us to collect samples, to Dominik Vondráček, Petr Stiblík, Petr Táborský, František Št'hlavský, Jan Nešněra, Jan and Ivana Ebrovi, Eliška Zadrobílková, Ildar Youssupov, Anna Bauerová, and Vilém Helešic for collecting numerous samples, and to Dr. Miroslav Hyliš from Charles University for kindly assisting with the scanning microscopy procedures. We also thank Dr. Erna Aeschb of the Biology Centre of the Upper Austrian Museum in Linz, Austria for the loan of type and voucher slides and valuable nomenclatural advice. JR was supported by the Charles University Grant Agency (project 389915) and Charles University specific research grant no SVV 260 434/2017. We also thank the anonymous reviewers for their constructive criticism and helpful suggestions.

## Appendix A. Supplementary data

Supplementary data associated with this article can be found, in the online version, at <http://dx.doi.org/10.1016/j.ejop.2017.07.003>.

## References

- Aesch, E., 2001. Catalogue of the generic names of ciliates (Protozoa, Ciliophora). Denisia 1, 1–350.
- Biagini, G.A., Hayes, A.J., Suller, M.T.E., Winters, C., Finlay, B.J., Lloyd, D., 1997. Hydrogenosomes of *Metopus contortus* physiologically resemble mitochondria. Microbiology 143, 1623–1629.
- Bourland, W.A., Wendell, L., 2014. Redescription of *Atopospira galeata* nov. comb. and *A. violacea* nov. comb. with redefinition of *Atopospira* nov. stat. and *Brachonella*. Eur. J. Protistol. 50, 356–372.
- Bourland, W.A., Hampikian, G., Vd'ačný, P., 2012. Morphology and phylogeny of a new woodruffiid ciliate, *Etoschophrya inornata* sp. n. (Ciliophora, Colpodea, Platyphryida), with an account on evolution of platyphryids. Zool. Scr. 41, 400–416.
- Bourland, W.A., Wendell, L., Hampikian, G., 2014. Morphologic and molecular description of *Metopus fuscus* Kahl from North America and new rDNA sequences from seven metopids (Armophorea, Metopidae). Eur. J. Protistol. 50, 213–230.
- Bourland, W., Rotterová, J., Čepička, I., 2017. Redescription and molecular phylogeny of the type species for two main metopid genera, *Metopus* es (Muller, 1776) Lauterborn, 1916 and *Brachonella contorta* (Levander, 1894) Jankowski, 1964 (Metopida, Ciliophora), based on broad geographic sampling. Eur. J. Protistol. 59, 133–154.
- Dragesco, J., 1996. Infraciliature et morphométrie de cinq espèces de ciliés mésopsammiques méditerranéens. Cah. Biol. Mar. 37, 261–293.
- Dragesco, J., Dragesco-Kernéis, A., 1986. Ciliés libres de l'Afrique intertropicale. Faune Trop. 26, 1–559.
- Esteban, G.F., Fenchel, T., Finlay, B.J., 1995. Diversity of free-living morphospecies in the ciliate genus *Metopus*. Arch. Protistenkd. 146, 137–164.
- Fenchel, T., Finlay, B.J., 1990. Anaerobic free-living protozoa: growth efficiencies and the structure of anaerobic communities. FEMS Microbiol. Lett. 74, 269–275.
- Foissner, W., 1980. Taxonomische Studien über die Ciliaten des Grossglocknergebietes IX. Ordnungen Heterotrichida und Hypotrichida. Ber. Nat.-Med. Ver. Salzburg 5, 71–117.
- Foissner, W., 2005. Two new flagship ciliates (Protozoa, Ciliophora) from Venezuela: *Sleighbophrys pustulata* and *Luporinophrys micelae*. Eur. J. Protistol. 41, 99–117.
- Foissner, W., 2006. Biogeography and dispersal of micro-organisms: a review emphasizing protists. Acta Protozool. 45, 111–136.
- Foissner, W., 2016a. *Heterometopus meisterfeldi* nov. gen. nov. spec. (Protozoa, Ciliophora), a new metopid from Australia. Eur. J. Protistol. 55, 118–127.
- Foissner, W., 2016b. Terrestrial and semiterrestrial Ciliates (Protozoa, Ciliophora) from Venezuela and Galápagos. Denisia 35, 1–912.
- Foissner, W., Agatha, S., 1999. Morphology and morphogenesis of *Metopus hasei* Sondheim 1929 and *M. inversus* (Jankowski, 1964) nov. comb. (Ciliophora, Metopida). J. Eukaryot. Microbiol. 46, 174–193.
- Foissner, W., Berger, H., Kohmann, F., 1994. Taxonomische und ökologische Revision der Ciliaten des Saprobiensystems. Band III: Hymenostomata, Prostomatida, Nassulida, vol. 1/94. Informationsberichte des Bayer. Landesamtes für Wasserwirtschaft, pp. 1–548.
- Foissner, W., Agatha, S., Berger, H., 2002. Soil ciliates (Protozoa, Ciliophora) from Namibia (Southwest Africa), with emphasis on two contrasting environments, the Etosha region and the Namib Desert. Part I. Denisia 5, 1–1063.
- Foissner, W., Müller, H., Agatha, S., 2007. A comparative fine structural and phylogenetic analysis of resting cysts in oligotrich and hypotrich Spirotrichea (Ciliophora). Eur. J. Protistol. 43, 295–314.
- Gentekaki, E., Kolisko, M., Boscaro, V., Bright, K.J., Dini, F., Di Giuseppe, G., Gong, Y., Miceli, C., Mode, L., Molestina, R.E., Petroni, G., Pucciarelli, S., Roger, A.J., Strom, S.L., Lynn, D.H., 2014. Large-scale phylogenomic analysis reveals the phylogenetic position of the problematic taxon *Protocruzia* and unravels the deep phylogenetic affinities of the ciliate lineages. Mol. Phylogenet. Evol. 78, 36–42.
- Grain, J., 1984. Cinétosome, cil; systèmes fibrillaires en relation avec le cinétosome. In: Grassé, P.-P. (Ed.), Traité de Zoologie. Masson Paris, Milan, Barcelone, pp. 35–179.
- Hall, T., 1999. BioEdit: a user-friendly biological sequence alignment editor and analysis program for Windows 95/98/NT. Nucleic Acids Symp. Ser. 41, 95–98.
- Hoek, A.H.V., Sprakel, V.S., Alen, T.A., Theuvenet, A.P., Vogels, G.D., Hackstein, J.H., 1999. Voltage-dependent reversal of anodic galvanotaxis in *Nyctotherus ovalis*. J. Eukaryot. Microbiol. 46, 427–433.
- Hu, X., 2014. Ciliates in extreme environments. J. Eukaryot. Microbiol. 61, 410–418.
- ICZN (The International Commission on Zoological Nomenclature), 1999. International Code of Zoological Nomenclature. International Trust for Zoological Nomenclature, London.
- Jankowski, A.W., 1964a. Morphology and evolution of Ciliophora I. The new system of sapropelobiotic Heterotrichida. Zool. Zh. 43, 503–517.
- Jankowski, A.W., 1964b. Morphology and evolution of Ciliophora III. Diagnoses and phylogeny of 53 saprolobionts, mainly of the order Heterotrichida. Arch. Protistenkd. 107, 185–294.
- Jankowski, A.W., 2007. Phylum Ciliophora Doflein, 1901. In: Alimov, A.F. (Ed.), Protista. Part 2, Handbook on Zoology. Russian Academy of Sciences, Zoological Institute, St. Petersburg, pp. 371–993.
- Kahl, A., 1927. Neu und ergänzende Beobachtungen heterotricher Ciliaten. Arch. Protistenkd. 57, 121–203.
- Kahl, A., 1932. Urtiere oder Protozoa I: Wimpertiere oder Ciliata (Infusoria) 3. Spirotricha. Tierwelt Dtl. 25, 399–650.
- Katoh, K., Misawa, K., Kuma, K., Miyata, T., 2002. MAFFT: a novel method for rapid multiple sequence alignment based on fast Fourier transform. Nucleic Acids Res. 30, 3059–3066.
- Levander, K.M., 1894. Beiträge zur Kenntnis einiger Ciliaten. Acta Soc. Fauna Flora Fenn. 9, 1–87.
- Lynn, D.H., 2008. The Ciliated Protozoa: Characterization, Classification and Guide to the Literature, 3rd ed. Springer, Dordrecht.
- Lynn, D.H., Small, E.B., 2002. Phylum Ciliophora, Doflein, 1901. In: Lee, J.J., Leedale, F.G., Bradbury, P.C. (Eds.), An Illustrated Guide to the Protozoa, vol. 1. Society of Protozoologists, Lawrence, pp. 371–656.
- McMurrich, J.P., 1883. Notes on some Canadian Infusoria. Proc. Can. Inst. 1, 300–309.

- McMurrich, J.P., 1884. A new species of infusorian. *Am. Nat.* 18, 830–832.
- Medlin, L.K., Elwood, H.J., Stickel, S., Sogin, M.L., 1988. The characterization of enzymatically amplified eukaryotic 16S-like rRNA-coding regions. *Gene* 71, 491–499.
- Narayanan, N., Priya, M., Haridas, A., Manilal, V.B., 2007. Isolation and culturing of a most common anaerobic ciliate, *Metopus* sp. *Anaerobe* 13, 14–20.
- Omar, A., Zhang, Q., Zou, S., Gong, J., 2017. Morphology and phylogeny of the soil ciliate *Metopus yantaiensis* n. sp. (Ciliophora, Metopida), with identification of the intracellular bacteria. *J. Eukaryot. Microbiol.*, 1–24, <http://dx.doi.org/10.1111/jeu.12411-4934>.
- Paiva, T., do Nascimento Borges, B., Silva-Neto, I.D., 2013. Phylogenetic study of Class Armophorea (Alveolata, Ciliophora) based on 18S-rDNA data. *Genet. Mol. Biol.* 36, 571.
- Petz, W., Valbonesi, A., Schiftnner, U., Quesada, A., Cyan Ellis-Evans, J., 2007. Ciliate biogeography in Antarctic and Arctic freshwater ecosystems: endemism or global distribution of species? *FEMS Microbiol. Ecol.* 59, 396–408.
- Ronquist, F., Teslenko, M., van der Mark, P., Ayres, D.L., Darling, A., Höhna, S., Larget, B., Liu, L., Suchard, M.A., Huelsenbeck, J.P., 2012. MrBayes 3.2: efficient Bayesian phylogenetic inference and model choice across a large model space. *Syst. Biol.* 61, 539–542.
- Roskov, Y., Abucay, L., Orrell, T., Nicolson, D., Flann, C., Bailly, N., Kirk, P., Bourgoin, T., DeWalt, R.E., Decock, W., De Wever, A. (Eds.), 2016. Species 2000: Naturalis, Lei-den, the Netherlands (ISSN 2405-884X). Digital resource at [www.catalogueoflife.org/annual-checklist/2016](http://www.catalogueoflife.org/annual-checklist/2016). (Accessed 9 April 2017).
- Saccà, A., 2012. The role of eukaryotes in the anaerobic food web of stratified lakes. In: Altenbach, A.V., Bernhard, J.M., Seckbach, J. (Eds.), *Anoxia: Evidence for Eukaryote Survival and Paleontological Strategies. Cellular Origin, Life in Extreme Habitats and Astrobiology*, vol. 21. Springer, pp. 403–419.
- Santos, S.M., Guinea, A., Fernández-Galiano, D., 1986. Etude de l'infraciliature et du process de bipartition chez *Nyctotherus ovalis* Leidy, 1850 (Ciliophora, Heterotrichida). *Protistologica* 22, 351–358.
- Silva-Neto, I.D., Paiva, T., do Nascimento Borges, B., Harada, M.L., 2016. Fine structure and molecular phylogeny of *Parametopidium circumlabens* (Ciliophora: Armophorea), endocommensal of sea urchins. *J. Eukaryot. Microbiol.* 63, 1–16.
- Small, E.B., Lynn, D.H., 1985. Phylum Ciliophora Doflein, 1901. In: Lee, J.J., Hutner, S.H. (Eds.), *An Illustrated Guide to the Protozoa*. Society of Protozoologists, Lawrence, pp. 393–575.
- Sola, A., Serrano, S., Guinea, A., Longás, J.F., 1992. The infraciliature of two sapropelic heterotrich ciliates, *Ciranter mobilis* and *Saprodnium dentatum* (Ciliophora, Heterotrichida). *Arch. Protistenkd.* 142, 51–57.
- Sonneborn, T.M., 1970. *Paramecium* research. *Methods Cell Physiol.* 4, 241–339.
- Stamatakis, A., 2014. RAxML version 8: a tool for phylogenetic analysis and post-analysis of large phylogenies. *Bioinformatics* 30, 1312–1313.
- Tucolesco, J., 1962. Études protozoologique sur les eaux Roumaines. I. Espèces nouvelles d'infusoires de la Mer Noire et des bassins salés paramarins. *Arch. Protistenkd.* 106, 1–36.
- Wetzel, A., 1928. Der Faulschlamm und seine Ziliaten Leitformen. *Z. Morphol. Ökol. Tiere* 13, 179–328.
- Vd'ačný, P., Foissner, W., 2017. A huge diversity of metopids (Ciliophora, Armophorea) in soil from the Murray River floodplain, Australia. I. Description of five new species and redescription of *Metopus setosus* Kahl, 1927. *Eur. J. Protistol.* 57, 35–76.